University of Strathclyde Engineering

A Hybrid Modelling Approach to Evaluating the Effects of a Vessel's Biofouling State on Hull & Propeller Performance

Author: Iliya Valchev

Supervisor: Dr Andrea Coraddu & Dr Maurizio Collu

A thesis submitted in partial fulfilment for the requirement of degree of MPhil Naval Architecture & Marine Engineering

May 2025

Copyright Declaration

Signed:

Date: Thursday 29th May, 2025

Abstract

With the sophistication of shipboard systems, maintenance is becoming more time-consuming and skill-dependant. Precise and timely planning, which can be achieved through Condition Based Maintenance, is key in overcoming these challenges, as well as ensuring the longevity and efficiency of assets. The rapid growth of ship monitoring systems means that failures and performance shifts can be linked to variations in measured parameters. This knowledge can be used to limit performance losses, through the identification of undesirable trends. The current project seeks to predict the health status of the hull and the propeller, through the combination of performance modelling approaches from two distinct schools, first-principle techniques and data-driven methods, with the data collection capabilities of modern vessels. Reductions of the vessel's performance at a certain operational and environmental setting, when compared to a reference 'clean vessel state' can be traced to the extent of fouling of the hull & propeller, whose condition can be determined separately. A hybrid methodology, combining the accuracy, speed, and flexibility of data-driven methods with the physical knowledge of first-principle models is considered the ideal candidate for the above tasks. The main aim of the research project is to develop a set of real-time fault detection, which can be used to supplement a maintenance strategy, reducing maintenance loads and crew requirements. The developed novel hybrid prediction models utilise both data-driven and first-principle approaches, which has not been previously applied to the problem of evaluating the vessel performance shift due to biofouling. Finally, a case study is employed to demonstrate the numerical tool's ability to identify shifts in ship capability. Due to the generous collaboration of DAMEN Shipyards and The Royal Netherlands Navy, the developed methodology is validated and tested on real-world data.

Acknowledgments

I would like to take this opportunity to thank a few important individuals who made this work possible through their support, encouragement, and guidance. It has truly been a journey of ups and downs, starting off in late 2020 as a PhD project with the worst possible timing, and later, through a transition to an MPhil degree, helping make way for other career opportunities.

First and, by far, the foremost, I would like to thank my incredible partner. You were endlessly patient, endured every tough moment with me, and joined me in celebrating all the small victories throughout this journey. Victoria, I could not have come where I am without you, and can only hope to support you at least half as much as you - me.

Moreover, I would like to thank my supervisors for the knowledge and guidance they have provided. Andrea, thank you for making this whole journey possible and for all that you have taught me. Your patience, guidance, and generosity will be forever appreciated. Even after moving to a different university & country shortly after this all started, you always made an effort to be available, and were willing to sacrifice your time and attention. Dr Collu, thank you for acting as my supervisor after Andrea left the university, and for spending time with me brainstorming novel concepts for my methodology.

A lot of gratitude is also owed to the Royal Netherlands Navy for funding the initial PhD project and for generously providing the data necessary to develop the project methodology.

Last but not least, I am grateful for my personal perseverance throughout these last years and the high quality work that has been completed. Even though the initial plan did not come to fruition, I believe that what is presented as part of this thesis is novel and truly beneficial to the Maritime industry and the engineering community. I can only be proud of the final outcome.

Contents

List of Figures

List of Figures

List of Tables

1 Background

The last decade has been characterised by growing concerns about greenhouse emissions and their increasingly apparent effects on climate change [1]. The problem of global warming has been internationally recognised [2] and has been one of the biggest drivers in most fields of current research and regulation. The shipping industry is no exception, and several promising technologies have been and are under development towards a net-zero carbon footprint [3].

1.1 Introduction

The increase in globalisation of trade comes partially as a result of a raising demand for the transport of resources [4]. In this field, shipping has been identified as the most efficient mode of transport to face this demand when compared to its land and air alternatives [5]. This is due to a relatively low energy consumption and, therefore, a low cost per unit of carried weight [6], as well as a high degree of cargo safety [7]. As a result, shipping has become responsible for 90% of global trade and a seemingly low, in comparison, global transport emission share of 2.9% [8, 9, 10]. Maritime seems to be less damaging to the environment when compared to its land and air alternatives, however, sulphur oxides, nitrogen oxides, particulate matter, and carbon dioxide emissions due to shipping are still a significant contributor to air pollution [11].

Following the growth observed in the last 40 years [5], the volume of waterborne transport work is expected to further increase, potentially doubling by 2030 [12]. Moreover, the shipping industry only recently started the uptake of new technologies (e.g., alternative fuels [13, 14]) and still primarily relies on fossil fuel energy [15]. Consequently, a rapid increase in shipping's Green House Gas (GHG) emissions volume and emissions share is expected due

to the increase in transport volumes and the quicker decarbonisation of other industries respectively [16]. For example, the most recent Fourth GHG Study by the International Maritime Organisation (IMO) [10] observed that the decrease in carbon intensity of shipping operations (i.e., due to the use of new technologies) was outweighed by the growth of total shipping emissions (i.e., due to the increase in waterborne transport volume). Specifically, emissions are still expected to increase from about 90% of 2008 levels in 2018 to 90-130% of 2008 emissions in 2050 for a range of possible scenarios [10]. As an attempt to rectify this, the IMO has been actively taking regulatory action. The development and enforcement of the EEDI (Energy Efficiency Design Index) by the Marine Environment Protection Committee (MEPC) and, since 2011, the requirement for ship owners to incorporate the Ship Energy Efficiency Management Plan (SEEMP) [17] in line with the IMO are some examples of the IMO's efforts. A vessel's EEDI measures the ratio between produced GHG emissions and the amount of useful work it delivers. A minimum energy efficiency level is required, depending on ship type and size, in line with a phased implementation plan where increasingly stricter energy efficiency thresholds are enforced. This process started in 2013, following a two-year buffer, and is planned to introduce the strictest regulatory efficiency requirements by 2025. Nevertheless, stricter regulations will be required in the future (such as the one on sulphur content requirements for marine fuel inside and outside Emission Control Areas (ECAs) [18]) to achieve the IMO's ambitions towards a net-zero environmental footprint of shipping by the end of the century, following a 50% reduction by 2050 [19].

The means of achieving the required emission reductions still remains an open question. In its second GHG study [8], the IMO suggests a combination of technological and operational improvements. The authors of [5] review studies on ship energy efficiency increasing (and/or emission reducing) technologies and practices currently available in academia and industry. They reach the conclusion that a 75% reduction in emissions is possible by 2050 based on current technologies, including the adoption of alternative fuels. Unfortunately, they also state that widespread deployment of these technologies and practices is currently not happening fast enough or at the required scale. The authors of [20] come to similar conclusions when analysing

the implementation of over 30 candidate technologies. GHG reducing technologies (i.e., fuel cells, batteries, dual-fuel engines) and alternative fuels (i.e., ammonia and hydrogen) will have a substantial impact on the future [5], however, the current fleet cannot be realistically retrofitted in the short-medium term. For this reason, it is mandatory to keep current propulsion systems at their best efficiency. Improving vessel efficiency is also in line with ship owners' desire to reduce fuel costs, which often contribute to more than half of a ship's operational costs [7]. In fact, an emission reduction of 33% by 2030 could be possible because most energy efficiency improving measures are cost efficient [21]. Nevertheless, despite these being financially feasible, the adoption of new technologies is rare among vessel owners and operators. This is the so-called 'energy efficiency gap', which is caused by unrealised potential for improvement, and affects many other fields [22]. Focusing our attention on the shipping industry, there are many factors causing this gap (e.g., safety, reliability, technological uncertainty, and market constraints) that act as a barrier for the implementation of new energy efficiency improving technologies [23].

Regardless of the emission reducing technologies employed, a vessel and its systems are and will always be subject to performance decay. Effective maintenance can be responsible for up to 40% of total operational costs [24] and, therefore, is a perfect candidate for optimisation and improvement. Moreover, effective maintenance of systems and system components reduces the disruptions that can be caused by faults or failures on-board [25], ensuring that the vessel is operating at its best efficiency. Therefore, using intelligent tools as a decision-support instrument in maintenance planning is a potential source of operational improvements [26]. However, improvements need to be economically viable for vessel owners, as well as effective in reducing environmental impact [27]. A good example is the problem of biofouling, which is the focus of the current work. Direct exposure to seawater, which is both highly corrosive and filled with living organisms, is the main cause of surface roughness increases that negatively impact the hydrodynamic performance of a ship [28]. This increase is responsible for higher GHG emissions due to the consumption of additional fuel. While novel systems that combat biofouling [29] are becoming available, two main methods of biofouling control are widely

implemented [30, 15], namely antifouling coatings and periodical cleaning. Nevertheless, no coating can fully stop biofouling [31] and the coating needs to be periodically replaced during dry-docking. Financially, the higher fuel consumption translates to substantial increases in operational costs, especially since between $60 - 70\%$ of the operational costs of a ship result from its energy requirements [32]. On the other hand, periodical cleaning is a time-consuming and costly maintenance activity, which prevents the vessel from performing its particular mission. The above brings about a curios trade-off between the two sources of monetary expenditure in operating a vessel. For this reason, being able to monitor and evaluate the biofouling state and its effects on vessels' hull and propeller performance is of paramount importance for optimum maintenance planning. Existing research [33] has hinted that even modest improvements in the fouling condition of a hull potentially outweigh the costs of developing technical solutions or improving management strategies. Unfortunately, due to the dynamic and multifaceted nature of the problem, this remains a difficult task [34]. The reasons in why the author has chosen the topic of biofouling are expanded on in the following Chapter 2, and will, for now, be omitted in favour of delivering a holistic description of the higher level challenges and opportunities the Maritime industry faces.

To avoid only conducting maintenance when a fault or failure occurs, there is a need for a mature knowledge of a vessel and its operation. In this respect, the development of the necessary decision-support tools associated with constructing a maintenance schedule is an important avenue for research. This can be looked at in terms of both making the implementation of new technologies easier through a good foundation for their upkeep, encouraging owners to adopt them, as well as the above-mentioned connection to fuel economy, which currently is of big importance due to the currently high carbon content of marine fuels. Throughout history, many maintenance strategies have been developed with varying requirements in terms of knowledge and information.

1.2 Maintenance Approaches

According to the British Standard EN 13306:2017 [35], the term maintenance refers to the *'combination of all technical, administrative and managerial actions during the life cycle of an item intended to retain it in, or restore it to, a state in which it can perform the required function'*, whereas a maintenance strategy is a *'management method used in order to achieve the maintenance objectives'*. As mentioned above, the uptake of an appropriate maintenance strategy in terms of a vessel is essential. This both minimises down time and costs, increasing profitability, as well as ensuring the long life of an operator's assets. The preferred strategy has naturally changed with the modernisation of industry and continues to evolve based on technological trends. Lazakis et al. [36] appropriately list the evolutionary steps of owners' and operators' view of maintenance in shipping. Initially, it was considered a nuisance, however, necessary for the continued operation of one's ships. Eventually, the possibility to reduce operational down time and costs through the optimisation of the maintenance strategy and scheduling meant an opportunity to increase profitability and as such started being seen in a more positive light. In today's age, maintenance has become integral, where much thought and planning is put into the selection of the most appropriate strategy. Of course, this has not happened solely due to the 'change of heart' of the Maritime industry, the modernisation of the world has meant that more robust and advanced strategies came into existence, providing increasingly benefits to owners and operators, in a way bringing incentive for their interests.

The classification and separation of maintenance strategies, however, is no easy task. Upon review, there is no internationally accepted structure across the whole industry, a conclusion which other research has also reached [37]. However, the underlying understanding which has lead researchers to varying classifications of maintenance types is constant. The author prefers the structure presented in [36], among other works. The initial stages of maintenance deployment in shipping made use of corrective maintenance, where a component is only replaced or serviced when a failure or fault occurs. Even though there is a certain level of cost saving that comes from fully utilising the lifetime of a part before replacing it, the unexpected occurrence

of failures results in a higher chance for serious faults and subsequently longer down periods [24]. As an attempt to remedy this and decrease operational downtime or a need to operate with a severely reduced efficiency/performance, a more proactive approach was developed. The so-called preventive maintenance draws upon previous experience and applies a time-based maintenance interval, where components are replaced preemptively. Preventive maintenance reduces failure rates and down time, in this way seeking to maximise cost savings, however, often a lot of the remaining useful life of components is wasted [36]. Looking at the so-far mentioned maintenance strategies, it can be seen that they are almost each other's opposite. Corrective maintenance prioritises the full exploitation of components, sacrificing vessel operability, whereas the preventive approach sacrifices some useful life of vessel parts and focuses on maximising operational up-time. In reality, apart from very specific use cases, the optimum approach is somewhere in between. Not surprisingly, the next step in shipping maintenance strategy evolution seeks the minimum possible costs through a balance between the two previous approaches. Predictive maintenance strategies utilise the advancement of technology and research to detect the need for maintenance in real-time during operation [38]. According to [36, 37], predictive maintenance can be further split up into Reliability-Centered Maintenance (RCM), Risk-Based Inspection (RBI) and Condition Monitoring (CM). Figure 1.1 shows the above described evolution of maintenance strategies.

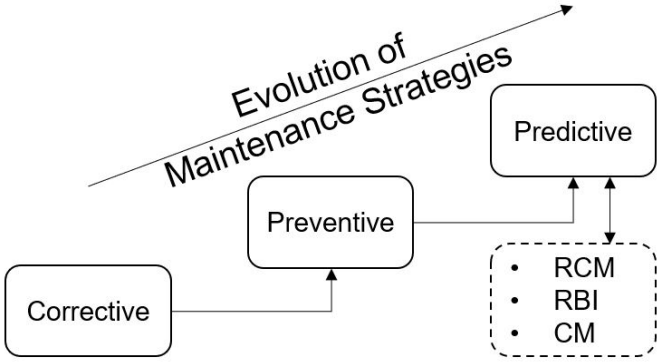

Figure 1.1: Evolution of Maintenance Strategies

The current work is interested in CM, which seeks to determine the health status of ma-

chinery through the use of sensory data and ultimately provide insight into when and what maintenance is required before failure occurs [38]. Knowledge about the health status of vessel components at any given moment is extremely valuable when ensuring maximal exploitation of resources, allowing operational downtime only when a failure is expected to occur soon. The trends of key performance indicators, which are recorded through the aforementioned sensory readings, are normally used in advanced performance modelling methods in combination with historical data and engineering expertise to conduct the necessary condition evaluation. Naturally, the choice of an appropriate performance modelling avenue is a very important factor in achieving good quality results. The development of the state-of-the-art in modelling and the resulting availability of better insight in terms of vessel systems & subsystems can thus be seen as directly linked to the improvement of the existing maintenance framework in the Maritime industry, which is an essential factor going forward. The necessary steps towards the decarbonisation of shipping cannot be done on a weak foundation of knowledge due to its complicated and high-consequence nature. Owners and operators can only commit to technological improvement if they know what to expect as a result.

1.3 Datification in Shipping

Currently, following the trends in other industries, shipping is going through a technological revolution where the smart use and recording of digital data is improving operational and design processes [39]. Due to both a steady transition from the previous manual means of operational monitoring to new cyber-centered methodologies and the ever increasing computational power available for exploitation, new data-driven techniques for evaluating vessel performance are being developed. While the potential benefit of these tools is vast, it can only be brought to fruition through the availability of high quality and quantity data [40].

Traditionally, operational performance in shipping has been monitored utilising manual data logging through the so-called noon reports (NR). These log books are used on all ships and the frequency of logging of new entries is either daily or every watch, where a 24-hour average is en-

tered into the NR. Which variables get recorded depends on the needs of the shipping company, the availability of instruments for conducting the actual measurement, the training and motivation of the crew etc. [41]. In fact, due to the dependence of noon reports on manual human data logging, they are often exposed to certain shortcomings due to insufficient crew training, inadequate data collection protocols and, of course, human error on data entry. Most operators collect very similar data (ship position, speed, propeller RPM, fuel consumption, draft, environmental conditions, etc.), however, there is no standard format for this, which makes using NR data for performance analysis very difficult if the goal is an approach which would work for different vessels and operators. Irregardless of that, some researchers have seen success in utilising noon reports for the analysis of vessel performance [9, 15, 42], while there are even some who have used NR data in the development of Machine Learning (ML) algorithms [43, 44].

Technological advancements have resulted in the implementation of automatic data acquisition systems for vessels, also known as Continuous Monitoring (CM) systems, where data is being recorded with much higher sampling frequency, accuracy, and reliability than the previously used noon reports [45]. Sensory readings from the ship's instrumentation normally get fed to this central system, where they are available for storage and subsequent analysis or for on-the-go decision making through data-driven tools. The digitisation and unification of performance data allows for easy exchange between vessels and land-based data centers, which will most definitely be of paramount importance in the future, for example if current interest in the development of autonomous shipping is to be believed. It is interesting to note that despite the superior capabilities of automatic systems, operators are often not provided with transparency on how the data is being handled and processed within commercial systems [41]. Nevertheless, in the scope of using data-driven techniques for the determination of vessel performance characteristics, the amount of additional data that the higher sampling frequency entails results in higher accuracy and reliability models. The lack of need for crew involvement in data collection also enables the use of automatic equipment monitoring.

Both manual parameter logging through noon reports and automatic data acquisition systems are greatly reliant on the use of different sensors installed throughout the ship, each with

unique characteristics and operating conditions [39]. For example, higher frequency data collection is used for machinery analysis, while low frequency sampling is utilised in the determination of environmental conditions [46]. As a result, the extent and quality of available sensory data are directly related to these devices, whose functionality is essential for any performance evaluations. In this sense, while sufficient data quality is needed, it is not currently guaranteed. On-board ship sensors are prone to malfunction due to harsh operating conditions and are often duplicated to increase redundancy [41]. Additionally, sensory noise is inevitable due to the presence of unobserved phenomena whose effect on readings is unknown, and should be addressed in the data handling pipeline. Nevertheless, the modernisation of industry is an undisputed trend which is bound to better availability and quality of sensory equipment and as such the reliability and volume of recorded data is naturally going to increase. Ultimately, if the information is available, it can then be used to better the Maritime industry through multiple avenues.

1.4 Chapter Conclusion

The shipping industry is seeing substantial and increasing pressure to reduce its environmental footprint, all the while maintaining the operational efficiency of its assets. As such, the current reliance on fossil fuels and the imminent growth in global trade require urgent action to substantially reduce greenhouse emissions. Technological advancements and alternative power sources offer promise in the long-term, however, their widespread adoption is hindered by various hurdles in the short-term, including the previously mentioned 'energy efficiency gap' and the inherent challenges of retrofitting/replacing the existing fleet.

Biofouling significantly affects vessel performance, further complicating the path towards decarbonisation. Moreover, it is a consistent issue which will continue to hinder shipping regardless of advancements in vessel powering. The growth of marine life on a ship's hull is the main contributor to increases in surface roughness as a ship ages, leading to higher requirements in terms of power input for the same overall performance. Currently, this translates to increased

emissions, and while antifouling coating and periodic cleaning are being used as a deterrent, these methods are not fully effective, are also costly, and time-consuming. Consequently, the ability to monitor the state of biofouling on a ship's underwater surfaces, and its impact on vessel performance is key for developing a robust and optimal maintenance strategy. The latter have continuously evolved, from corrective to predictive and proactive approaches, highlighting the importance of advanced condition monitoring systems in ensuring vessels operate in an optimum condition, despite challenges such as biofouling. With the industry's movement towards greater levels of 'datification', high quality operational sensory data is becoming more readily available, facilitating more sophisticated analysis and estimation of vessel performance and empowering existing maintenance practices.

Ultimately, the successful decarbonisation of the shipping industry will require a holistic approach that integrates technological innovation, effective maintenance strategies, and the smart use of data. By embracing these advancements, the maritime sector can both achieve significant emission reductions in the short-term, and build the foundations of a more efficient future. The current project seeks to develop the current best practice in terms of biofouling impact estimation by introducing novel numerical modelling methods that have not yet been considered for this application, but have highlighted substantial promise in other fields of engineering.

1.5 Structure of Thesis

Following the brief introduction given in the current Chapter, a detailed investigation into the available literature on the target topic is conducted in Chapter 2. This critical review and its findings has also been published as a separate journal article [47]. Based on the identified research gaps as per the later, the aims & objectives of the current research project are outlined in Chapter 3. In order to meet the set goals, a sophisticated methodology is constructed and validated in Chapter 4, resulting in a robust ship speed prediction model. Moreover, to demonstrate the value of the above in terms of supplementing a vessel's maintenance strategy, a case study is performed in Chapter 5 to compare the new approach against the current industry method of

estimating the performance impacts of biofouling. Finally, after a discussion on the observed results, the author reflects on what has been achieved and its future prospects within Shipping in Chapter 6, providing a conclusion to the research project.

2 Critical Review

Throughout the years, researchers have attempted to develop numerical methods which can effectively be used as a guide for vessel biofouling centered maintenance strategies. To better understand these numerical models, it is worth first describing the biofouling phenomenon in more detail. In the current section, the state-of-the-art of such methods is critically reviewed, following a description of biofouling, its impact, and methods of prevention. A conclusion from the performed review, open problems, and future direction of this field of research is detailed at the end of the chapter. The chapter, in its entirety, has also been separately published as a journal article in Ocean Engineering [47].

2.1 Introduction

Biofouling is an unwanted process, characterised by several stages of formation, which results in the growth of marine life on a ship's wetted surfaces. According to [48], ship hull biofouling can be characterised by three categories: weeds, shells, and slime. The former two are referred to as macrofouling and the latter as microfouling. Macrofouling forms on vessels with longer nonoperational periods and has more pronounced negative effects on ship performance [49]. Instead, ships with high operational speeds and low periods of down time commonly experience earlier and less detrimental stages of biofouling, such as the formation of a biofilm and the growth of algae, also termed as microfouling [49, 50]. The initial biofouling stage is the formation of a slime film with varying thickness, depending on the growth stage. Once a biofilm has been formed, its presence makes the further growth of weed and shells much easier [51]. This development is not uniform over the vessel's entire underwater surfaces [15]: the separate

regions of an underwater body experience varying conditions, for example in terms of fluid flow, due to the general non-uniformity of a ship hull, providing different levels of facilitation for organism growth.

Moreover, this development also varies between vessel types and missions, depending on their operational characteristics [52]. In fact, navy ships often spend long periods in port, whereas commercial vessels rarely remain stationary for a prolonged period of time due to their need to complete transport work in order to remain profitable. Such differences in activity result in major variability in the type and extent of fouling formation. It has been widely observed that marine life finds it much easier to attach to vessel surfaces at lower speeds, ultimately a stationary vessel being the optimum 'host' [49]. In contrast, higher vessel speeds result in increased frictional shearing forces, which often dislodge less hardy organisms from a ship's underwater surfaces or, at least, make their survival much harder, especially when experienced for prolonged periods of time [49]. Therefore, a container carrier, that often completes long voyages at constant high speeds, most likely will experience the onset of fouling to a lesser extent when compared to a sedentary navy ship [49].

A vessel's operational envelope has a substantial influence on biofouling, however, there are other important factors as well. Environmental variables (e.g., water temperature, salinity, pH, nutrient composition, flow velocity, depth, and light) affect the properties of biofouling [53]. Biofouling organisms thrive in warmer weather [15], which not only means that there is a geographical influence on their development, but also seasonal variations. The majority of marine lifeforms prefer higher water temperatures and steady environmental conditions, therefore, less organisms are able to survive on the submerged surfaces of vessels whose operation involves rapid and frequent changes in environmental conditions [49]. The biofouling phenomenon is very complex and multifaceted, meaning that even vessels with identical operational behaviour will most likely experience different biofouling development if they do not operate in the same region.

2.2 Impact of biofouling on vessels

Biofouling results in severe operational drawbacks and dangers. In particular, it negatively impacts vessel efficiency in terms of performance and costs [54] (see Sections 2.2.1 and 2.2.2), as well as resulting in damages to the environment when combined with the global nature of shipping [55] (see Section 2.2.3).

2.2.1 Impact on performance

In order for a vessel to move through water at a certain speed, its propulsion system must generate an appropriate amount of thrust, which overcomes the inherent resistance associated with this movement. The total experienced resistance is a combination of several components concerning friction, as well as pressure variations due to wind, waves, and the hull's movement through water [56]. The biggest and most influential contribution to the total resistance (up to 90% according to [57]) is the skin friction of a vessel's underwater hull. It originates from the viscosity of water and is directly affected by the smoothness/roughness of the underwater surfaces of a ship. Thus, it is easy to observe that the condition of a vessel's hull, propeller, and other appendages has a direct correlation with this important frictional element of the total resistance. Biofouling has a negative effect on the roughness of the subjected surface, resulting in an altered hydrodynamic profile and a higher total resistance. Recent research has identified that hull roughness also has an impact on other resistance components [58], which has previously been assumed to be negligible.

The negative impact of an increase of the hull's resistance due to biofouling can be evaluated in two ways [50]. To maintain a desired speed, there must be an appropriate increase in the delivered thrust by the propulsor, i.e. there will be a higher power demand. If the delivered power is to be kept constant, the increase in total resistance due to biofouling results in a natural decrease of the vessel's speed. Additionally, if the former perspective is taken into account, the increase in delivered power can also be considered with regards to fuel economy. These different evaluation methods exist in literature, making it difficult to easily compare the results

of different research works [15]. A constant between all interpretations of the problem is that fouling decreases a vessel's range [59], which is a serious issue for some ship types (e.g. navy vessels).

Each of the above-mentioned biofouling stages is different with regard to the scale of its negative impact on a vessel's performance [57]. Even the initial stage of biofouling, the formation of a slime film, has a pronounced impact on hydrodynamic performance. For example, Watanabe et al. [60] reported an $8 - 15\%$ increase of frictional resistance due to the presence of slime. This has been further confirmed by Farkas et al. [50] where a Computational Fluid Dynamics (CFD) implementation was exploited to determine the impact of different stages of slime film development. An increase in total resistance ranging from 0.5 to 25.8% was observed when different biofilm stages were examined. Moreover, in [57] the effects of biofouling on ship resistance and powering were studied and it was discovered that a light slime film resulted in around a 10% increase in shaft power and total resistance, whereas heavy slime films could result in around a 20% increase.

Macrofouling affects the total resistance to a greater extent. The estimation of added resistance due to weed biofouling is difficult and of minor interest [48]. Instead, the impact of hard calcareous fouling on hull resistance, propeller performance, and propulsion characteristics is often the subject of research in the field. For example, Kempf et al. [61] conducted an experimental campaign on pontoons with varying coverage and height of shells with the goal of predicting added resistance due to biofouling. In [62] towing tank experiments using flat plates covered with artificial barnacles of varying size and coverage were performed. The results, extrapolated at full-scale, showed that barnacle size has a significant effect on added resistance due to biofouling, where a 10% coverage with 10mm diameter and 5mm height artificial barnacles led to the same 44.6% increase in effective power requirement that was observed for a 50% coverage with 2.5mm diameter and 1.25mm height shells. The above results confirmed the assumption of [63] that the height of the largest barnacles (part of a fouling layer) has the largest impact on drag. In [57] an increase of required shaft power between 35% for lesser and 86% for heavy calcareous fouling was reported. This was observed at cruising speed through a

Table 2.1: Performance impact of biofouling.

Ref.	Method	Microfouling impact	Macrofouling impact
[60]	Rotor and Towing tank experiments	Frictional resistance increase $8-15\%$	N/A
[50]	CFD	Total resistance increase $0.5-25.8\%$	Total resistance increase $50-120\%$
[57]	Laboratory-scale drag measurements and boundary layer similarity law analysis	Total resistance increase of around 10% for a light slime film and around 20% for a heavy one	Total resistance increase ranging from $35-86\%$

method of predicting the effects of coating roughness and fouling on a full-scale ship by utilising model tests. Finally, the authors of [50] exploited CFD simulations with varying extents of hard fouling on different ship and propeller types to determine the impact of hard fouling on ship performance. They observed increases in total resistance in the range between $50-120\%$ across different hull forms, along with increases in required delivered power between $75-213.4\%$. Using effective power as an indicator of fouling effects neglects the decreased propeller performance due to the fact that when fouled a ship propeller's efficiency decreases and its operational region may be shifted away from optimal conditions.

For the sake of completeness, a brief summary on the performance impact that has been attributed to biofouling is reported in Table 2.1.

2.2.2 Financial impact

As discussed in the previous section, over time biofouling decreases the efficiency of a vessel, requiring additional fuel for achieving the same mission. An increase in the fuel quantity required for powering is accompanied by extra financial strain, especially since between $60-70\%$ of the operational costs of a ship result from its energy requirements [32].

There is a direct monetary cost to maintaining a fouling-free vessel, as well as accompanying down periods, where the vessel is unable to perform its mission. Therefore, there is an obvious trade-off between the costs of hull and propeller maintenance activities and the costs due to increases in total resistance. In fact, it is crucial to develop tools which are able to effectively estimate the loss in efficiency (and the increase in costs) due to the vessel's biofouling state in

order to detect the optimal point in time for conducting hull and propeller maintenance [64]. The most influential and widely known study to address the financial aspects of ship biofouling is that done by Schultz et. al [33]. An in-depth analysis and breakdown of the costs associated with the fouling of an entire class of naval vessels allowed the researchers to quantify the financial expenditure that is needed to combat the usual performance deterioration with time. The above lead to a conclusion that even modest improvements in the fouling condition of a hull could save enough money to cover the costs of development, acquisition, and implementation of even relatively expensive technical or management solutions.

The financial aspects are not only ground for the creation of tools and strategies which can help fouling management, but there is also a need and desire for such developments [65].

2.2.3 Environmental impact

As stated in the introduction, the energy efficiency gap in Maritime is a serious problem that needs to be addressed. The overall efficiency decrease due to biofouling has a severe environmental impact caused by the increase in the amount of pollutants expelled to the atmosphere through exhaust gases. The IMO has previously estimated that the deterioration in hull and propeller performance of the world fleet is accountable for $9 - 12\%$ of Maritime's GHG emissions [66]. Being able to assess the vessel's performance decrease due to fouling in real-time and, subsequently, to use this information to improve current maintenance practice then becomes fundamental. Moreover, these tools are inexpensive and relatively easy to exploit on both old and current vessels. In fact, researchers have been able to achieve this using Noon Reports (NR) [43] which are widely available for most ships and even if not, their creation is solely dictated by company operational practice.

Another aspect to take into consideration is that a single vessel can travel across very long distances and often connects geographical locations with entirely different marine life, becoming a vector for the transportation of species across the globe. This becomes a problem when considering potentially invasive organisms, which threaten the biodiversity of the oceans. In fact, there is evidence that fouling is even more likely to cause the transfer of foreign species

than ballast water [67, 68]. The chance of spreading non-indigenous species through fouling has been observed to increase with the age of the hull and propeller's antifouling coating [68]. Interestingly, microfouling is far less likely to result in the spread of non-indigenous species when compared to macrofouling because the organisms that slime films are comprised of lack reproductive structure [68]. Maintaining a vessel's hull at earlier stages of fouling development, while also collecting the resultant waste, could be considered as a viable option in reducing this environmental risk [33, 15].

2.3 Fouling control

To mitigate biofouling's negative effects, two main means of mitigation and control are used in combination.

Antifouling (AF) coatings are normally applied to the exposed surfaces of ships to protect against, or at least slow down, the build-up of biomass. Different coating technologies exist, utilising different approaches. As described by [53], the main ones are Self-Polishing Copolymers (SPC), Controlled Depletion Polymers (CDP), and Foul-Release coatings (FR), which can be further split up into biocidal (SPC and CDP) and non-biocidal (FR). Ultimately, the former release chemicals to prevent the formation of biofouling, whereas the latter reduce the attachment strength of marine life and facilitate the release of biofouling from treated surfaces when the vessel is moving. Biocidal coatings have a long history of environmental damage: for a long time tributyl tin (TBT) was used industry-wide because of its very high effectiveness in preventing fouling, however, was ultimately banned due to its serious environmental impact [48] and replaced with copper-based biocidal coatings. However, these are now also being banned regionally [48]. Hard coatings, on the other hand, have been found neutral to the ocean with a lifespan of at least 10 years, where they may even extend the life of the hull [69]. None of the technologies mentioned above provide full protection (i.e., biofouling still occurs on the hull and propeller of vessels). The application of antifouling coatings only reduces fouling accumulation between cleaning events and allows for longer periods between them [31].

Regardless of the relative effectiveness of AF coatings, none of the technologies provide full protection, i.e., biofouling still occurs on the hull & propeller of vessels, be it at a reduced rate, and if left unchecked would result in severe frictional resistance increases. Manual cleaning of the hull and propeller is the second method of fouling control, which can either be done underwater by divers with specialised brushes and Remotely Operated Vehicles (ROVs) or when the vessel is dry-docked [69, 70]. Dry-docking is the more effective of the two methods as it allows for cleaning, sandblasting, and re-coating of the hull with a new antifouling coating and results in a larger reduction in total resistance [15]. Moreover, it is the only method which allows for the neutralisation of invasive species [15]. Unfortunately, dry-docking is also expensive and thus is undertaken only when necessary, usually every 3 to 5 years [71]. Underwater cleaning of the hull and propeller has been observed to have roughly half the beneficial effect on reducing fouling resistance when compared to dry-docking [15], however, it is much cheaper. In fact, in [59], authors state that underwater cleaning costs would get accounted for in between 14 and 24 operational hours through fuel savings. The replacement of divers with specialised ROVs for underwater cleaning can be identified as another option [72]. Unfortunately, for the easily damaged foul-release silicone coatings, underwater cleaning is not suitable [42]. Additionally, it also does not allow for the collection of biological waste and can lead to the rapid discharge of antifoulants from biocidal ship hull coatings, which without proper filtration can cause severe environmental damage [73]. For this reason, classic underwater cleaning is banned in many ports across the world [49]. Nevertheless, methods for addressing the shortcomings of underwater cleaning, namely capture technology, are currently under development [74]. Additionally, underwater cleaning is often combined with hard coatings which avoids the discharge of toxic particles [69].

2.4 Preliminaries

Before reviewing the methods available in the literature, this section provides a concise explanation of biofouling-related parameters and collectible data useful for monitoring and eval-

uating the relevant effects on hull and propeller performance. It is important to have a clear understanding of what phenomena can be measured or simulated by means of endogenous (i.e., vessel specific) or exogenous (e.g., environmental) data collection. Specifically, a parameter is referred to as exogenous if it is determined outside of a vessel's operation and cannot be influenced by the examined system, whereas endogenous measurements describe factors over which there is control. For example, environmental conditions are exogenous as they describe the environment in which the ship has to operate and cannot be influenced. In fact, exogenous parameters are the main subject of filtering because of the inherent difficulty of estimating their effects on a vessel. Knowledge about exogenous parameters is extremely valuable because it allows approaches to take the influence of outside conditions into consideration, irregardless whether this is done as part of a deterministic approach for evaluating added resistances due to wind, waves etc., or as part of a data-driven approach where the phenomena are captured in a purely artificial way.

For this reason, the data that can be available will first be described, followed by what quantities it is possible to estimate for the purpose of monitoring and evaluating biofouling effects on hull and propeller performance.

2.4.1 Available Data Sources

The quality, volume, and variety of collected data varies between vessels and is highly dependent on the particular equipment installed on board [75]. Due to the long life cycle of ships, data recording capabilities vary substantially, depending on a ship's age [39]. Retrofitting sensory equipment is an option which many ship owners actually pursue [76]. Considering the task of a vessel's operational monitoring, for both newbuilding and retrofitting, selecting the array of sensors is a complex ship-specific problem, which depends on the particular monitoring application, the shipowner's needs and the desired capabilities [77]. In fact, many different metrics need to be taken into account, such as the cost of the sensors and their probability of failure, the costs and the complexity of the installation, and the estimated benefits (e.g., environmental, economical, etc.) [76]. The final array of sensors available for the vessel's monitoring directly

affects the condition monitoring system's capabilities, quality, and accuracy [78]. As a matter of fact, collecting high frequency and quality operational data facilitates the development of enhanced monitoring capabilities but, at the same time, increases the cost of the installation, its maintenance, and the operation of the monitoring system itself [79]. Most commonly, it is required to exploit, in an opportunistic way, all the measures and sensors already available and still obtain good results without investing in retrofitting or modifying newbuiding projects [49]. Note that, some information, can be also retrieved via virtual sensors which do not require any physical sensor installation [76]. Although virtual sensors might lead to less accurate estimation, this approach still provides some benefits of having a physical sensor without the associated capital cost [80].

Table 2.2 briefly reviews the biofouling-related operational measurements as well as example sensory equipment. Some sensory features are inherently less reliable than others due to the nature of the target parameter and the nature of the sensor exploited [81]. A lot of variables are not included (e.g., light intensity, water nutrient composition, and water pH etc.) despite them being influential in terms of the speed and type of biofouling formation, partially because of the difficulties associated with their measurement [53]. Moreover, the current work is focused on methods for determining the biofouling performance impact rather than the specifics of the biofouling growth process.

Table 2.2: Typical biofouling-related operational measurements.

Parameters	Description	Source	Sensors	Reliability
Water Depth	The value of a water depth measurement in terms of vessel performance modelling comes with respect to estimating shallow water effects. With decreasing water depth, these become more impactful	Exogenous	Depth sounder (also called echo sounder or depth finder) or Pressure-based depth sensor	High
Water Properties (e.g., Temperature, Density, Viscosity, and Salinity)	Variations in water properties directly affect the hydrodynamic performance of a vessel	Exogenous	Various sea water sensors	High
Sea State Properties	Knowledge of the sea state allows for the estimation of wave effects on the ship	Exogenous	Shipboard sensors, Satellite data, or Wave buoys	Medium/ High
Water Current Properties	Knowledge of the water current speed and direction with respect to the vessel could allow for the use of speed over ground instead of speed over water (SoW). This helps curtail the low reliability of SoW measurements.	Exogenous	Acoustic Doppler current profilers	High
Wind State Properties	Knowledge of the wind state allows for the estimation of wind effects on the ship.	Exogenous	Anemometer	High
Air Properties (Temperature, Pressure, Humidity etc.)	Variations in air properties directly affect the aerodynamic performance of a vessel.	Exogenous	Shipboard sensors such as temperature sensor, barometer, humidity sensor, etc.	High
Draft & Trim	Draft & Trim are key hydrostatic properties, which directly affect hydrodynamic performance.	Endogenous	Hydrostatic level sensors in multiple locations across ship length	High
Vessel Speed through Water	Speed through water (also LOG speed) helps determine a vessel's operational efficiency and rate of fuel consumption. It is complicated to calculate accurately, requiring knowledge of currents and other forces acting on the vessel.	Endogenous	Paddle wheel speed sensor, Ultrasonic speed sensor, Electromagnetic speed sensor, or, most recently, Doppler log which is more accurate	Medium/ High
Vessel Speed over Ground	Speed over Ground (GPS speed) is the speed at which the vessel moves with respect to its geographical position.	Endogenous	GPS signal	High

ME RPM & Torque	The power output of the engine through its RPM and Torque indicates operational setting.	Endogenous	Rotational speed sensor (for example a tachometer) and a Torque sensor	High
ME Fuel Consumption	Fuel is the source of propulsive power and so it is directly linked to energy efficiency.	Endogenous	Mass flow meter	High
Fuel Properties	Fuel properties such as heating values, density, temperature, etc. vary and are important parameters related to the energy input into the power plant.	Endogenous	Fuel quality sensor & Fuel heating value sensor	High
Shaft Torque, RPM, and Power	The shaft power is a good indicator of the power available for propelling the vessel.	Endogenous	Shaft power (torsion) meter	Medium/ High
Propeller Thrust	A propeller's generated thrust is the vessel's moving force, which opposes total resistance.	Endogenous	Thrust meter, usually an optical sensor	High
Propeller Pitch	The propeller's pitch sets its operational point. For a vessel with a controllable pitch propeller, this can be varied.	Endogenous	Propulsion Control System	High
Rudder Angle & Activity	Angling the rudder results in a sideways force, which turns the vessel. Rudder activity also results in power losses, i.e. added resistance.	Endogenous	Rudder angle sensor	High

2.4.2 Parameters to Estimate

For what concerns the scope of this review, the most important parameter to estimate is the impact that biofouling has on the vessel's hull and propeller performance. In particular, it is often required to compare the actual 'real-life' performance to the case when the hull and propeller are 'clean' (i.e., not fouled) [82]. Commonly, data recorded during ship sea trials is used to represent this unfouled scenario [83, 42, 84, 85, 86]. Nevertheless, this approach is not always the correct one since, in time, other vessel components are subject to decay [87] and this may lead to an overestimation of the biofouling effects on hull and propeller performance. Additional vessel fuel consumption is usually exploited to translate the added resistance due to biofouling into a measure that can be easily converted into a monetary cost [33]. However, due to many other exogenous factors that can potentially influence the fuel consumption, it has been proven to be inaccurate for describing the added resistance due to biofouling [88]. In fact, Carchen et al. [88] argue the need for new measures (in addition to speed loss, added power requirements and fuel consumption) which provide enhanced insight into vessel hydrodynamic performance changes due to biofouling. Specifically, they propose three novel parameters, i.e., hull viscous drag, effective wake, and propeller sectional drag, which have the potential to improve the ability to evaluate biofouling's impact on ship hydrodynamic performance. Nevertheless, these parameters are difficult to relate to commercial shipping practice. For example, the use of simpler parameters such as speed loss is useful in translating the delay in vessel operations into financial losses [64]. The same can be said regarding increases in power and fuel requirements [33].

Table 2.3 summarises the main parameters that are usually estimated and exploited to measure the biofouling impact.

2.4.3 Modelling Approaches

To estimate the parameters described in Section 2.4.2 based on the data described in Section 2.4.1, the most effective and cost-efficient approach is to use numerical methods [98]. These numerical models can build upon the physical knowledge of the problem [50], or on

Table 2.3: Typical parameters for biofouling impact estimation

Ref.	Parameter	Link to shipping practice
[64, 84, 85, 86, 49, 50, 89, 90, 26]	Speed loss	Can be translated into longer voyage times and bigger delays in schedule.
[49, 83, 15, 91, 50]	Additional fuel consumption	Direct connection to increased fuel costs and, therefore, operational costs.
[43, 53, 62, 50, 56, 57, 42, 92, 58, 33, 89, 42, 93, 94, 95, 96, 26]	Additional power requirement/Added resistance	Can result in overloading of the vessel's engine and is indicative of higher energy needs/lower ship efficiency.
[97, 34]	Change in propeller open-water performance (i.e Thrust coefficient, Torque coefficient & efficiency)	Indicative of a shift in propeller performance envelope and can be used to guide modifications towards optimal vessel operation.

historical data about the biofouling phenomenon [64], or on both [99]. According to what type of information is used to formulate the model, physical knowledge of the problem and/or collected historical data, the construction of the model changes. In particular, three different types of modelling approaches can be identified: Physical models (PMs), Data-driven models (DDMs), and Hybrid models (HMs). PMs are built based on a-priori, mechanistic knowledge of the real system (i.e., the numerical description of the biofouling growth and related added resistance) [98]. DDMs, instead, are built based on historical collections of observations of the vessel in operation (i.e., vessel speed, fuel consumption, delivered power, wind, waves, sea currents data), exploiting state-of-the-art Machine Learning (ML) techniques [64]. In the case of an HM, the PM and the DDM are combined to build models which use both a-priori physical information of the underlying phenomenon and historical data [100]. Figure 2.1 reports a graphical representation of these three modelling approaches and how they are built.

Since PMs are based on the knowledge of the physical laws governing the phenomenon, they can be very reliable. In fact, by construction, they only produce physically plausible predictions. The expected accuracy of the results grows with the increase of the detail in modelling the physical phenomenon [56]. However, usually, increasing the accuracy of PM results in quite a high request in terms of computational requirements [98]. This fact limits their use in the wild where substantial computational capabilities are seldom available [98].

DDMs, instead, do not require any a-priori knowledge of the physical system, but rather are built on historical data collected from the real system. They usually require a large amount

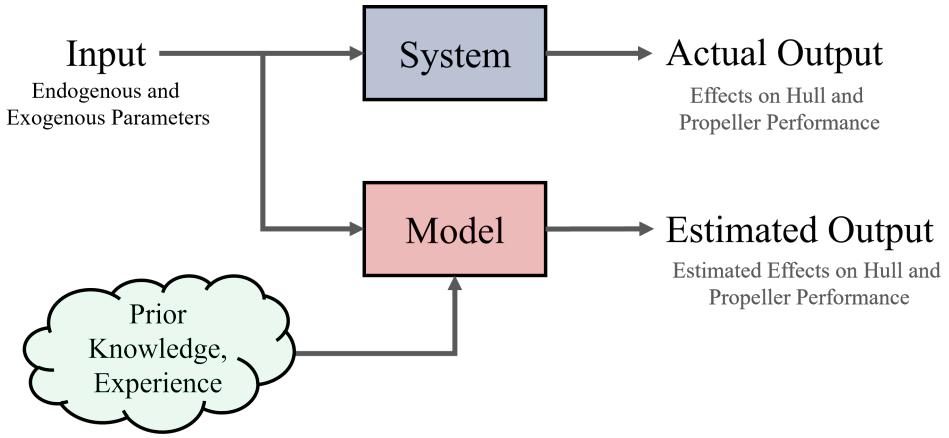

(a) Physical Models (PM)

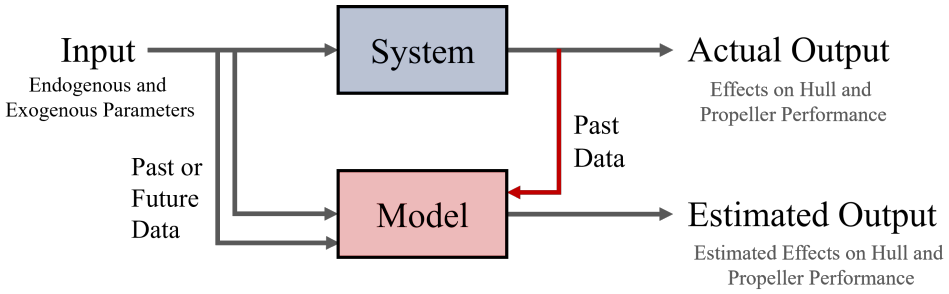

(b) Data-Driven Models (DDM)

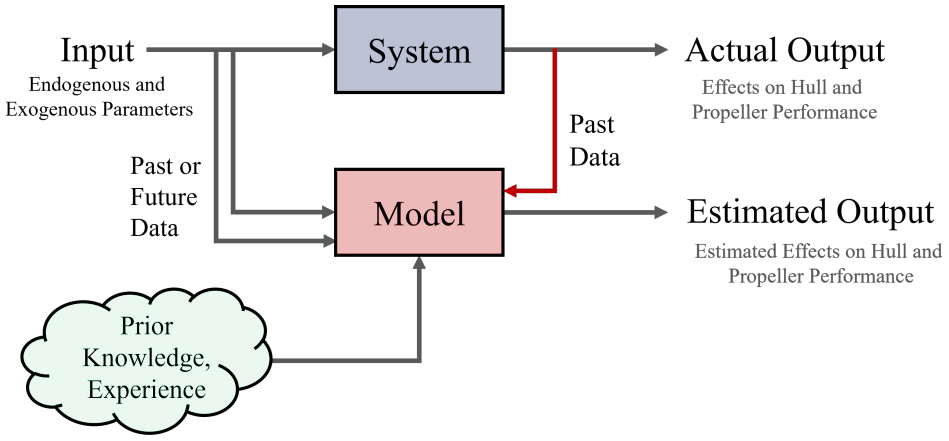

(c) Hybrid Models (HM)

Figure 2.1: The three performance modelling approaches

of data and a large amount of computational resources to be constructed (i.e., the learning phase) to reach a satisfying performance in terms of model accuracy [101]. Instead, once the model is constructed, its use for making predictions (i.e., the forward phase) is computationally inexpensive [102] and this has a big added value for DDMs as only the forward phase needs to be exploited in order to use them in operation. However, since they rely only on historical observations, DDMs work well in the statistical sense (i.e., on average), but they can produce implausible estimations (i.e., not physically plausible estimations) in particular situations [99].

HMs have been developed to fill the gaps of PMs and DDMs and develop models able to take the best of the two worlds [103]. HMs, in fact, can be able to: exploit the mechanistic knowledge of the system and avoid implausible predictions, reduce the computational requirements of a PM by exploiting historical data, and reduce DDMs' need for large amounts of historical data by starting from an already good approximation of the phenomenon provided by PMs [100].

Advantages and disadvantages of PMs, DDMs, and HMs for estimating the impact of biofouling on vessel's hull and propeller performance will be discussed in detail in the following sections, presenting and analysing examples of models proposed in the literature belonging to each one of these categories. For each example, the accuracy obtained by the model on real-word or synthetic data has been reported, if available.

2.5 Analytical Review

It is now hopefully clear why biofouling is so undesirable, not only does it affect the profitability/effectiveness of a vessel, but also negatively impacts the environment through increased GHG emissions and fouled ships endangering the biodiversity of the planet's oceans. The extent of these setbacks is so immense that it completely warrants research interest and the development of specialised tools, which can be used to minimise fouling's impact. The continuous progress of technology and, subsequently, simulation and analysis capabilities enable the creation of such decision support instruments. More particularly, the decision that owners and operators have to make on when to invest in cleaning their vessels is greatly important in

minimising the effects of fouling and needs to backed by a vigorous analysis of vessel performance. This, in combination with the rare situation that improvements in fouling management are beneficial in terms of both environmental and financial considerations, has resulted in the development of various methodologies for predicting the fouling state of ships and its effects on performance. The information that the latter provide is used to develop appropriate maintenance strategies, therefore, it is of great interest for players in the maritime sector and is highly valuable in terms of environmental preservation.

A long history of biofouling research has resulted in many excellent publications and analyses which utilise a wide array of approaches, some more successful than others. These can be grouped in terms of their underlying ideas into deterministic (also physical, first-principle, white box), data-driven (also black box), and hybrid (also grey box). Hybrid models are still in their infancy with only a limited number of implementations in research. As a result, when considering the evaluation of the hull & propeller's fouling condition and its effects, as far as the author is aware, grey box models have not yet seen adoption. While some of these methodologies consider their own real-world application and usefulness, many focus on bettering human understanding of the underlying variation in physical phenomena that can be observed as a result of the aspects of fouling. The latter are very insightful and vigorous in terms of their theoretical basis, however, more often than not are not applicable to dynamic on-the-go decision making and as such bring little value from a practical viewpoint. A review of the current state-of-the art is to follow. In this review, PMs, DDMs, and HMs proposed in literature for estimating the impact of biofouling on vessel's hull and propeller performance have been analysed. In particular, among the variety of methods proposed in the literature, the models presented in this work have been chosen to represent all the different approaches to the problem.

Methods to be presented for each category were selected according to these criteria: recently developed models (from 2015 to 2021) or models between 2000 and 2015 with at least 25 citations.

In the case of PMs, the most exploited and effective methods for predicting the hull and propeller's deterioration due to fouling are CFD models which incorporate fouling condition

specific roughness properties into the wall function of the CFD software [104, 58, 93, 97, 94, 50, 91, 34, 28]. Other commonly exploited models are based on Granville's boundary layer similarity law scaling [57, 33, 105, 62, 92, 53], which extrapolate flat plate experimental results into full-scale resistance and powering predictions for vessels.

In the case of DDMs, instead, the most exploited and effective methods for determining biofouling's impact on performance are based on artificial neural networks [43, 64, 95, 96, 26]. Additionally, classification methods based on neural networks are used to identify different levels of biofouling [106, 107] and biofouling species [108].

For what concerns HMs, this approach has been less investigated in the literature and no methods have so far been proposed for assessing biofouling's impact on the vessel's hull and propeller performances.

In the following sections, advantages and disadvantages of PMs, DDMs, and HMs and relevant examples have been analysed in detail. Moreover, for each class of models, tables have been reported summarising the following aspects (if available):

- Input data: the data that the models require to make the desired estimation;
- Data origin: synthetic data or real-world data collected during sea-trials or operations by on-board sensors or by exogenous sources;
- Amount of data: the amount of data exploited to build and validate the models;
- Method: the technique used by the models to predict the output;
- Output: what parameter(s) the model actually estimates;
- Accuracy: the accuracy obtained by the models;

A section is also dedicated to show how, in some cases, PMs have been translated into industry standards (Section 2.5.2). Physical models have been around the longest, therefore they are considered by actors in Maritime to be more robust and trustworthy [98].

2.5.1 Physical Models

PMs are the most well-established numerical approach when it comes to assessing the biofouling state [89]. PMs, as already explained before, rely on the a-priori physical knowledge of the

phenomenon and are built upon a set of governing laws and assumptions [98]. The complexity, the accuracy, and the computational requirements of a PM vary by adding or removing some assumptions [56]. To model the hydrodynamic performance of a ship and then quantify the negative impact of the different stages of the biofouling, PMs estimate the total resistance of a vessel or its different components (i.e. wind, waves, currents, and sometimes the rudder effect) through experiment and simulation [15]. As PMs are the most popular numerical approach, many exist in literature with different levels of complexity.

Among PMs, Experimental Fluid Dynamics (EFD) represents the baseline for biofouling state estimation. EFD consists of conducting experiments in a controlled test environment, such as towing tanks and cavitation tunnels, with the goal of quantifying a target effect on hydrodynamic performance [98]. There is a long history of research utilising such techniques, which is well described by Demirel et al. [62] who utilise a series of towing tests on flat plates using artificial 3D printed barnacles to determine the effects of barnacle height and coverage on vessel resistance and powering. The main drawback of EFD is their high associated costs and the limitation to specific experimental conditions. It is both time and cost intensive to conduct a rigorous experimental procedure which covers many operational scenarios [98]. Moreover, experimental facilities often are not suitable for full-scale testing, limiting EFD to model scale and leading to results often being extrapolated to full-scale for further analysis. For example, for the analysis of biofouling's impact on vessel performance, the Granville's similarity law scaling procedure [109, 110] is often used to translate laboratory-scale results into a prediction of the impact of fouling. This procedure was first introduced by Schultz [63, 57] and it has been employed extensively in research even since [33, 105, 62, 92, 53, 91]. Ultimately, EFD is not often used on its own to determine fouling effects, but rather as a source of information employed in more advanced PMs [53, 50, 57, 58, 62, 63, 92, 56].

Another approach, an alternative to EFD, to determine biofouling's impact on ship performance, involves estimating the total resistance and then correcting for its various components which allows the isolation of fouling's contribution [15]. This estimation has often been performed with resistance modelling methods [89, 15], which were originally developed by

Todd [111]. A collection of separate empirical and non-empirical methods for each resistance component can be exploited [89, 43]. A good example is the work by Foteinos et al. [42], where an engine model in the MOTHER software is first calibrated according to shop test and sea trial reports and then used to estimate total ship resistance; empirical formulae are used to determine calm water resistance, air resistance, and wave-added resistance, which are then subtracted from the total ship resistance to obtain the contribution of hull & propeller fouling. Researchers include different levels of detail in their decomposition of total resistance [89]. For example, Carchen et al. [98] developed a real-time biofouling impact monitoring system on the basis of automatic data collection and resistance modelling. The authors considered not only the wind, wave, and calm water resistance (which are usually taken into account [42]) but also the steering and shallow water effects. Resistance modelling is based on a-priori physical knowledge and, therefore, results in only physically plausible results. However, these results are often inaccurate, partially due to a need for estimating several unknown friction-related coefficients [43].

The state-of-the-art PMs are surely the ones based on CFD, which often replace or supplement EFD and resistance modelling [98]. CFD demonstrate high accuracy using computers to solve complex Navier-Stokes equations describing fluid flow. However, CFD are very computationally expensive when compared to other methods [26]. Similar to EFD methods, CFD simulations are confined to the analysis of a single flow or operational condition at a time, which limits their practical real-time applicability [98]. Nonetheless, a large body of research relies on CFD to measure biofouling impact [50, 28, 34, 58, 56, 91, 93, 94, 104, 97]. The CFD approach to estimating the biofuling state is to consider increases in the vessel's surface roughness due to specific biofouling conditions and incorporate these in the wall function by means of appropriate roughness functions [57]. The specific roughness functions are usually determined using experimental methods [63]. Additionally, data collected from EFD is used to validate this type of PMs [104, 58, 93, 97, 50, 91, 28, 34].

PMs are quite useful not only to get an estimation of the biofouling state but also to gain a better understanding of the hydrodynamic behaviour of fouled vessels and surfaces [88]. How-

ever, even nowadays, there are still specific physical phenomena which cannot be easily modelled through PMs [112]. Consequently, in realistic scenarios, PMs often lack in accuracy or are too computationally demanding.

For a more precise view of the current state-of-the-art approaches, Table 2.4 summarises the most relevant contributions in the field of PMs for biofouling state estimation.

Table 2.4: Summary of PMs for monitoring and evaluating the biofouling state and effects on vessels' hull and propeller performance

Ref.	Method	Input data	Data origin	Amount of data	Output	Accuracy
[57, 33]	Granville's similarity law analysis based on laboratory-scale experimental results.	Fouling condition and antifouling paint specific roughness functions, vessel geometry & particulars.	Experiment derived roughness functions.	Roughness functions for 7 surface conditions.	Predictions of full-scale ship resistance and powering for a range of fouling conditions and roughness.	Extrapolated full-scale results are compared with trial results for similar hull forms: Reference values of 24% and 8%, compared to extrapolated results of $22-32\%$ and 9%.
[89]	Propeller power absorption technique which uses the propeller as an instrument to estimate speed or power.	Propeller particulars, ship performance data.	Automated data acquisition systems installed on-board.	After filtering, 3326 entries were used.	Power increase and/or speed loss due to fouling.	Average speed and shaft horsepower absolute errors of 1.8% and 0.9% respectively.
[42]	Shaft torque prediction through an engine simulation software fed with recorded engine data, coupled with resistance modelling	Engine shop test data, sea trial reports, performance reports, noon reports, engine and vessel geometry	Real-world engine & vessel trial and operation.	Four Panamax vessels' operational data.	Estimation of resistance due to fouling through increases in the Propeller Law and Fouling Resistance coefficients.	Results with more than 5% deviation from sea trials were discarded from analysis.
[105, 62]	Granville's similarity law analysis based on a series of flat plate towing tests for different artificial barnacle heights & coverage.	Barnacle size and coverage values.	3-D scans of actual barnacles.	10 different combinations of barnacle size and coverage.	Added resistance diagrams are plotted using predictions of added resistance and the effective power of ships for varying barnacle fouling conditions.	Uncertainties estimated through repeatability tests based on a procedure defined by the ITTC: Friction coefficient uncertainty below 4%; Roughness function uncertainty was mostly under $+/-6\%$, however, for small barnacles it was below 28%.

[92]	A prediction code based on Granville's similarity law is used to predict the effects of different fouling states.	Roughness height, roughness functions, corresponding roughness Reynolds numbers and desired ship lengths.	Experiment derived roughness functions from [57].	Roughness functions for 7 surface conditions.	Frictional resistance coefficient values which are used to generate added resistance diagrams for the prediction of increases in frictional resistance coefficients and effective power of ships due to a range of surface conditions.	The authors provide no information on the accuracy of the used method.
[98, 88]	A ship performance monitoring system based on real-life data collection and resistance modelling.	Time, SoG, Course over Ground, Heading, SoW, Propeller speed, Propeller Torque, Propeller Thrust, Rudder angle, Wind speed, Wind direction, Wave amplitude, Wave spectrum, Wave properties	Automatic on-board monitoring system.	Data from sea trials and normal service with 1 Hz sampling frequency.	Normalised delivered power, apparent wake fraction, effective wake fraction, fouling coefficient, and change in frictional resistance coefficient	The authors present no validation study, which would give indication into the accuracy of their method.
[53]	A time-dependent biofouling growth model based on field test data coupled with a frictional resistance and powering prediction model based on Granville's similarity law.	Vessel idle time, field test data for AF coatings, water temperature, biofouling condition specific roughness functions & ship particulars.	Static field tests from a paint company.	Test from one to three years in two regions.	Fouling Rating, calcareous fouling surface coverage, percentage increase in frictional resistance & percentage increase of effective power.	Following the validation of their model, the authors conducted a case study in which the model committed a 4% error when estimating the increase of effective power due to fouling.

[104]	CFD implementation utilising biofouling state specific roughness functions.	Fouling conditions' specific roughness functions, geometry and particulars of KCS hull.	Experiment derived roughness functions from [62].	Roughness functions for 10 fouling conditions.	Fouling effects on the resistance components, form factors, wake fractions and flow characteristics.	Verification study based on grid convergence index (GCI) method: GCIs under 1%. As part of a validation study, the modified wall-function results from CFD were compared with experimental results, however, the exact values for committed errors are not given.
[58]	CFD implementation utilising biofouling state specific roughness functions.	Fouling conditions' specific roughness functions, geometry and particulars of KCS and KVLCC2 hulls.	Experiment derived roughness functions from [62].	Roughness functions for 3 surface conditions.	Fouling effects on the resistance components, form factors, wake fractions and flow characteristics.	Verification study based on grid convergence index (GCI) method: GCIs under 1%. Validation study by comparison with experimental results: observed errors are within 5% of reference values.
[93]	CFD implementation utilising biofouling state specific roughness functions.	Fouling conditions' specific roughness functions, geometry and particulars of the KP 505 propeller and the KCS hull.	Experiment derived roughness functions from [62].	Roughness functions for 10 surface conditions.	Effects of fouling on full-scale ship resistance and powering, as well as flow characteristics.	Verification study based on grid convergence index (GCI) method: GCIs under 0.1%. Validation study by comparison with experimental results: observed errors are within 5.5% of reference values.
[97]	CFD implementation at full-scale utilising biofouling state specific roughness functions.	Fouling conditions' specific roughness functions, full-scale KP505 propeller geometry and particulars	Experiment derived roughness functions from [62].	Roughness functions for 10 surface conditions.	Propeller open water performance (i.e., Thrust coefficient, Torque coefficient and open-water efficiency)	Verification study based on grid convergence index (GCI) method: GCIs under 1%. As part of a validation study, the results from CFD were compared with experimental results, however, the exact values for committed errors are not given.

[94]	A validated RANS solver (OpenFOAM) utilised according to experimentally investigated surface roughness properties.	Fouling conditions' & hull coatings' specific roughness functions, geometry and particulars of the KCS hull.	Experiment derived roughness functions.	Experiments for 4 marine coatings.	Impact of fouling on ship total resistance and frictional resistance.	Verification study based on grid convergence index (GCI) and correction factor (CF) methods: GCIs and CFs around 10%. Validation study by comparison with synthetic CFD results from [104]: average deviation of 5% for drag coefficient and 5% for frictional resistance coefficient.
[50]	CFD implementation utilising biofouling state specific roughness functions.	Fouling conditions' specific roughness functions, geometry and particulars of the KP 505 propeller and KCS hull.	Experiment derived roughness functions from [113, 114].	Roughness functions for 8 surface conditions.	Impact of biofilm on ship propulsion characteristics.	Verification study based on grid convergence index (GCI) method: GCIs under 3.5%. Validation study by comparison with experimental results: observed errors are within $+/-6\%$ of reference values.
[91]	The ITTC 1978 Performance Prediction Method is modified by incorporating Granville's similarity law scaling in combination with CFD.	Roughness functions, vessel geometry and particulars, results from towing tank experiments.	Experiment derived roughness functions from [113].	Roughness functions for 8 surface conditions.	Impact of fouling on ship resistance and propulsion characteristics.	Verification study based on grid convergence index (GCI) method: GCIs under 4.9%. Validation study by comparison with experimental results: observed errors are within 4.2% of reference values.
[34]	CFD implementation utilising biofouling state specific roughness functions.	Fouling conditions' specific roughness functions, geometry and particulars of WB, KP505 & KP458 propellers	Experiment derived roughness functions from [113, 63].	Roughness functions for 14 surface conditions.	Open water performance (i.e., Thrust coefficient, Torque coefficient and open-water efficiency) of propellers	Verification study based on grid convergence index (GCI) method: GCIs under 5%. Validation study by comparison with experimental results: observed errors are within 2.7%, 2.5%, and 5.4% of reference values for WB, KP505 & KP458 respectively.

[28]	CFD implementation utilising biofouling state specific roughness functions.	Fouling conditions' specific roughness functions, geometry and particulars of KCS, KVLCC2 & BC hulls	Experiment derived roughness functions from [113].	Roughness functions for 8 surface conditions.	Impact of fouling on ship resistance and propulsion characteristics.	Verification study based on grid convergence index (GCI) method: GCIs under 4.2%. Validation study by comparison with experimental results: observed errors are within 2.1%, 4.2%, and 2.6% of reference values for KCS, KVLCC2 & BC respectively.

2.5.2 Industry Standards

The current industry standard for estimating changes in ship hull and propeller performance consists of applying the ISO 19030 developed by the International Organisation for Standardisation (ISO). The aim of the ISO 19030 is to prescribe practical methods for measuring changes in ship specific hull and propeller performance and to define a set of relevant performance indicators for hull and propeller maintenance, repair, and retrofit activities [84]. The ISO 1903 consists of three parts:

1. an explanation of the general principles that are adopted [84];
2. a description of the default and most accurate method that can be applied for determining metrics for changes in hull and propeller performance [85];
3. a set of alternative methods that can be used in case the default procedure cannot be adopted [86], enhancing the range of applicability of the standard.

ISO 19030 has been identified as a good starting point for vessel owners and operators to track hull and propeller performance, considering the previous lack of an official standard [49]. However, it has received criticism for its underlying methods [115], e.g., the suggested corrections and filtering procedure [64, 50] and its performance assessment [116]. In fact, most performance monitoring approaches utilise a reference condition, which is then compared to real-time performance to determine any noticeable shifts [115]. However, these corrections are often done through simplistic methods with narrow ranges of applicability which demonstrate inaccurate results. The ISO 19030 is no different as it requires filtering out of operating points that are outside of the applicability of the methods' assumptions [64]. While the ISO 19030 standard is considered a positive step forward from previously non-existent official guidance to hull and propeller monitoring, it is still affected by issues which have not yet been resolved [116].

2.5.3 Data-Driven Models

In recent years, DDMs have been growing in popularity in the field of ship performance modelling [117]. Unlike PMs, they do not require any a-priory knowledge about the underlying physical principles [64]. In the field of biofouling, DDMs are built by applying predictive ML algorithms on historical data, collected from automatic on-board data logging systems [64, 83, 96], noon reports [118, 15], and vessel inspections and surveys [107]. Generally, the main limitations of DDMs are the need for high quantity and quality data [11] and their possible lack of physical meaning [99]. Nevertheless, DDMs can account for many ship-specific and environmental phenomena, that might be difficult, or even impossible, to model with PMs [64], with very limited computational overhead.

DDMs have been successful and have increasingly received the attention of researchers and the Maritime industry because modern on-board equipment is capable of recording and storing large amounts of good quality historical data [96]. In fact, advanced data logging systems are nowadays a standard in newbuilds, as well as being conveniently installed during the retrofitting of older vessels [76]. This trend is expected to continue in the future [39].

Research that exploits DDMs for biofouling state estimation is still in its infancy and a limited number of works are available in the literature. Nonetheless, DDMs have already showed promising results when compared to PMs [43, 118] and the ISO 19030 standard [64].

DDMs, in fact, can also easily leverage on structured information like images and videos [119] to better estimate the biofouling state. For example, Wang et al. [106] were able to accurately classify fouling conditions through image recognition techniques, combined with an Artificial Neural Network. Due to an excellent accuracy, despite using research-tailored input images, they argue that manual underwater surveys could be replaced with artificial methods. Bloomfield et al. [107], similarly to Wang et al. [106], leveraged on Convolutional Artificial Neural Networks to classify underwater survey images of a vessel's hull according to a tiered fouling level framework. The achieved accuracy is shown to be very close to expert agreement rates on a sub-sample of the used image library. Chin et al. [108] collected an image database containing

entries for 10 common fouling species from internet sources and used it in combination with an image processing technique to train a Convolutional Artificial Neural Network. The latter is then used to classify biofouling according to species that are present and fouling density.

Apart from DDMs which leverage on images of the hull, other methods can be used to determine the biofouling state. For example, Coraddu et al. [83], utilising just a set of real data collected on-board from a real vessel, developed an unsupervised DDM based on outlier detection ML algorithms to estimate the hull and propeller biofouling condition. Through a rigorous and statistically robust approach, using as little as 10 manually labelled samples, a very high accuracy is achieved. In fact, the research by Coraddu et al. [83] demonstrates that DDMs can be effective without using very large historical datasets, which is the common opinion.

Even though having an indication of a vessel's biofouling state is valuable for maintenance-related planning and decision making processes, being able to evaluate the exact impact that biofouling has on performance is surely much more valuable [84]. In this context, DDMs have shown a very high potential and effectiveness in many studies. For example, Coraddu et al. [64] proposed DDMs based on deep learning models able to quantify the speed loss due to biofouling in real-time by using just data coming from the vessel's on-board monitoring systems. The developed DDMs show to outperform the state-of-the-art ISO 19030 industry standard, providing more reliable and actionable results. Other DDMs have also been developed to determine speed loss due to biofouling [90].

Apart from using a speed loss prediction as proxy for the biofouling state estimation, the most popular performance metric in terms of quantifying biofouling is shaft power [43, 118, 95, 96, 26]. Recently, Laurie et al. [96] employed and compared a set of ML techniques (i.e. linear regression, decision tree, k-nearest neighbours, artificial neural networks, and random forest) when predicting the shaft power of a fouled vessel. Considering the complex nature of biofouling phenomena, a very high prediction accuracy (errors below 2%) was observed for some of the statistical methods. In fact, DDMs can accurately estimate vessel performance in a broad range of operating conditions because they are built on historical data, as opposed to the majority of PMs.

Another aspect that needs to be carefully taken into account when estimating the biofouling state is the impact of hull and propellers cleaning. For example, Adland et al. [15] investigated the impact of hull and propeller cleaning on vessel performance. In particular, they proposed a DDM capable of determining the performance impact of the underwater cleaning and the dry-docking of a vessel. To asses the validity of the proposal, the authors rely on a dataset of daily noon reports combined with a historical log of cleaning instances.

For a more precise view of the current state-of-the-art approaches, Table 2.5 summarises the most relevant contributions in the field of DDMs for biofouling state estimation.

Table 2.5: Summary of DDMs for monitoring and evaluating the biofouling state and effects on vessels' hull and propeller performance

Ref.	Method	Input data	Data origin	Amount of data	Output	Accuracy
[108]	Convolutional Neural Network paired with OpenCV image processing.	A database of images of different fouling organisms and fouling density.	Internet.	1825 images of 10 common fouling species.	Classification of the fouling species and density of fouling.	Mean classification accuracy of 74.75% & standard deviation of 7.92%. No model accuracy is provided for determining fouling density.
[83]	One-Class Support Vector Machines and Global k-Nearest Neighbour methods for outlier detection.	A featureset, comprised of measured values from the ship monitoring systems and wave buoy data.	On-board monitoring systems & wave buoys.	39(+10) features, unspecified number of samples.	Hull and propeller fouling is identified and labelled.	Even with as little as 10 labelled samples, the proposed model has impressive accuracy when classifying whether the ship is fouled, achieving 0.04+/-0.001 Average Misclassification Rate.
[107]	Convolutional Neural Network.	A dataset of underwater images of ship hulls, labelled according to their Simplified Level of Fouling (SLoF).	In-water surveys of around 300 vessels.	10263 images with SLoF labels.	Estimates for SLoF based on input image.	Mean average precision of 0.796, standard deviation of 0.023.
[15]	Before-after and difference-in-differences estimators.	A dataset consisting of daily vessel parameter measurements, combined with a historical log of hull & propeller cleanings.	Daily noon reports & maintenance logs.	7868 daily observations after data cleaning & 28 maintenance activities.	Impact of hull & propeller cleaning activities on the average fuel consumption of examined vessels.	The proposed procedure is applied at an arbitrary point in time, instead of the time of a known cleaning for validation. This is repeated 1000 times and the results indicate an encouraging 0.002%+/-0.086% average change in fuel consumption at these arbitrary points.

[43]	Artificial Neural Network.	A dataset comprised of measured values from the ship monitoring system.	On-board monitoring.	4 8-feature datasets, consisting of a total 679 10-minute averages.	A 10-minute average propulsion power estimate.	A 2.7% cross-validation error is reported, however, there is no indication of its interval of confidence. Also, there is no unbiased test of the model where a set of data, omitted in training and validation, is used.
[64]	Deep Extreme Learning Machine.	A dataset comprised of measured parameters from the ship's monitoring system, combined with a historical log of hull & propeller cleanings.	Data logging systems & maintenance logs of two Handymax tankers.	15 minute averages over nearly 5 years for 17 features & 9 cleaning events.	Speed through Water & speed loss percentage, as well as estimates for timing of maintenance activities	The proposed method shows a higher level of reliability when compared to the state-of-the-art ISO 19030 industrial standard. Additionally, all changes corresponding to a cleaning event are detectable. No indication of accuracy of the DELM when predicting Speed through Water.
[95]	Artificial Neural Network	A featureset, comprised of measured parameters from a ship's monitoring system, as well as environmental features.	VLCC automatic monitoring system.	11 features, unspecified number of samples.	Shaft power estimate.	Graphs on the error distribution are provided, however, authors provide no indication on which the final selected model is and its exact accuracy.
[90]	Curve fitting and Detrended Fluctuation Analysis (DFA)	Two datasets, collected 9 months apart, that include ship speed, propulsion power, fuel consumption, generated power, battery power, aft & fore draught.	Alarm monitoring system of an electric ferry.	A week of data at the start & one after 9 months (1 sample per minute).	Speed loss estimate after 9 months of operation.	Only Motor power vs Vessel speed curve fitting accuracy is provided: best fit R-square & RMSE - 0.9999 & 0.07248 before and 0.9999 & 0.05637 after 9 months.

[96]	Multiple Linear Regression, Decision Tree (AdaBoost), KNN, ANN and Random Forest.	A dataset from a ship's monitoring system, expanded through artificial feature generation and additional wave information.	On-board automatic ship monitoring & CMEMS.	20 features with 10571 entries after cleaning.	Shaft power.	MAPEs & RMSPE: Multiple Linear Regression - 6.453% 0.0930%, Decision Tree - 6.987% 0.0932%, KNN - 1.245% 0.0302%, ANN - 1.893% 0.0317% and Random Forest - 1.171% 0.0264%.
[26]	Artificial Neural Network	A dataset from a ship's monitoring system, expanded through artificial feature generation.	Container ship continuous monitoring system.	14 (+5) features - 1 minute samples over 19 months.	Main Engine Fuel Oil Consumption (t/24hr) or Shaft Power (kW) estimate.	RMSE & R-square for Fuel Consumption - 0.78 & 0.998 with and 0.96 & 0.997 without fouling feature. RMSE & R-square for Shaft Power - 132.07 & 0.999 with and 203.19 & 0.997 without fouling feature.

2.5.4 Hybrid Models

HMs are a hybridisation between PMs and DDMs. In a HM, the PM and the DDM are combined to build a model which uses both a-priory physical information for the underlying phenomenon as well as historical data [98]. For example, the prediction of a PM can be used as an initial estimate to feed into a DDM [99]. HMs aim to address the main setbacks of PMs (i.e., computational requirements and accuracy) and DDMs (i.e., possible lack of a physical interpretation and need for large amount of data).

By looking at the literature, no applications of HMs to biofouling have yet been proposed and this represents a clear research gap. In fact, there is an opportunity to utilise the large amount of high-quality PMs in literature to supplement DDMs. A simple combination of state-of-the-art approaches may result in an HM able to outperform the original model in terms of accuracy, computational complexity, data requirements, and physical interpretability. In fact, HMs have shown their potential within other niches of vessel performance modelling with favourable results [100]: Leifsson et al. [103] successfully utilised a HM, which outperformed both a PM and a DDM, for predicting vessel speed and fuel consumption in the scope of vessel operational optimisation; Similarly, Coraddu et al. [101] compare the performance of PMs, DDMs and HMs in predicting the fuel consumption of a vessel in a real scenario and conclude that HMs improve upon the accuracy of PMs and the data requirements of DDMs; Additionally, in [11], Coraddu et al. utilise the latter to effectively optimise vessel trim in real operational conditions; Swider et al. [120] look into the complementarity potential between PMs and DDMs and reach encouraging conclusions, which are supplemented by an example application of an HM for predicting the speed/power of an offshore vessel; Coraddu et al. [121] utilise a HM to accurately predict engine temperatures during operational dynamic manoeuvring based on engine models and engine measurements for a Holland class patrol vessel and show that, for this, a hybrid approach greatly outperforms a DDM; Yang et al. [122] use real operational data from a crude oil tanker over a 7-year sailing period to demonstrate the accuracy and reliability of a genetic algorithm-based HM in predicting vessel fuel consumption; Montewka et al. [112] suc-

cessfully incorporate the use of a HM for evaluating ship performance in ice-covered water in a route planning methodology for an ice going bulk carrier; Liu et al. [123] build a digital twin based on a HM which provides a satisfying prediction of ship speed and fuel consumption and demonstrate the application effects of the HM through an arrival time forecast and a weather routing showcase; Finally, Coraddu et al. [99] combine PMs and DDMs to build a fast, accurate, and physically grounded model that can be used for real-time prediction of engine performance parameters in dynamic conditions in order to identify emerging failures early on and establish trends in performance reduction.

2.6 Open Problems and Future Perspectives

After providing a complete review of the numerical methods for monitoring and evaluating the biofouling state and effects on vessels' hull and propeller performance in Section 2.5, the current section summarises the open problems and future perspectives of this field of research.

For what concerns the open problems, there are at least two main aspects that are worth discussing. Firstly, regardless of the numerical methods adopted, filtering out unfavourable exogenous factors which might alter the biofouling state estimation and the effect of the environmental conditions is of great importance. In this respect, robust filtering and outlier detection procedures should be carried out to feed the PMs, DDMs, or HMs with reliable data. Secondly, some of the proposed approaches are computationally expensive which might prevent their use in real-time for maintenance-related decision making processes. Although DDMs can be considered computationally inexpensive in the forward phase, the training phase (to build or update the model) can be quite taxing (especially if this phase is performed on-board). Moreover, the additional burden of detecting and filtering outliers has to be accounted for real-time applications. For this reason, researchers should focus their attention on the development of numerical frameworks which also take into account computational burden.

Focusing our attention on the future, the author foresees a wider use of hybridisation techniques for biofouling assessment. As reported in Section 2.5.4, to the best of the author's

knowledge, no applications of HMs to biofouling have yet been proposed. Leveraging on state-of-the-art PMs, in the upcoming years, researchers have the unique opportunity to exploit the on-board operational data to develop HMs for a more accurate, reliable, computationally inexpensive, and physically grounded biofouling state assessment. In fact, HMs have the potential to offer the accuracy, speed, and flexibility of data-driven approaches, while maintaining some physical knowledge of the problem through simplistic PMs, making them an ideal candidate for supporting real-world maintenance strategies. For this reason, the development of HMs could unlock the continuous real-time evaluation of the hull and propeller status, enabling shipowners and operators to select the optimal trade-off between cleaning costs and increased fuel consumption due to biofouling. While adopting HMs for biofouling state and effects estimation is surely a new field for future research, there is still space for improvement for the current approaches. For example, the effects of exogenous factors are not accurately represented by PMs, resorting to simple filtering procedures of the unmodeled conditions. DDMs, by construction, can handle this condition by simply considering these exogenous factors in the data collection, nevertheless this requires a large amount of historical data to sample all conditions that the model needs to learn. For this reason, the development and implementation of more and more advanced data logging and storing systems over the entire global fleet (newbuilds and retro-fittings) is becoming essential. Finally, given the relevance of the topic and its impact on the global shipping footprint, there is a need for an update of the current industry standard to reflect the state-of-the-art in monitoring capabilities providing enhanced and certified numerical procedures for biofouling state assessment.

2.7 Chapter Conclusion

The scope of this section was to review the numerical methods for monitoring and evaluating the biofouling state and effects on vessels' hull and propeller performance. For this reason, the problem of biofouling was first described, its impact on performance, which is summarised in Table 2.1, and gave insight into the preliminary steps in biofouling related performance mod-

elling such as data acquisition, ideal parameter requirements, listed in Table 2.2, and desired outputs for impact estimation, summarised in Table 2.3. The above was then followed by a critical review of approaches to biofouling state and effects estimation. In particular, the approaches were grouped into three families of numerical methods, i.e., PMs, DDMs, and HMs, and analysed them from a practical real-world view point. For each family, strengths and weaknesses were discussed, as well as reviewing the most important approaches that exist in literature and listed these approaches in Table 2.4 for PMs and Table 2.5 for DDMs. In short, PMs are based fully on the physical knowledge of the phenomena (providing also the ground for the current industrial standards); DDMs fully rely on historical data to learn the desired model; while HMs are able to exploit both sources of information. Summary tables were created as an additional supplement to the review. Finally, the current open problems and future direction of this important field of research were expanded on.

In summary, PMs have, so far, been the standard approach to biofouling analysis and can achieve good prediction accuracy, however, this is achieved at the expense of an increased requirement for computational resources that prevent their use in real-time applications. DDMs, instead, have the advantage of providing a more accurate near real-time prediction at the cost of a computational expensive training phase. Unfortunately, DDMs can, in some cases, provide results that are not physically plausible due to their statistical nature, however, they have been observed to work well on average For this reason, HMs, which are able to take the best from PMs and DDMs, can potentially offer the optimum solution as they are able to deliver physically plausible results in near real-time. Nevertheless, at the time of writing, HMs have not yet been employed or sufficiently investigated for the specific application of biofouling state and effect estimation.

3 Research Idea, Aims & Objectives

The critical review, performed in Chapter 2, categorises the currently existing numerical methods for modelling the effects of biofouling on ship performance. While both Physical Models and Data-Driven Models have been employed extensively, the more novel field of hybrid modelling has not been explored in the field of biofouling.

As discussed in Section 2.5.4, Hybrid Models have successfully been used for performance modelling of other subjects in Maritime, where they most often exhibit better performance than purely Physical or Data-Driven methods. Therefore, there is a potential to reduce the data requirements of biofouling impact estimation DDMs, while also incorporating much needed physical knowledge into their methodology, allowing the resulting HMs to be used in real-time applications, and in a decision-support role for biofouling management maintenance strategies. Consequently, a hybrid methodology was identified as a plausible step forward in improving the current state-of-the-art in modelling biofouling's effect on vessels.

Further considerations are also important and can bring value to the research project. Robust pre-processing might facilitate better numerical performance, as well as filtering out exogenous factors that contribute to sensory noise. While hybridisation could prove to better model accuracy and lower data requirements, it is also important to determine the exact benefits of a 'physically-grounded' hybrid approach. Whether these are accuracy-based and become apparent when the hybrid model is used to evaluate vessel performance trends, or whether just the act of embedding physical methods into a data-driven approach brings a higher degree of trustworthiness to the methodology is to be determined.

Considering all of the above, the main Aim of the current thesis is to combine state-of-the-art

approaches from Machine Learning and Marine Engineering and develop hybridised decision-support tools for supplementing predictive maintenance strategies. This aim is achieved through specific objectives that also attempt to rectify current research gaps:

- To critically review the literature on current state-of-the-art practice in terms of vessel biofouling monitoring in order to determine research gaps and opportunities for research.;
- To utilise robust data pre-processing & filtering approaches in order to optimise numerical model performance.;
- To create a state-of-the-art Data-Driven Model based on vessel operational data in order to estimate biofouling-related performance drops in real-time.;
- To identify and employ suitable Physical Models in order to expand a sensory dataset from an on-board automatic monitoring system by adding additional features.;
- To create an advanced hybrid model for predicting biofouling effects on ship performance in real-time by combining the previously developed Data-Driven Model with the pre-processed dataset, expanded through Physical Modelling, in order to improve numerical model performance.;
- To validate the real-time hybrid model against the current state-of-the-art i.e., current industry standard (i.e. ISO19030), as well as the pre-hybridisation data-driven methodology.
- To demonstrate how the models can be used as a decision-support tool, part of a holistic biofouling management plan based on current and past vessel performance.

4 Methodology

The current chapter describes the development of a hybrid modelling methodology which attempts to predict the effect biofouling has on a vessel's performance. This has been based on the critical analysis of existing research in the field, conducted in Chapter 2. A description of the available real-word data, and how it has been cleaned and pre-processed for use in the various developed models in Section 4.2, is followed by a breakdown of current industrial best practice in terms of biofouling impact estimation, i.e. ISO19030 in Section 4.3. Further in Section 4.4, the processed dataset is used to develop a set of Data-driven models, based on various Machine Learning algorithms, ranging from simple methods such as Regularised Least Squares (RLS) to more sophisticated approaches such as Random Forest (RF) and Artificial Neural Networks (ANN). Section 4.5 provides a description of the physical knowledge that can be extracted from the available information about the subject vessel through first-principle methods, as well as the author's approach in doing so. Additionally, some further feature engineering is applied in an attempt to incorporate existing knowledge into the methodology in Section 4.6. Finally, through incorporating the simple but valuable physical models that have been constructed into the data-driven framework, Section 4.7 outlines the resulting hybrid methodology that is the main outcome of the current research project. The chapter is then concluded in Section 4.9, following an analysis of the performance of Data-driven & Hybrid models demonstrate when trying to predict a certain vessel Key Performance Indicator (KPI) in Section 4.8, which can then be studied to evaluate the impact of biofouling.

Further chapters utilise the state-of-the-art hybrid methodology in a realistic case study with the aim of providing the reader with an understanding of how the former can be used in a

practical environment. While these further sections of the report contain their own detailed methodology, in order to provide the reader with a better understanding of the overall process followed within this research project, a holistic view over the entire project's methodology is provided visually in Figure 4.1.

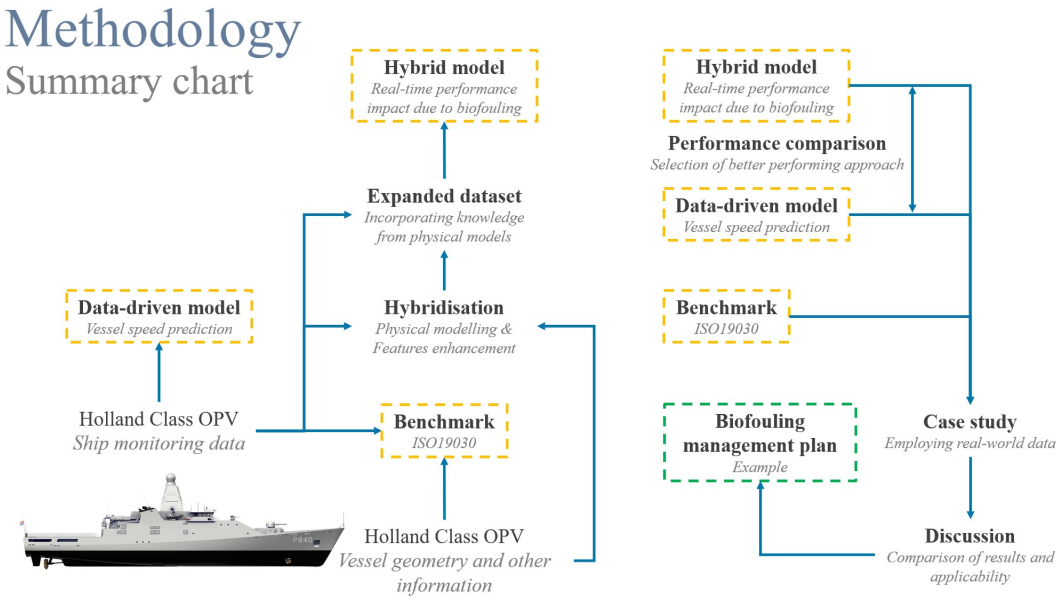

Figure 4.1: Project Methodology Flow Chart

4.1 Data Description

Both Data-driven and Hybrid models have a high reliance on data quality in achieving good performance, therefore, it is essential for a methodology that evaluates vessel performance and relies on DDMs and HMs to do so, to be built upon a robust dataset. Furthermore, the latter needs to be expansive enough so as to successfully capture a sufficient, for the purposes of the current project, amount of data on the different environments and settings that a vessel operates within.

The current work utilises a set of high-quality data for a medium-sized craft, which contains over 70 features. These features range from indicators of the environmental conditions surrounding the vessel, to readings of the various settings of her propulsion systems and their

performance. Table 4.1 lists all of the relevant features which have been used in model development further in the current work. The different Machine Learning algorithms, described in Section 4.4, each employ a selection strategy to select the optimal subset of features with the best results.

The dataset spans over 2 years, however, due to a substantial gap after only a few months in the beginning of that period, a subset is used here, covering approximately a year of operation. The vessel is cleaned prior to this period, therefore, the beginning of the data subset has been assumed as representative of a clean-hull condition. While this is only an approximation due to the high speed of fouling development, in the context of the observed time frame, the initial period is undeniably going to be the 'cleanest' state for the hull & propellers, assuming no underwater cleaning has been conducted. Because the utilised data begins months after the ship was drydocked, at the start of the recorded period, a biofilm would have already been formed and would be impacting her performance in open water. Unfortunately, the industrial partner that kindly provided the sensory dataset had also not kept record of underwater cleaning activities conducted when the vessel was at port. However, it was noted that even if underwater cleaning had occurred, it would have been infrequent and low-scale, therefore, the expectation is that the biofouling levels of the underwater hull & propellers continuously increased within the year. Whether or not the above assumptions is correct will undoubtedly become apparent further in this work.

A relatively high granularity exists within the dataset with a data point every 3 seconds in the vessel's operating periods. This high frequency of the automatic ship monitoring system and the expansiveness of the produced dataset allows the capture of information on various environmental & operational phenomena, that are too rapidly occurring and, therefore, too short-lived to be otherwise captured. As previously mentioned in Chapter 2, this is a common problem within the field of biofouling performance estimation, where researchers have had to base their novel methods on subpar datasets, which often only include a few averaged readings every few minutes. In this way, the current work leverages on the capabilities of recent data acquisition systems which are becoming more readily available in shipping, and seeks to demonstrate the

benefits & possibilities when such a system is present.

4.2 Data Pre-processing

Data pre-processing is a crucial and indispensable step in the data analysis and machine learning pipeline. It involves cleaning, transforming, and organizing raw data to enhance its quality and make it suitable for analysis or model training. Prior to being shared, the sensory dataset described in the previous section had already went through simple pre-processing and cleaning as part of its compilation, however, it was observed that there were still erroneous entries remaining that would have caused issues when training and testing the various models. Therefore, a simplistic and visual pre-processing process was employed. Additionally, due to the target application of the current research, it was decided that model accuracy would be greatly increased if transient periods of acceleration, deceleration, and change of course (i.e. turning manoeuvres) were discarded.

Ultimately, the pre-processing methods described below result in roughly a 60% reduction of the available dataset's size to a final size of around 2 million data points. The author believes this to be large enough to contain sufficient information about the target phenomenon over a broad range of operational conditions and, as such, is suitable for the Machine Learning methods explored in Section 4.4.

4.2.1 Removal of Erroneous entries, Outliers & Sensory noise

Empty entries in a sensory dataset refer to missing data points or fields that do not contain any information for a particular data point. These missing entries can occur for various reasons, such as malfunction of a sensor or issues with data transmission, and can significantly impact the integrity and usefulness of the dataset, therefore, it is essential that they are dealt with early on.

Depending on the nature of the missing data, various techniques can be employed, such as data imputation (filling in missing values using statistical methods), excluding incomplete

Table 4.1: List of dataset features

Variable Name	Units	Variable name	Units
Air Temperature	$^{\circ}C$	DG2 Produced power	kW
Speed through water	$knots$	DG3 Produced power	kW
Relative humidity	$\%$	DG1 Load	$\%$
Relative wind angle	$^{\circ}$	DG2 Load	$\%$
Relative wind speed	$knots$	DG3 Load	$\%$
Sea temperature	$^{\circ}C$	SB Patrol Electric Motor speed	rpm
Eastward wind speed	m/s	PS Patrol Electric Motor speed	rpm
Northward wind speed	m/s	SB Main DE speed	rpm
Spectral significant wave height	m	PS Main DE speed	rpm
Spectral significant primary swell wave height	m	Bow thruster absorbed power	kW
Spectral significant primary wind wave height	m	Draft at bow	m
Primary swell wave period	s	Draft at stern	m
Wind wave period	s	True wind speed	$knots$
Wave period at spectral peak	s	True sea water velocity	$knots$
SB Propeller shaft speed	rpm	True wind speed in x direction based on COG	$knots$
PS Propeller shaft speed	rpm	True wind speed in y direction based on COG	$knots$
SB Propeller pitch ratio	$\%$	Mean direction of wind based on COG	$^{\circ}$
PS Propeller pitch ratio	$\%$	Mean primary swell wave direction based on COG	$^{\circ}$
SB Propeller shaft torque	Nm	Mean wave direction based on COG	$^{\circ}$
PS Propeller shaft torque	Nm	Mean wind wave direction based on COG	$^{\circ}$
Roll angle	$^{\circ}$	True sea water velocity in x direction based on COG	$knots$
Trim angle	$^{\circ}$	True sea water velocity in y direction based on COG	$knots$
SB Main DE fuel consumption	kg/h	Mean direction of current based on COG	$^{\circ}$
PS Main DE fuel consumption	kg/h	True wind speed in x direction based on Heading	$knots$
SB Main DE fuel rack position	$\%$	True wind speed in y direction based on Heading	$knots$
PS Main DE fuel rack position	$\%$	Mean direction of wind based on heading	$^{\circ}$
SB Rudder angle	$^{\circ}$	Mean primary swell wave direction based on Heading	$^{\circ}$
PS Rudder angle	$^{\circ}$	Mean wave direction based on Heading	$^{\circ}$
SB Patrol Electric Motor absorbed power	kW	Mean wind wave direction based on Heading	$^{\circ}$
PS Patrol Electric Motor absorbed power	kW	True sea water velocity in x direction based on Heading	$knots$
DG1 Fuel consumption	l/h	True sea water velocity in y direction based on Heading	$knots$
DG2 Fuel consumption	l/h	Mean direction of current based on Heading	$^{\circ}$
DG3 Fuel consumption	l/h	Drift angle - difference between heading and COG	$^{\circ}$
DG1 Produced power	kW	Rate of turn based on COG	$^{\circ}/s$

samples, or applying machine learning algorithms that can handle missing data. It is important for researchers to carefully assess the data available to them when choosing between the above techniques. Due to the large amount of available data points and the complexity of the dataset, it was decided to delete any samples that have an erroneous or missing value for any of the features. Examples of erroneous samples in the current scope were considered to be:

- Negative values for strictly positive physical quantities (e.g. negative fuel consumption or negative significant wave height).
- Values outside of acceptable sensory ranges (e.g. direction angles outside of the $0° - 360°$ range or percentages outside of the $0\% - 100\%$ range).
- NaN entries, indicative of a sensory fault, data transmission fault, or corrupted data point.

In the current case, the high quality of the data meant there were relatively few discarded samples (less than 1% of the total size of the dataset).

Additionally, erroneous data that was not captured as part of the above, was treated using Inter Quartile Range (IQR) filtering [124] which is a simple and robust statistical method for filtering out outliers within a dataset. The data is organised in ascending order and divided through Quartiles, which are values that separate the data in four equal parts. The middle 50% of the dataset is contained between the first (Q1) and third (Q3) quartile, which is defined as the IQR. Values which sit outside of $Q1 - 1.5 * IQR$ to $Q3 + 1.5 * IQR$ are then considered as outliers and, in the current work, removed from the dataset. Features, subject to IQR preprocessing, were identified through visual histogram representation of the dataset. An example (Relative Wind Speed) can be seen in Figure 4.2, showing the difference before and after IQR filtering.

4.2.2 Removal of Transient periods

Transient periods of acceleration, deceleration, or turning manoeuvres are characterised by complex physical phenomena which become difficult for data-driven methods to predict due to their inherent lack of first-principle knowledge. Ultimately, for a methodology which aims

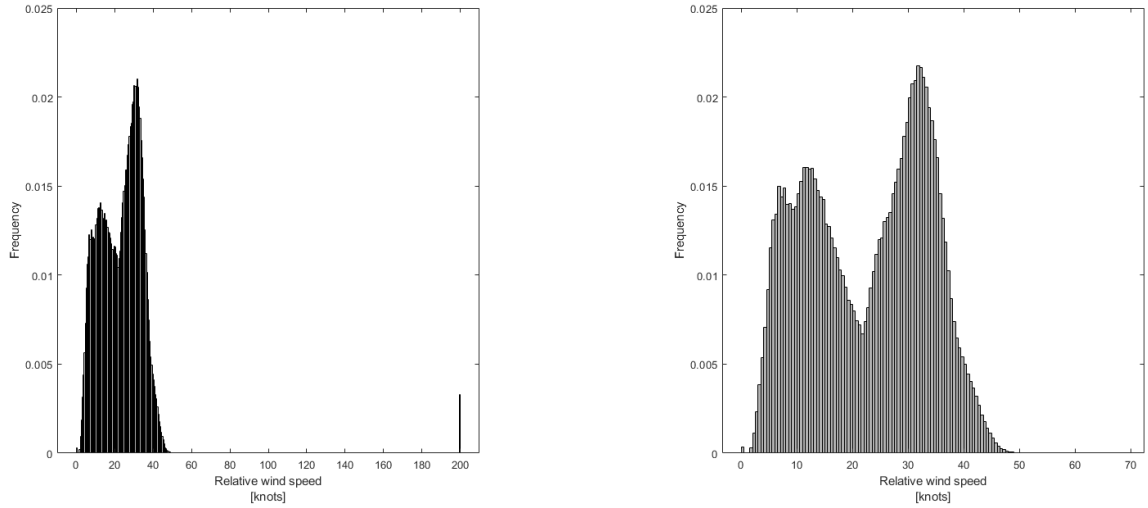

(a) Relative Wind Speed distribution prior to IQR filtering

(b) Relative Wind Speed distribution after IQR filtering

Figure 4.2: IQR filtering of Relative Wind Speed

to assess the impact biofouling has on vessel performance, the ability to do so during volatile periods of operation is unimportant and striving to achieve it could only compromise the overall quality of the model, perhaps lowering its predictive performance. Therefore, here it has been decided to filter out these operational scenarios in order to preserve model performance.

In particular, low speed operation is normally characteristic during manoeuvring in port or shallow and difficult waters. There, the vessel is impacted by additional outside factors such as the presence of other craft, wave refraction from channel walls, shallow water effects, etc.. Subsequently, the author decided it appropriate to filter out all data points which contain a Speed through Water of under 5 knots, and hopefully prevent most of the uncertainties of low-speed operation from having an effect on any subsequent analyses.

Additionally, for a few key features that are indicative of changes in vessel operation (Vessel speed, Propellers' rotational speed, Rudder angle, Patrol Electric Motor rotational speed, and Main Engines' rotational speed), a 5% per second threshold was set for variation between subsequent data points. This was observed to be greatly important for the accuracy of developed models. As can be seen in Table 4.2, the chosen threshold balanced between losing too much

Table 4.2: Model accuracy versus Size of dataset after steady-state filtering

Filtering threshold (% per second)	% of data points lost	% change in model accuracy (RLS)
20%	−15.9%	+6.65%
10%	−30.1%	+9.48%
5%	−49.9%	+11.24%
3%	−64.4%	+13.88%
1%	−86.3%	+23.80%
0.5%	−93.6%	+28.89%

of the operational data, and increasing model performance when compared to no filtering of transient operation. Lowering this further to 3%, 1% or 0.5% per second greatly reduced the data points available after filtering without making the model better at predicting the vessel's speed. In fact, an artificial increase in accuracy could be seen when the majority of the data was filtered out.

4.2.3 Data Normalisation

The sensory dataset that was available for the the current work includes a large selection of different features, which are measured using varying units, and subsequently scales. For example, while Relative Humidity is measured in percentage, the Power generated by the vessel's engines is often in the range of thousands or tens of thousands of kW. In order for the developed models to utilise variables with such vastly different scales, the variables need to be standardised through normalisation. The most commonly used methods for normalising data are:

- Min-Max normalisation.

  The minimum value observed in the dataset is subtracted from every data point. The resulting number is then divided by the difference between the maximum and minimum value:

  $$x_{norm} = \frac{x - x_{min}}{x_{max} - x_{min}} \in [0, 1] \tag{4.1}$$

  This approach results in values within the range of $[0, 1]$, however, can be adjusted to

result in different ranges, such as $[-1, 1]$:

$$x_{norm} = 2 * \frac{x - x_{min}}{x_{max} - x_{min}} - 1 \in [-1, 1] \tag{4.2}$$

- z-score normalisation.

  The mean of the data is subtracted from every data point. The resulting number is then divided by the standard deviation of the dataset. In this way, data points equal to the mean are normalised to be 0, whereas ones which differ from the mean by a standard deviation are transformed to 1:

$$x_{norm} = \frac{x - \mu}{\sigma} \tag{4.3}$$

Whichever method of normalisation is chosen, the data variables are processed into a consistent scale and range throughout the dataset. This enhances the performance of numerical models and, in a data-driven environment, prevents distortion between the weight of different features. For the current work, Min-Max normalisation in the range $[0, 1]$ was chosen for all features.

4.3 Benchmark Method - ISO19030

As described in Section 2.5.2, ISO19030 [84, 85, 86], developed by the International Organisation for Standardisation, represents the state-of-the-art industrial approach for estimating performance changes for ships. In the current scope, it is used as a benchmark, as it was deemed to be the most indicative method of highlighting and evaluating the performance of the developed data-driven and hybrid methods on the currently available data, outlined in Section 4.1. In fact, a decision was made to not validate the developed approaches against other works in literature due to the unique nature of the operational envelopes of different vessels, and the variation between the datasets that have been utilised in other similar research.

The steps followed in applying the ISO19030 procedure to the raw unprocessed data features described in Table 4.1 are as follows:

1. Extraction of features, required for ISO19030.

   As expected, not all 68 available features are required for applying the ISO 19030 method, as it is quite simplistic in its estimation. In particular, only Air temperature, Speed through water, Relative wind angle, Propeller shaft speed, Speed over ground Propeller shaft torque, Draft & Trim were utilised.

2. Removal of NaN entries within the dataset.

3. Application of Chauvenet's Criterion for data filtering

   ISO 19030 relies on Chauvenet's Criterion [125] for the detection and removal of outliers and erroneous entries within the input data. Firstly, the mean, μ, and standard deviation, σ, of the dataset are computed, followed by the absolute difference between the values within the dataset and the calculated mean, Δ_i. By then assuming a normal distribution, the probability of a data point with a certain deviation from the mean is calculated and compared to a threshold value, which is used to govern whether a datum is flagged as an outlier. Points are considered to be outliers if:

$$erfc\left(\frac{\Delta_i}{\sigma * \sqrt{2}}\right) * N < 0.5 \tag{4.4}$$

   Where $erfc$ is the complimentary error function and N is the total number of data points.

4. Additional filtering

   Entries were also omitted if the speed over water was less than $10\ knots$. This was done to avoid to avoid misrepresentation of the results for low speeds when calculating the percentage speed loss.

5. Correction for Wind Resistance

   ISO 19030 includes corrections to the delivered power, P_D, due to the influence of wind,

which are computed by:

$$\Delta P_W = \frac{(R_{rw} - R_{0w}) * v_g}{\eta_{D0}} + P_D \left(1 - \frac{\eta_{DM}}{\eta_{D0}}\right) \tag{4.5}$$

where

$$R_{rw} = \frac{1}{2} * \rho_a * {v_{wr}}^2 * A * C_{rw}(\Psi_{wr,ref}) \tag{4.6}$$

and

$$R_{0w} = \frac{1}{2} * \rho_a * {v_g}^2 * A * C_{0w}(0) \tag{4.7}$$

where:

- ΔP_W - Wind correction, $[W]$;
- R_{rw} - Wind resistance due to relative wind, $[N]$;
- R_{0w} - Air resistance in no-wind condition, $[N]$;
- v_g - Ship speed over ground, $[m/s]$;
- v_{wr} - Relative wind speed at reference height, $[m/s]$;
- C_{rw} - Wind resistance coefficient, dependent on wind direction of relative wind $\Psi_{wr,ref}$;
- C_{0w} - Wind resistance coefficient for head wind;
- ρ_a - Air density, $[kg/m^3]$;
- A - Transverse projected area in current loading condition, $[m^2]$;
- $\Psi_{wr,ref}$ - Relative wind direction at reference height, $[\circ]$;
- η_{D0} - Propulsive efficiency coefficient in calm condition;
- η_{DM} - Propulsive efficiency coefficient in actual voyage condition

The corrected power, $P_{D,corr}$, is then:

$$P_{D,corr} = P_D - \Delta P_W \tag{4.8}$$

For the current case, P_D is calculated using the Propeller shaft torque and speed readings from the dataset:

6. Calculation of expected speed based on reference Power curve

   Power curves for the vessel, representative of a clean vessel condition, were generated according to the methodology in Section 4.5.1 for a large set of drafts and trims. Based on these, by using the corrected delivered power, $P_{D,corr}$, as well as an observed Draft and Trim, an expected speed, v_e is estimated.

7. Calculation of speed loss

   The percentage speed loss, v_{loss}, can then be calculated using the expected speed, v_e, and the measured speed through water, v_w:

$$v_{loss} = 100 * \frac{v_m - v_e}{v_e} \tag{4.9}$$

In ISO19030, the speed loss is then used as the main KPI for evaluating a vessel's performance. As part of Section 2.4.2, different vessel performance metrics were discussed in the scope of evaluating the effects of biofouling. The choice of KPI is highly dependant on the perspective from which the problem of biofouling is considered. For example, when talking about a commercial vessel, increases in power requirements and fuel consumption to achieve a set speed are more important due to the monetary/profitability considerations of merchant vessels. However, as is in the current case with a Naval craft, for some vessel types, speed loss can be seen as the ideal KPI due to the importance of high-speed operation. Therefore, speed and, particularly, speed loss due to the effects of biofouling over time are considered as the target variable in the current work.

4.4 Data-driven Methods

For any statistical learning problem, a general modelisation framework can be defined, characterised by an input space $\mathcal{X} \subseteq \mathbb{R}^d$, an output space $\mathcal{Y} \subseteq \mathbb{R}^d$, and an unknown relation $\mu : \mathcal{X} \longrightarrow \mathcal{Y}$ to be learned [126, 127]. Within the current work, $\mathcal{X}$ contains the features listed in Table 4.1 excluding the target parameter which is representative of $\mathcal{Y}$. In the current work, the latter is the vessel's Speed through water. In this context, the authors define the model $h : \mathcal{X} \longrightarrow \mathcal{Y}$ as an approximation of μ. The aim of the current work is to develop a model h that is able to estimate the expected 'clean' vessel speed given the operational and environmental conditions that the ship is operating in at a specific point in time. A subsequent comparison to the 'real' recorded speed through water at that time then allows for an approximate indication of the state of the hull & propeller. Moreover, by applying this methodology to a long operational period (as is represented by the available dataset, described in Section 4.1), it should become possible to observe a notable shift in performance over time, draw conclusions based on this trend, and, ultimately, make maintenance decisions.

The approximating model h can be obtained through different types of techniques, for example, requiring some physical knowledge of the problem, as in physics-based methods, or the acquisition and utilisation of large amounts of data, as in data-driven methods. While physical models (PMs) are utilised further in this work in Section 4.5 with the aim of introducing first-principle knowledge into the existing dataset, the current Section focuses on adopting a data-driven Machine Learning (ML) approach in order to translate the prediction of a vessel's speed through water into a typical regression problem [128, 129]. In fact, ML techniques aim at estimating the unknown relationship μ between input and output through a learning algorithm $\mathcal{A}_{\mathcal{H}}$ which exploits historical data to learn h and where $\mathcal{H}$ is a set of hyperparameters which characterises the generalisation performance of $\mathcal{A}$ [130]. The historical data consists of a series of n examples of the input/output relation μ and are defined as $\mathcal{D}_n = \{(\mathbf{x}_1, y_1), ..., (\mathbf{x}_n, y_n)\}$, where $\mathbf{x} \in \mathcal{X}$ and $y \in \mathcal{Y}$.

Each learning algorithm is characterised by a unique set of hyperparameters that define it,

however, the appropriate process of choosing the hyperparameters' values is standard across all different methods. Since hyperparameters influence the model's ability to approximate μ, a proper Model Selection (MS) and Error Estimation (EE) procedure is required to tune them [130]. Resampling techniques such as k-fold Cross Validation [131], the nonparametric Bootstrap [132], or Monte Carlo simulation [133] are normally used when dealing with real-world scenarios, as these have been observed to perform well in practice [99]. When utilising Resampling techniques, the original dataset $\mathcal{D}_n$ is resampled a number of times (n_r), with or without replacement, to build three independent datasets called learning, validation and test sets, respectively $\mathcal{L}_l^r$, $\mathcal{V}_v^r$, $\mathcal{T}_t^r$, with $r \in \{1, ..., n_r\}$, such that

$$\mathcal{L}_l^r \cap \mathcal{V}_v^r = \oslash,\ \mathcal{L}_l^r \cap \mathcal{T}_t^r = \oslash,\ \mathcal{V}_v^r \cap \mathcal{T}_t^r = \oslash \tag{4.10}$$

$$\mathcal{L}_l^r \cup \mathcal{V}_v^r \cup \mathcal{T}_t^r = \mathcal{D}_n \tag{4.11}$$

Following this, to perform the MS process and select the best set of hyperparameters $\mathcal{H}^*$ from the set of all possible ones $\mathfrak{H} = \{\mathcal{H}_1, \mathcal{H}_2, ...\}$ for the specific algorithm $\mathcal{A}_\mathcal{H}$, the following procedure must be applied:

$$\mathcal{H}^* : arg \min_{\mathcal{H} \in \mathfrak{H}} \sum_{r=1}^{n_r} M(\mathcal{A}_\mathcal{H}(\mathcal{L}_l^r), \mathcal{V}_v^r), \tag{4.12}$$

where $h = \mathcal{A}_\mathcal{H}(\mathcal{L}_l^r)$ is a model built with the algorithm $\mathcal{A}$ with its set of hyperparameters $\mathcal{H}$ and with the data $\mathcal{L}_l^r$ and where $M(\mathcal{A}_\mathcal{H}(\mathcal{L}_l^r), \mathcal{V}_v^r)$ is a desired metric. Since the data in $\mathcal{L}_l^r$ is independent of the data in $\mathcal{V}_v^r$, $\mathcal{H}^*$ should be a set of hyperparameters, which allows $\mathcal{A}_\mathcal{H}$ to achieve good performance on unseen data. Furthermore, for the EE phase, the optimal model $h_\mathcal{A}^* = \mathcal{A}_{\mathcal{H}^*}(\mathcal{D}_n)$ is evaluated according to:

$$M(h_\mathcal{A}^*) = \frac{1}{n_r} \sum_{r=1}^{n_r} M(\mathcal{A}_{\mathcal{H}^*}(\mathcal{L}_l^r \cup \mathcal{V}_v^r), \mathcal{T}_t^r) \tag{4.13}$$

Similarly to the process of MS, since the two datasets ($\mathcal{L}_l^r \cup \mathcal{V}_v^r$ and $\mathcal{T}_t^r$) are independent,

$M(h^*_{\mathcal{A}})$ estimates the true performance of the final model without bias [130].

In the current work, the MS procedure is completed using Monte Carlo simulation without replacement [133]. Within this, $l = 0.7n_s$, $v = 0.15n_s$, and $t = 0.15n_s$, where n_s is the number of data points to be resampled from $\mathcal{D}_n$ in each Monte Carlo iteration. The latter is implemented as a user input, which balances the computational requirement of the model and the accuracy & confidence of its results. Some of the algorithms used in the following sections utilise the entire dataset $\mathcal{D}_n$, i.e. $n_s = n$, however, for others this is impossible due to the size of $\mathcal{D}_n$ and the associated computational demand. For what concerns the error metric M, Mean Square Error (MSE) is adopted due to its convexity, smoothness, and statistical properties [134]. Additionally, to analyse and ensure the performance of the developed model, Mean Absolute Percentage Error (MAPE) is utilised, as well as a range of visualization methods.

Sections 4.4.1 through 4.4.6 will now describe the theory behind the various algorithms that have been explored as possible options for the prediction model. This includes explanations of each method's unique hyperparameter set, as well as a top-level description of their underlying concepts, logic, and application to the particular problem.

4.4.1 Regularised Least Squares (RLS)

The idea behind RLS can be summarised as follows. During the training phase, the quality of the learned function $h(\mathbf{x})$ is measured according to a loss function $l(h(\mathbf{x}), y)$ [134] with empirical error

$$\hat{L}_n(h) = \frac{1}{n}\sum_{i=1}^{n} l(h(\mathbf{x}_i), y_i). \tag{4.14}$$

A simple criterion for selecting the final model during the training phase could then consist in simply choosing the approximating function that minimises the empirical error $\hat{L}_n(h)$. This approach is known as empirical risk minimisation (ERM) [128]. However, ERM is usually avoided in ML as it leads to severe overfitting of the model on the training dataset. In fact, in this case, the training process could choose a model, complicated enough to perfectly

describe all the training samples (including the noise that afflicts them). In other words ERM implies memorisation of data rather than learning. A more effective approach is to minimise a cost function where the trade-off between accuracy on the training data and a measure of the complexity of the selected model is achieved [135], implementing the Occam's razor principle

$$h^* : \min_h \ \hat{L}_n(h) + \lambda C(h). \tag{4.15}$$

In other words, the best approximating function h^* is chosen as one that is complicated enough to learn from the data without overfitting. In particular, $C(h)$ is a complexity measure: depending on the Machine Learning approach used, different measures are realised. Instead, $\lambda \in [0, \infty]$ is a hyperparameter, that must be set a-priori and is not obtained as an output of the optimisation procedure: it regulates the trade-off between the overfitting tendency, related to the minimisation of the empirical error, and the underfitting tendency, related to the minimisation of $C(h)$. The optimal value for λ is problem-dependent, and requires tuning. In RLS, models are defined as:

$$h(\mathbf{x}) = \mathbf{w}^T \mathbf{x}, \tag{4.16}$$

The complexity of the models, in RLS, is measured as:

$$C(h) = \|\mathbf{w}\|^2, \tag{4.17}$$

i.e., the Euclidean norm of the set of weights describing the regressor, which is a standard complexity measure in ML [126, 136]. Regarding the loss function, the square loss is typically adopted due to its convexity, smoothness, and statistical properties [134]:

$$\hat{L}_n(h) = \frac{1}{n} \sum_{i=1}^{n} l(h(\mathbf{x}_i), y_i) = \frac{1}{n} \sum_{i=1}^{n} [h(\mathbf{x}_i) - y_i]^2. \tag{4.18}$$

Consequently, Problem (4.15) can be reformulated as:

$$\mathbf{w}^* : \min_{\mathbf{w}} \sum_{i=1}^{n} [\mathbf{w}^T \mathbf{x} - y_i]^2 + \lambda \|\mathbf{w}\|^2. \tag{4.19}$$

Equation 4.19 can then be represented in its matrix form:

$$\mathbf{w}^* : \min_{\mathbf{w}} \|\mathbf{w}^T \mathbf{X} - \mathbf{y}\|^2 + \lambda \mathbf{w}^T \mathbf{w}, \tag{4.20}$$

where $\mathbf{y} = [y_1, ..., y_n]^T$, $\mathbf{X} = [\mathbf{x}_1, ..., \mathbf{x}_n]^T \in \mathbb{R}^{nxm}$, $\mathbf{w} = [w_1, ..., w_m]^T$, and the identity matrix $I \in \mathbb{R}^{mxm}$. By setting the gradient equal to 0 w.r.t. $\mathbf{w}$, it is possible to state that:

$$(\mathbf{X} + \lambda \mathbf{I})\mathbf{w}^* = \mathbf{y}, \tag{4.21}$$

or

$$\mathbf{w}^* = (\mathbf{X}^T \mathbf{X} + \lambda \mathbf{I})^{-1} \mathbf{X}^T \mathbf{y}, \tag{4.22}$$

RLS is characterised by a single hyperparameter, λ, which is tuned in the MS phase, as described in Section 4.4 and controls the Bias-Variance trade-off, prevents overfitting, and greatly improves generalisation performance.

4.4.2 Kernel Regularised Least Squares (KRLS)

In KRLS, models are defined as:

$$h(\mathbf{x}) = \mathbf{w}^T \varphi(\mathbf{x}), \tag{4.23}$$

where φ is an a-priori defined Feature Mapping (FM) [126] allowing to keep the structure of $h(\mathbf{x})$ linear. The complexity of the models, in KRLS, is measured the same as in RLS i.e. according to equation 4.17. Similarly, the square loss is also adopted. In this case, Problem (4.15) can be reformulated as:

$$\mathbf{w}^* : \min_{\mathbf{w}} \sum_{i=1}^{n} [\mathbf{w}^T \varphi(\mathbf{x}) - y_i]^2 + \lambda \|\mathbf{w}\|^2. \tag{4.24}$$

By exploiting the Representer Theorem [137], the solution h^* of the Problem (4.24) can be expressed as a linear combination of the samples projected in the space defined by φ:

$$h^*(\mathbf{x}) = \sum_{i=1}^{n} \alpha_i \varphi(\mathbf{x}_i)^T \varphi(\mathbf{x}). \tag{4.25}$$

It is worth highlighting that, according to the kernel trick, it is possible to reformulate $h^*(\mathbf{x})$ without explicit knowledge of φ, and consequently avoiding the curse of dimensionality of computing φ, using a proper kernel function $K(\mathbf{x}_i, \mathbf{x}) = \varphi(\mathbf{x}_i)^T \varphi(\mathbf{x})$:

$$h^*(\mathbf{x}) = \sum_{i=1}^{n} \alpha_i K(\mathbf{x}_i, \mathbf{x}) \tag{4.26}$$

Several kernel functions can be found in the literature [138, 139], each with a particular property that can be exploited according to the problem under examination. Usually, the Gaussian kernel is chosen:

$$K(\mathbf{x}_i, \mathbf{x}) = e^{-\gamma \|\mathbf{x}_i - \mathbf{x}\|^2}, \tag{4.27}$$

because of the theoretical reasons described in [140, 141] and because of its effectiveness [142, 143]. γ is another hyperparameter, which regulates the non-linearity of the solution that must be tuned as will be described later. Basically, the Gaussian kernel is able to implicitly create an infinite dimensional φ, and because of this, KRLS is able to learn any possible function [140]. The KRLS problem of Eq. 4.24 can be reformulated by exploiting kernels as:

$$\boldsymbol{\alpha}^* : \min_{\boldsymbol{\alpha}} \|\mathbf{Q}\boldsymbol{\alpha} - \mathbf{y}\|^2 + \lambda \boldsymbol{\alpha}^T \mathbf{Q} \boldsymbol{\alpha}, \tag{4.28}$$

where $\mathbf{y} = [y_1, ..., y_n]^T$, $\boldsymbol{\alpha} = [\alpha_1, ..., \alpha_n]^T$, the matrix $\mathbf{Q}$ such that $\mathbf{Q}_{i,j} = K(\mathbf{x}_j, \mathbf{x}_i)$, and the identity matrix $I \in \mathbb{R}^{nxn}$. By setting the gradient equal to 0 w.r.t. $\boldsymbol{\alpha}$, it is possible to state that:

$$(\mathbf{Q} + \lambda I)\boldsymbol{\alpha}^* = \mathbf{y}, \tag{4.29}$$

or

$$\boldsymbol{\alpha}^* = (\mathbf{Q}^T\mathbf{Q} + \lambda\mathbf{I})^{-1}\mathbf{Q}^T\mathbf{y}, \tag{4.30}$$

which is a linear system for which effective solvers have been developed over the years, allowing it to cope with even very large sets of training data [144].

For KRLS, there are two hyperparameters, λ and γ, which are tuned in the MS phase, as described in Section 4.4. Concequently, the computational demand is higher than RLS, however, so is the expected accuracy.

4.4.3 Decision Trees

Tree-based algorithms progressively segment the feature space into a set of smaller and smaller regions, $R_1, R_2, ..., R_P$, and them model the response as a constant, c_p in each one [145]:

$$f(x) = \sum_{p=1}^{P} c_p I(x \in R_p). \tag{4.31}$$

A model is built by recursive binary splitting in order to reduce the sum of squares. Therefore, it is easy to see that the best $\hat{c}_p$ is just the average of y_i in region R_p [145]:

$$\hat{c}_p = ave(y_i|\mathbf{x}_i \in R_p). \tag{4.32}$$

A greedy algorithm is necessary, as it is computationally not feasible to find the best partition in terms of minimising the sum of squares [145]. Starting with all of the data, consider a splitting variable j and a split point s, and define the pair of half planes:

$$R_1(j, s) = \{X|X_j \leq s\} \quad and \quad R_2(j, s) = \{X|X_j > s\}. \tag{4.33}$$

Then we seek the j and s that solve:

$$j,\ s : \min_{j,\,s} [\min_{c_1} \sum_{\mathbf{x}_i \in R_1(j,s)} (y_i - c_1)^2 + \min_{c_2} \sum_{\mathbf{x}_i \in R_2(j,s)} (y_i - c_2)^2]. \tag{4.34}$$

For any choice of j and s, the inner minimisation is solved by:

$$\hat{c}_1 = ave(y_i | \mathbf{x}_i \in R_1(j,s)) \quad and \quad \hat{c}_2 = ave(y_i | \mathbf{x}_i \in R_2(j,s)) \tag{4.35}$$

For each splitting variable, the determination of the split point s can be done very quickly. Therefore by scanning through all of the inputs, determination of the best pair (j, s) is feasible. [145]

The process is repeated further on each of the two resulting regions and so on, and so on. It is clear that this process can be taken to the extreme, where the tree memorises and overfits the data, therefore a way of maintaining good generalisation performance i.e. a Bias-Variance balance is needed.

There are a number of hyperparameters that are typically exploited to tune Decision Tree models:

- Criteria - Measures the quality of the split in a decision tree. Can be Gini impurity or Information Gain.
- Maximum depth - Controls the maximum depth that the tree is allowed to grow to.
- Minimum split samples - The minimum number of samples needed to split a node.
- Minimum leaf samples - The minimum required number of samples to be present at a leaf node. This means that a split is only done when both resulting leafs will have the minimum required number of samples.
- Max features - unlike RLS and KRLS, a Decision tree does not have inherent feature selection, therefore, a maximum number of features needs to be tuned. This allows us to avoid the curse of dimensionality, while also maintaining the most valuable features.

4.4.4 XGBoost

The concept of boosting is the combination of many "weak" learners to form a powerful "committee" which produces a weighted estimate [145]. In particular, Extreme Gradient Boosting (XGBoost) is an optimised application of gradient boosting that uses decision trees [146]. Boosting algorithms are iterative, where subsequent iterations are trained to correct the errors of their predecessors with the goal of minimising a loss function.

A tree ensemble model uses K additive functions to predict the output [147]:

$$\hat{y}_i = \sum_{k=1}^{K} f_k(\mathbf{x}_i),\ f_k \in \mathcal{F}, \tag{4.36}$$

where $\mathcal{F} = \{f(\mathbf{x}) = w_{q(\mathbf{x})}\}(q\ :\ \mathbb{R}^m\ \longrightarrow\ T, w \in \mathbb{R}^T)$ is the space of regression trees. Here q represents that maps an example to the corresponding leaf index. T is the number of leaves in the tree. Each f_k corresponds to an independent tree structure q and leaf weights w.

To learn the set of functions used in the model, the following regularised objective is minimised [147]:

$$\hat{L}_n(h) = \sum_i l(\hat{y}_i, y_i) + \sum_k \Omega(f_k), \tag{4.37}$$

where

$$\Omega(f) = \gamma T + \frac{1}{2}\lambda \|w\|^2. \tag{4.38}$$

The term Ω penalises the complexity of the model. The additional regularisation term, λ, helps to smooth the final learned weights to avoid over-fitting.

For a more in depth explanation of the XGBoost algorithm, please refer to the original publication - [147].

4.4.5 Random Forest (RF)

The Random Forest (RF) algorithm [148] is based on the bagging (i.e. bootstrap aggregation) technique, which reduces the variance on an estimated prediction function [145]. It simultaneously fits the same regression tree to bootstrap sampled versions of the training data, and averages their result to produce its estimate:

$$\hat{y}_i = \frac{1}{K} \sum_{k=1}^{K} f_k(\mathbf{x}_i). \tag{4.39}$$

On top of the hyperparameters needed for Decision Trees, the size of the "forest" needs to be tuned for the particular application.

RF is a substantial modification of bagging that builds a large set of de-correlated trees. On many problems, it's performance is similar to boosting methods with the additional benefit that RFs are simpler to train and tune. [145]

4.4.6 Artificial Neural Network (ANN)

As the their name suggest, Artificial Neural Networks (ANNs) are inspired by the human brain and attempt to replicate a connected system of neurons. This is done through perceptrons (see Figure 4.3), which are organised in layers, connected together by weights or functions, which are progressively tuned based on the available data [149].

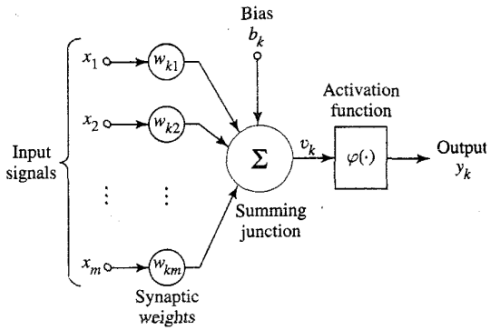

Figure 4.3: Nonlinear model of a neuron [149].

A typical Neural Network architecture includes three types of layers (see Figure 4.4):

1. Input layer - This layer receives the input data, where each node corresponds to a dataset feature.

2. Hidden layer - This intermediate layer process the information fed to them from the previous layer, applying a weighted sum of inputs and a non-linear activation function, which allows the network to capture complex relationships within the data.

3. Output layer - This final layer produces the output of the NN i.e. an estimate for the target feature(s).

Depending on the number of hidden layers in a NN, it can be referred to as Deep or Shallow.

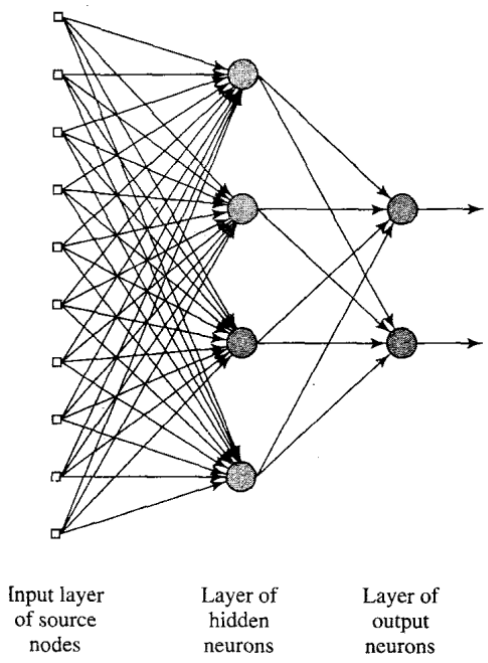

Figure 4.4: Fully connected feedforward network with one hidden layer and one output layer [149].

Training a feedforward ANN (i.e. signals are only fed in one direction from the input to the output side of the network) involves a few steps:

1. Forward propagation - The input data is fed into the input layer, and processed through the hidden layers by means of the initial weights and biases of their nodes. The output layer provides the initial estimate.

2. Error Estimation - After calculating an estimate of the target feature, the ANN assesses the difference between it and the actual value using a loss function (e.g. mean squared error for regression).

3. Backpropagation - The calculated loss is fed back through the network and used to calculate the gradients of the loss with respect to the weights of the network.

4. Optimisation - An optimisation algorithm is used to update the weights and biases based on the calculated gradients.

Considering the large amounts of data available for the current application, an ANN seems to be a good candidate. In particular, a Shallow network will be used due to its simplicity and the requirement for it to fit into a real-time approach.

4.5 Physical Modelling

In order to effectively implement physical knowledge into the existing data-driven methodology with the aim of developing a hybrid model, the features of the sensory dataset, described in Section 4.1, are used in combination with a 3D model of the Holland Class OPVs. A rough representation of the followed methodology is given in Figure 4.5.

A 3D model provides the opportunity to utilise the vessel's geometry and particulars in a hydrodynamic analysis software. In the current work, ShipX was used in order to gain first-principle knowledge about the vessel's operation, as is described in Section 4.5.1

Further, the open-water performance curves for the Holland Class OPVs' propellers were kindly provided by the Royal Netherlands Navy, and have been used in conjunction with dataset features to develop first-principle estimates for the Speed through Water (Section 4.5.2) and calm water Thrust (Section 4.5.3).

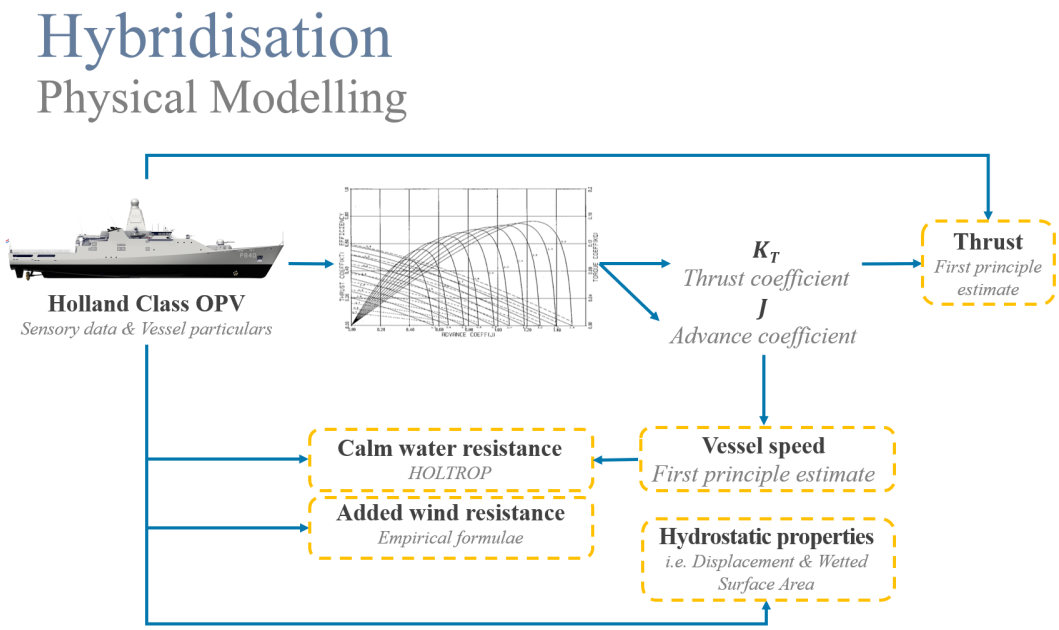

Figure 4.5: Physical Modelling Flow Chart

4.5.1 Calm Water Resistance & Hydrostatic Parameters

As depicted in Figure 4.6, the overall goal in conducting hydrodynamic simulation of the OPV in ShipX was to develop a database of calm water resistance curves. These can then be used as a look-up table or also a type of transfer function for the hybrid model in order to construct a new ”Calm Water Resistance” feature in the dataset.

On top of a 3D geometry for the vessel, ShipX requires a set of operational conditions for which to run the hydrodynamic simulation:

1. Draft
2. Trim
3. Vessel Speed
4. Simulation Method

By analysing the operational dataset (described in Section 4.1) ranges for the Drafts, Trims, and Vessel Speeds that need to be simulated in order to fully cover the operational range of the OPV

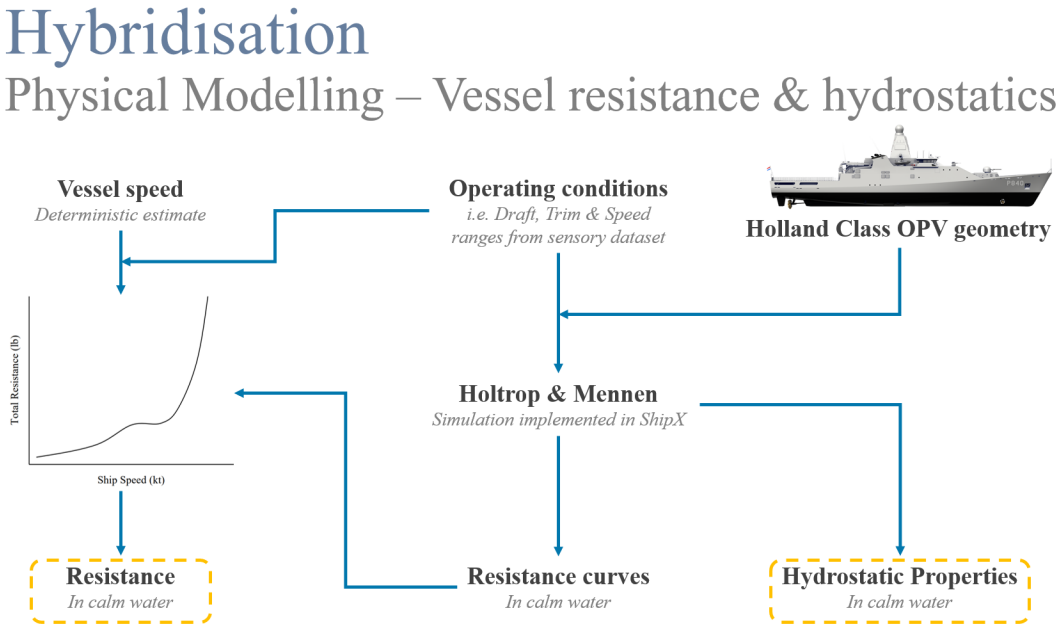

Figure 4.6: Vessel Calm Water Resistance & Hydrostatics Flow Chart

Table 4.3: Operational Parameter Grid

Parameter	Minimum value	Maximum value	Step
Draft	3.8m	5.0m	0.1m
Trim	−1.4m	0.8m	0.1m
Vessel Speed	5kn	25kn	0.5kn

are shown in Table 4.3.

The simulation method was set to HOLTROP84 which corresponds to the Holtrop & Mennen methodology [150], which is the most established and widely used first-principle approach for estimating the resistance of a vessel in calm water.

In total, 299 simulation runs were performed to develop 13 x 23 x 41 look-up tables for Vessel Calm Water Resistance, Wetted Surface Area, & Displacement. Using the first-principle estimate for the vessel's Speed through Water (Section 4.5.2), as well as existing OPV data, these "transfer functions" were then used to create new data features and improve the sensory dataset.

4.5.2 Speed through Water

On top of the sensory dataset, the Royal Netherlands Navy kindly provided some additional vessel information. Unfortunately, due to confidentiality, the majority of this cannot be disclosed. In particular, the availability of the Open Water performance characteristics of the two Holland Class OPV propellers meant that a first-principle estimate for the vessel speed could be calculated for each sample of the sensory dataset. This is a very powerful tool in the current work, because a 'clean' vessel speed estimate is the target feature of the data-driven models, outlined in Section 4.4, allowing them to be developed as a basis for a hybrid model. Ultimately, the ability to deterministically calculate the expected vessel speed, and implementing this physical knowledge of the target feature into the data-driven space, is what transforms the current methodology into a Hybrid Model.

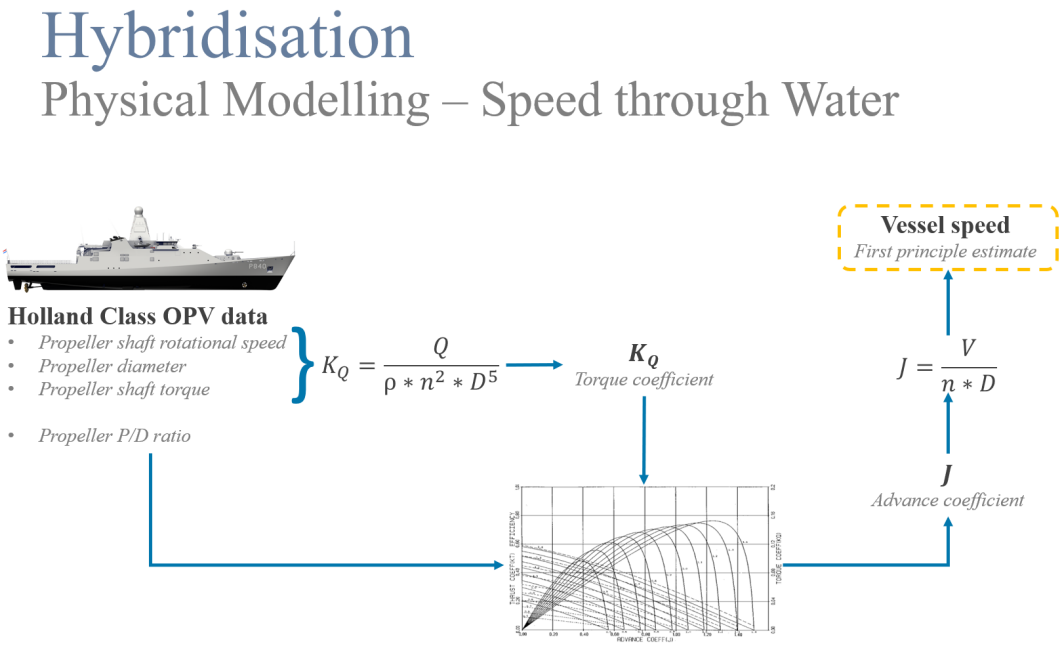

Figure 4.7: Vessel Calm Water Speed Flow Chart

As depicted in Figure 4.7, the speed of the vessel can be estimated through the open water curves of the vessel propellers. By calculating 2 out of the 4 performance parameters that are included in the graphs (i.e. Propeller Pitch/Diameter ratio, Torque coefficient, Thrust coeffi-

cient, and Advance coefficient), you can determine the remaining 2. Considering the available features of the dataset, it is possible to easily calculate the Torque coefficient, K_Q using Equation 4.40, as the propeller shaft rotational speed, n, & torque, Q, are included in the operational data (see Table 4.1), while the density of seawater, ρ and the diameter of the propellers, D are known. Moreover, the Propellers' Pitch/Diameter ratio is also part of the sensory signals.

$$K_Q = \frac{Q}{\rho * n^2 * D^5} \tag{4.40}$$

The Advance coefficient, J, can therefore be determined using the open water curves. By definition:

$$J = \frac{V}{n * D} \tag{4.41}$$

Equation 4.41 can then be rearranged and solved for vessel speed:

$$V = J * n * D \tag{4.42}$$

The above methodology is possible for each sample of the sensory data, therefore, the dataset was enriched further to include this deterministic estimate for vessel speed as an additional feature.

4.5.3 Thrust

Following a similar methodology to Section 4.5.2, Figure 4.8 depicts how the open water performance curves for the OPV's propellers can be used to also provide a deterministic estimate for Calm Water Thrust.

Using Equation 4.40, the Torque coefficient can be calculated and together with the Propeller Pitch/Diameter ratio is used to determine a Thrust coefficient, K_T. By definition:

$$K_T = \frac{T}{\rho * n^2 * D^4} \tag{4.43}$$

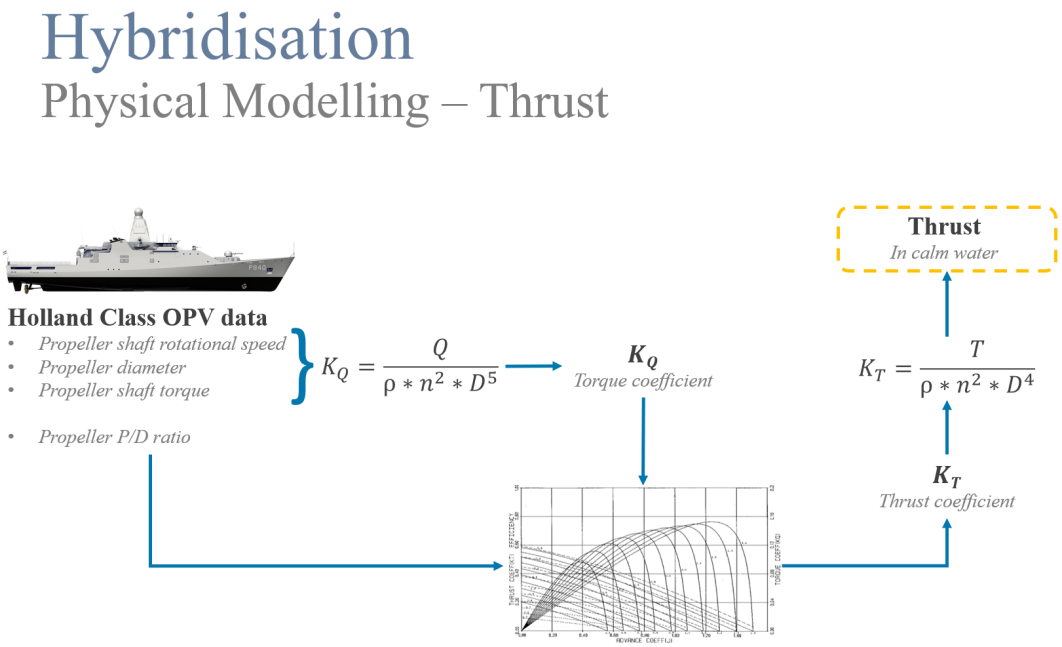

Figure 4.8: Propeller Thrust Flow Chart

Then Equation 4.43 can be rearranged and solved for Thrust, T:

$$T = K_T * \rho * n^2 * D^4 \tag{4.44}$$

The above methodology is again possible for each sample of the sensory data, and the dataset has been enriched with the physical estimate for the delivered Thrust in calm water.

4.5.4 Added Wind Resistance

Finally, following the methodology that was explained earlier in Section 4.3, the dataset was expanded by estimating the wind resistance for each data point.

4.6 Features Engineering

Improvements to the dataset can also go beyond incorporating physical knowledge through first-principle manipulation of the sensory features and vessel particulars. Particularly, a way to

encapsulate a vessel's exposure to biofouling generation enabling conditions into a numerical entity could be beneficial. As has already been discussed in Section 2.1, the time a ship spends stationary, as well as the overall operational time since a hull & propeller cleaning, are critical to the formation of micro and macro fouling on her underwater surfaces.

4.6.1 Time since Cleaning

The available Holland Class OPV operational data includes a timestamp for each reading. In fact, knowing a particular date/time when an underwater cleaning of the hull and propeller has been performed, it is possible to attempt to quantify the state of fouling formation.

An additional feature has been added to the dataset that simply quantifies the time elapsed (in hours) since her last drydocking or underwater cleaning.

This can be split further into two separate features if enough data is available to be exploited to train the data-driven/hybrid models. 'Enough data' refers to a dataset that spans a long enough timeframe within which the operational characteristics of the vessel have been continuously recorded, and the ship has been subjected to a number of cleaning operations. This would then ensure that the model can infer the typical operational characteristics following the different types of cleaning events.

4.6.2 Stationary Time

A step further can be done by, for each datapoint, calculating the total time duration that the ship has spent stationary since being cleaned. This knowledge can be very powerful in attempting to quantify the biofouling state of a ship's underwater body, as the majority of fouling is formed at very low vessel speed and mostly when she is stationary at port or anchored.

Similarly to Section 4.6.1, the above methodology can be expanded to differentiate between a full service of the hull and propeller of the ship during drydocking and an underwater cleaning performed by divers or robots. Again, this is highly dependent on the access to data.

4.7 Hybrid Models

Combining the developed PMs with a DDM which leverages the algorithms described previously in Section 4.4, Hybrid models are constructed. From the dataset features described in Table 4.1, Speed through Water is selected as the target feature. In the forward phase, this allows the comparison between the models' prediction and the sensory reading in order to determine the target KPI of $\%$ speed loss. Moreover, by having a first principle estimate for Speed through Water, an initial guess is available to the DDM, which is the defining characteristics of a HM as discussed in Section 2.5.4. Overall, the 'hybridisation' of the base data-driven model is achieved in two separate enhancements packages:

1. Hybridisation package $\#1$ (HP1):
    - Speed through Water;
    - Calm Water Resistance & Hydrostatic Parameters;
    - Thrust;
    - Added Wind Resistance;
2. Hybridistaion package $\#2$ (HP2):
    - Time since Cleaning;
    - Stationary time

In this work, a total of 24 models are therefore developed - 6 different Machine Learning Algorithms which are exploited on their own, combined with Hybridisation package $\#1$, combined with Hybridisation package $\#2$, or combined with both Hybridisation packages.

4.8 Performance Assessment & Comparison

In order to select the best-performing methodology, an exhaustive Model Selection approach was applied, utilising a subset of the available data which is representative of the cleanest vessel

Table 4.4: DDMs & HMs performance in predicting Vessel Speed through Water - July 2019

Algorithm	Error metric	DDM	HM (Package #1)	HM (Package #2)	HM (Package #1 & #2)
RLS	MSE	0.494 ± 0.003	0.237 ± 0.001	0.494 ± 0.003	0.232 ± 0.001
	MAPE	$4.308\% \pm 0.007\%$	$2.980\% \pm 0.006\%$	$4.312\% \pm 0.008\%$	$2.939\% \pm 0.005\%$
KRSL	MSE	0.108 ± 0.003	0.102 ± 0.002	0.106 ± 0.003	0.100 ± 0.002
	MAPE	$1.909\% \pm 0.011\%$	$1.882\% \pm 0.017\%$	$1.8984\% \pm 0.015\%$	$1.857\% \pm 0.009\%$
Decision Trees	MSE	0.234 ± 0.018	0.178 ± 0.012	0.235 ± 0.016	0.168 ± 0.010
	MAPE	$2.479\% \pm 0.054\%$	$2.275\% \pm 0.046\%$	$2.482\% \pm 0.044\%$	$2.263\% \pm 0.042\%$
XGBoost	MSE	0.123 ± 0.006	0.101 ± 0.005	0.121 ± 0.006	0.099 ± 0.004
	MAPE	$1.944\% \pm 0.034\%$	$1.8165\% \pm 0.022\%$	$1.930\% \pm 0.033\%$	$1.817\% \pm 0.026\%$
Random Forest	MSE	0.128 ± 0.007	0.097 ± 0.006	0.121 ± 0.007	0.093 ± 0.004
	MAPE	$1.882\% \pm 0.029\%$	$1.733\% \pm 0.030\%$	$1.852\% \pm 0.033\%$	$1.719\% \pm 0.031\%$
ANN	MSE	0.216 ± 0.006	0.157 ± 0.004	0.243 ± 0.013	0.146 ± 0.004
	MAPE	$2.203\% \pm 0.070\%$	$2.083\% \pm 0.049\%$	$2.234\% \pm 0.086\%$	$2.047\% \pm 0.045\%$

condition available. Moreover, the best model is then selected for a case study (Described in Chapter 5), where it is used to evaluate the speed loss of the subject vessel, and compared to the ISO19030 standard.

The training & test performance plots for each algorithm are depicted in Annex A for DDMs, and in Annex B for the best-performing HMs. Table 4.4 summarises the training performance of the DDMs/HMs in terms of MSE and MAPE. It can be seen that even the simplest explored ML algorithms, RLS & Decision Trees, result in a well-performing prediction model. However, these are still outperformed by the more advanced KRLS, XGBoost, Random Forest, and ANN. In particular, the Random Forest method has the most impressive estimation accuracy of $1.719\% \pm 0.031\%$ MAPE when coupled with the complete hybridisation package.

In terms of the optimum for each algorithm, the Hybrid methodology which combines both Hybridisation packages is consistently the best performer. This is more significant for simpler methods - RLS, for example, reducing its average MAPE by around 1.4%. On the other hand, the more complex and computationally expensive non-linear approaches do still benefit from hybridisation, however, this is to a lesser extend. In fact, the accuracy of these more sophisticated algorithms is already very high (around 1.9% MAPE for KRLS, Random Forest, and XGBoost) following a purely data-driven approach. Ultimately, the consistent accuracy improvement that HMs exhibit when compared to the base DDMs, demonstrates the benefits of incorporating physical knowledge into the methodology.

Looking further, the accuracy gained through HP2 is noticeably lower that HP1. Most likely, this is due to the fact that through HP1, a physical estimate of the target feature is fed into the ML framework, which acts as an initial 'guess' and guides the data-driven model towards the true value of the target feature. Furthermore, the benefit of the 'Time since Cleaning' and 'Stationary time' features is tied to the tracking and logging of cleaning operations. In the current work, knowledge of only the initial drydocking period in which the vessel's hull was repainted and its propeller - cleaned is available, which reduces these features' potential to improve the accuracy of the model's predictions. If information about smaller cleaning operations was available, a greater number of new features could be engineered and included in the methodology. Nevertheless, HP2 consistently improves upon the base DDM, even if only by a small amount.

In terms of complexity and computational effort, all hybridisation occurs prior to model training/testing, therefore inclusion of the additional features does not have a noticeable inverse impact on run times. In fact, even if performance gains due to HP2 are marginal in the current implementation, there is no significant downside to including it in the final model. Therefore, based on the results reported in Table 4.4, the Random Forest Hybrid Model (HP1 & HP2) was selected as the best performer and has been used in the Case study outlined further below.

Finally, despite showing a very high performance as per Table 4.4, the computational demand & accuracy of the best-performing model can be further improved. In fact, to achieve a fair comparison between the different algorithms, limitations were placed on the size of the Training and Cross-Validation datasets. Figure 4.9 shows the sensitivity of the Random Forest Hybrid Model with respect to the amount of data used for training & cross-validation in terms of MSE and MAPE. Both the size of the 95% confidence interval and the error naturally decrease with more data, however, the benefit of additional data gradually diminishes. Therefore, for the current application, a Training & Cross-Validation size of 20000 data points was determined to achieve the optimal balance between computational demand and accuracy. This is an increase on the 10000 used in the benchmark model from Table 4.4.

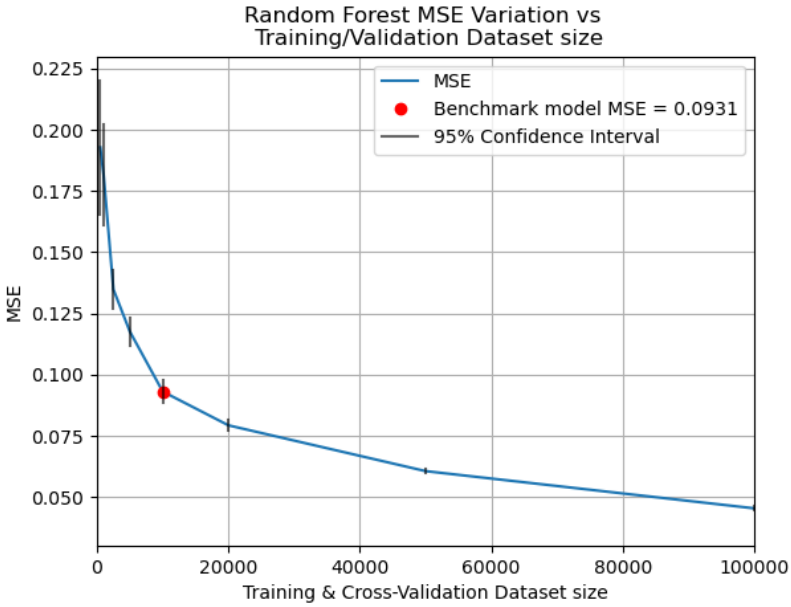

(a) MSE

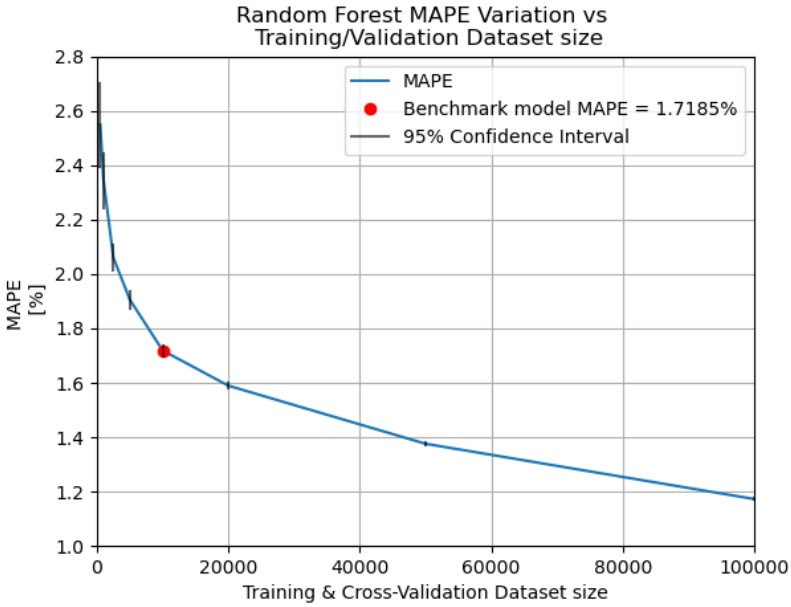

(b) MAPE

Figure 4.9: Random Forest HM - Training/Validation Dataset size vs Model Accuracy

4.9 Chapter Conclusion

A detailed description of the sensory dataset that has been collected during the operation of Holland Class Offshore Patrol Vessels was provided in Section 4.1, listing all parameter features, data granularity, data quantity, and data quality. As necessary with all data, appropriate cleaning and filtering steps have been taken to ensure a robust and high quality input is available to all constructed models, and that all volatile periods of transient operation have been excluded in order to better overall predictive performance. This is described in detail as part of Section 4.2.

Apart from preparation of the input data, the benchmark methodology that is currently used in industry i.e. the approach outlined as part of the ISO19030 standard, is broken down and explained in Section 4.3. An explanation of the workings of the developed DDMs is presented in Section 4.4, providing background into the underlying Machine Learning algorithms that have been exploited. Additionally, in Sections 4.5 manipulations are done using the input data, the vessel's particulars, and physical knowledge in order to provide a first-principle estimate of the target feature (i.e. vessel speed), as well as to enhance and supplement the sensory dataset with further features. Moreover, based on experience of the biofouling phenomenon, the elapsed time since the last cleaning of the vessel's underwater surfaces, as well as the cumulative duration that the ship has maintained stationary since cleaning, are included as dataset features in Section 4.6. Sections 4.5 & 4.6 are pivotal in terms of addressing the research gap that was identified as a result of the critical analysis in Chapter 2, and, therefore are what distinguish the current project from other similar studies on modelling the negative performance impacts of biofouling in real time.

Finally, an explanation of how the new features have successfully been incorporated together with the base DDMs to create the final state-of-the-art Hybrid Models has been given in Section 4.7. The chapter is concluded by utilising a subset of the sensory dataset, which is representative of 'clean' operating, in order to train and assess the performance of all developed models. The HMs, which are the main subject of the current work, were seen to consistently outperform DDMs, with the best model that utilises the Random Forest algorithm and the com-

plete suite of dataset features demonstrating very high predictive accuracy.

It can be said that, so far, a novel better-performing biofouling vessel performance impact estimation methodology has been successfully developed. The concept of hybrid models has successfully been translated into the field of biofouling, however, at this stage it is of little consequence as it has yet to be proven capable of generating useful knowledge and practical insight that can be used to guide a maintenance strategy. To do this, a case study is needed, which will determine whether the model, trained and tested on 'clean vessel' data in the previous section, is able to detect the performance shift that a vessel experiences as a result of the different stages of biofouling. Furthermore, if it does successfully pick up on this performance shift, there is a question as to whether it outperforms the standard practice as set out in the ISO19030 standard.

5 Case study

As discussed previously, a demonstration of how the newly-developed HMs can be used as a decision-support tool based on current and past vessel performance is necessary to provide validity to the research outcomes. Figure 4.1 previously outlined the overall approach of the research project. In the current work, HMs differentiate from DDMs only through the featureset used to train and validate them, as opposed to the incorporated ML algorithm or their structure. In fact, the more accurate of the two will inevitably outperform the other in terms of real-life application. However, to prove this, both the best performing DDM & HM, in our case - Random Forest, will be used in a direct comparison with ISO19030.

5.1 Analysis Setup

The three methodologies are tested on a large subset of the sensory data, which represents the most continuous and unbroken period of operation. In terms of timescale, this starts within a couple of months of the 'clean condition' data, used for training, and therefore it is expected that a reduction in vessel performance is naturally going to be observed. Furthermore, the subject data reflects 7 months of real-world operation. In fact, within this period of time, a successful biofouling performance impact estimation approach should be able to identify not only short-term changes in vessel performance within individual voyages / months, but also an overall long-term degradation.

In terms of data features, the ISO19030 approach only considers a small number of the available parameters and some additional information about the vessel, such as resistance curves, wind resistance coefficients, etc. as was discussed in detail in Section 4.3. The Random Forest

Method, instead, takes into account all original dataset features , with the caveat that for each individual tree estimator in the forest, a random subset of the complete featureset is considered. Additionally, physical knowledge about the ship is embedded into the method through hybridisation to form the HM, providing the model with an estimate of the target feature through novel manipulations of the dataset's features and vessel characteristics. Despite starting with the same exact data, the RF and ISO19030 approaches have differing strategies in terms of pre-processing and cleaning, where ISO19030 removes NaN entries from the dataset, applies Chauvenet's Criterion for data filtering, and removes entries with vessel speed under $10knots$. On the other hand, the HM & DDM incorporate the more sophisticated pre-processing steps described in Section 4.2.

The target KPI for ISO19030 is speed loss percentage, as per Equation 4.9, which utilises an expected speed based on the sensory data and the vessel's resistance curve, and compares it to the measured speed through water. Since the Random Forest models have also been trained to predict the same target feature, it is possible to take advantage of the same KPI and strategy. This allows for a fair comparison between methods.

5.2 ISO19030 Performance

Figure 5.1 shows the result of applying the ISO19030 approach on the available OPV data. In order to gain a better understanding of the results, a red trendline is fitted to the speed loss estimates for each month in order to visualise the short-term changes to vessel performance. Additionally, as a supplement and a showcase of long-term shifts, a green trendline is fitted to the entire suite of speed loss entries. In reality, a decrease in speed loss should be present if the vessel has been treated in some way, either through drydocking, polishing & repainting, or though underwater cleaning. An unbroken period of operation should normally be reflected by an increase in speed loss. It can be seen in Figure 5.1 that, according to ISO19030, the vessel's operational characteristics have actually improved during 4 of the 7 months. Moreover, through the entire period, there seems to be only a slight deterioration in performance. Both the long-

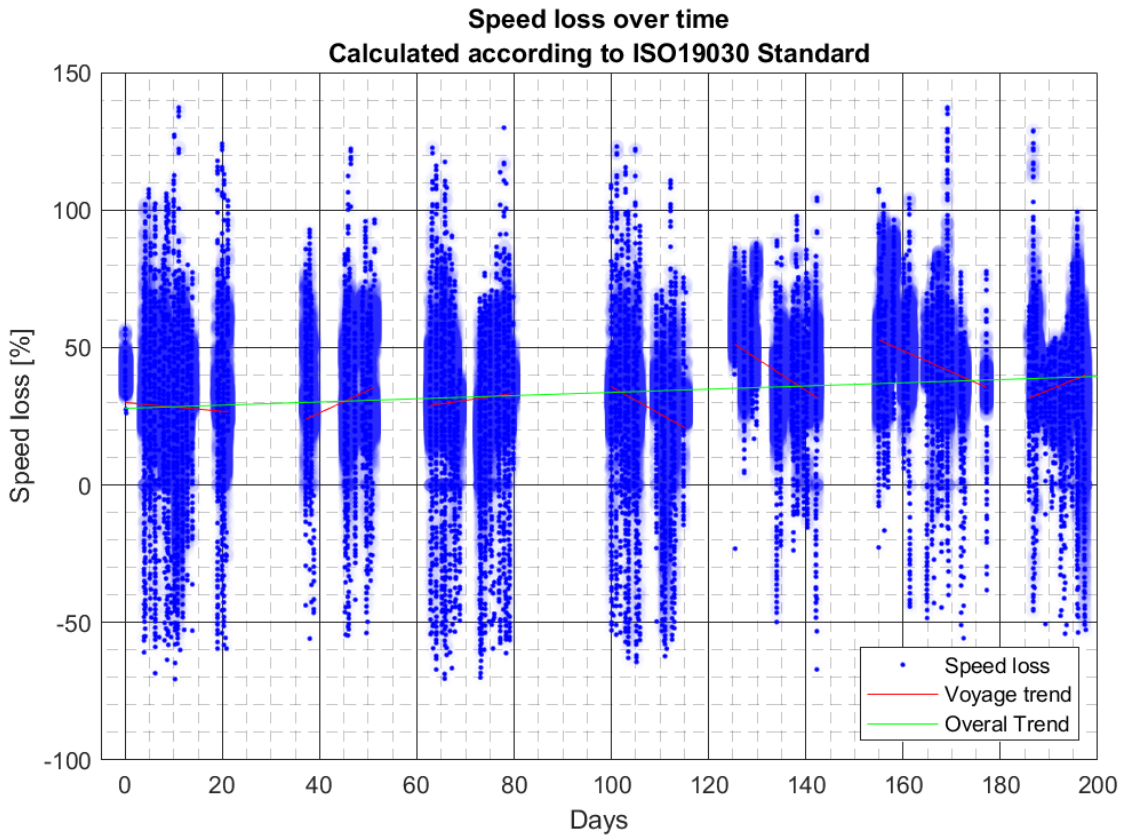

Figure 5.1: ISO19030 Speed Loss Prediction

term and short-term pictures painted by this analysis seem counterintuitive when considering the widely-observed negative effects of biofouling and their scale, which have been discussed previously in Chapter 2.

A possible explanation can be found in the fact that, apart from the major drydocking event, there is no information available about the frequency and extent of in-service underwater cleaning operations. Therefore, these could have happened both when the ship was in dock for an extended amount of time, or to a lesser extend when she was in port for a short period of a day or few.

At this point, the results can be seen as open to interpretation, and the approach should not be discounted until the outcome of the hybrid method is also observed.

5.3 Hybrid Model Performance

Figure 5.2 shows the result of applying the novel HM on the available OPV data. The same as with ISO19030, a red trendline fitted to the speed loss estimates for each month can be used to analyse performance shifts in the short-term, whereas a green one provides a visual representation of how the vessel degrades over the 7 months due to biofouling.

Based on the Hybrid method's output, the impact of biofouling seems to continuously degrade performance, which was highlighted as expected prior to the analysis. In the short-term, for each voyage / month apart from the last, there is a noticeable increase in the speed loss KPI. In fact, using Figure 5.2, estimates can be made in terms of when underwater cleaning has occurred and to what extent. Between days 20 and 40, representative of the first and second voyages, there is a substantial uplift in vessel performance (i.e. reduction in speed loss) which is most likely aligned with an underwater cleaning event. The same can be seen in the similar gap of around 20 days between the third and fourth voyage. On the other hand, between the second and third, as well as the forth and fifth, no cleaning seems to have been performed as the performance deterioration seems continuous. Of course, without knowledge of the exact maintenance log, no concrete conclusions can be made.

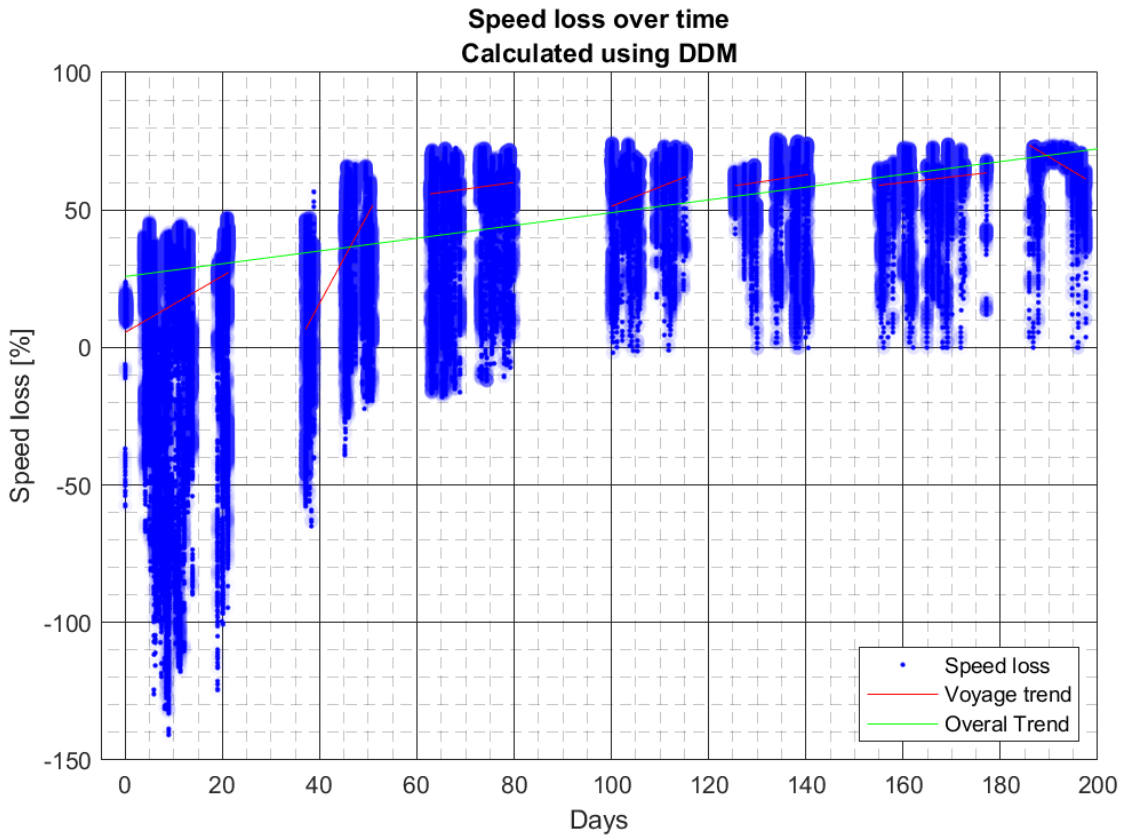

Figure 5.2: Hybrid Model Speed Loss Prediction

In terms of the higher-level trend over the entire 7-month operational period, a noticeable increase in speed loss is apparent. The simple first order polynomial trendline might not be fully accurate as a predictor of how the performance shifts over a longer period, however. In fact, the phenomenon does not seem linear in terms of time elapsed, but rather inverse logarithmic. This is physically sensible as, at some point in time, the entire underwater surface becomes subjected to macrofouling, and any further surface roughness gains are marginal. Ideally, countermeasures should be taken in terms of the ship's maintenance strategy prior to biofouling levels reaching that stage.

5.4 Data-Driven Model Performance

Figure 5.3 shows the result of applying the base DDM on the available OPV data. Again, the short and long-term trends are captured through trendlines.

There is an obvious disparity between the outputs of the two Random Forest Models. As was mentioned earlier, an improvement going from the DDM to the HM is expected due to the difference in prediction accuracy, however, the scale of this is surprising.

A possible explanation is the additional knowledge imparted into the methodology through Hybridisation Package #2, which includes time since cleaning and time spent immobile, which are directly related to the growth of biofouling and its impact on ship speed over time. Therefore, the benefit of HP2 could have potentially been underestimated in Section 4.8 by looking purely at prediction accuracy.

5.5 Method Comparison & Chapter Conclusion

All three methodologies have successfully been applied and visualisations of their results are shown in Figures 5.1, 5.2 & 5.3. As was highlighted when outlining the setup of the case study, the natural expectation is that a consistent deterioration in ship performance is to be observed due to the effect of biofouling. With the assumption that no small-scale cleaning events were conducted after the ship was in drydock, the above should be true for both the entire operational

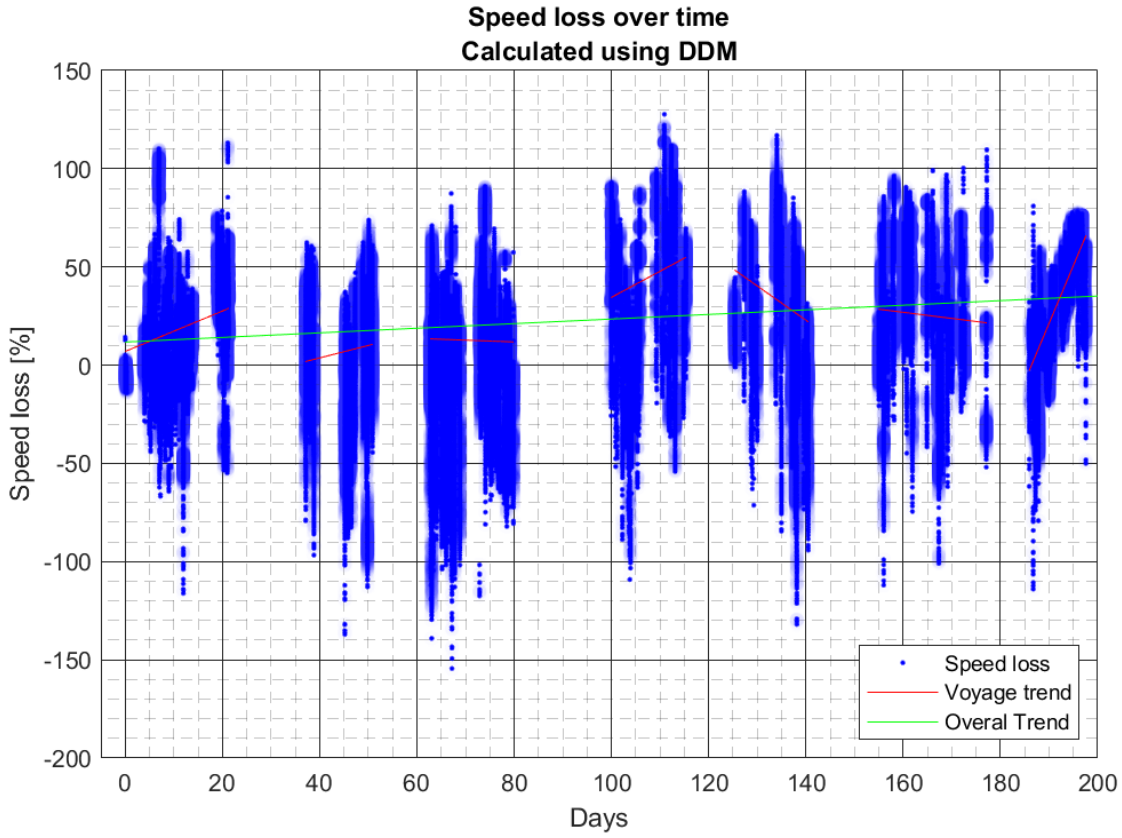

Figure 5.3: Data-Driven Model Speed Loss Prediction

period as a whole, as well as within the individual voyages that comprise it.

The ISO19030 approach only picked up a small shift in speed loss over the 7 months, as well as concluding that not only did performance not always reduce within the separate voyages, but in the majority of them, it got better. Based on the knowledge of the biofouling phenomenon, developed in Chapter 2, this is realistically not possible without external influence. The latter, of course, could not be fully discounted due to the lack of maintenance logs for the OPVs.

However, when looking at the results from the HM-based analysis, a more familiar scenario can be observed. That is, for the same operational conditions and propulsion settings, the vessel's speed through water continuously reduced in time both in the short and long-term. In order to be fully objective, it has to be said that in the final month / voyage of the operational time frame, the HM shows a performance uplift, which cannot be easily explained. There are days within this period where the ship was not in operation, which allows for the possibility of a cleaning event to have taken place.

In terms of the DDM, while it was easy to predict that its performance would be worse than that of its Hybrid counterpart, an interesting observation could still be made. In particular, a comparison between Figures 5.2 & 5.3 very clearly highlights the benefits of including real-world knowledge into the methodology through feature engineering.

On average, the novel HM method seemingly outperforms the ISO19030 approach when it comes to providing an insight into the status of biofouling's impact on vessel performance. This is true for both short-term and long-term observations. Therefore, the outcomes of the performed case study enforce the claim that HMs have a place in maintenance decision-support. In the current case, a lot of insight can be gained purely by having an operational dataset and some knowledge about the subject vessel, with a lot of potential for greater value if more information such as maintenance logs is available. Additionally, due to the nature of an OPV's mission (i.e. disjointed and highly transient as opposed to continuous and steady operation), even higher quality outcomes could be possible employing the developed strategy to commercial vessels. In fact, the latter are governed by optimised operation and maintenance schedule to a much higher extent to naval vessels, due to their extreme reliance on profitability and efficiency.

6 Project Conclusion

As was set out in Chapter 1, the current project has been developed towards addressing the critical challenges that the Maritime industry will be, and, in fact, already is, facing. Namely, there is a need to reduce Shipping's environmental impact, as well as its efficiency, through the improvement of maintenance methods and strategies. Although there are numerous promising technological advancements in different stages of development and implementation, none are mature enough to single-handedly address the issue at hand. Therefore, in the short-term, the best that can be done is to streamline the efficiency of vessel operations, as well as to maximise efficiency through optimal maintenance strategies. In fact, the above would continue to be beneficial in the future of the Maritime industry, even when currently immature technologies become ready for wide-scale implementation.

Biofouling, which leads to the deterioration of the surface condition of a vessel's underwater hull and propeller, and therefore - to the continuous growth in the ship's energy/fuel requirements in order to complete its particular mission, has been an active area of research effort for several decades. However, only recently has the availability of high quality and high enough quantity of operational data become common enough, to allow for the continuous monitoring of the biofouling state of underwater vessel surfaces, as well as its impact on ship performance. Within this research work, a new novel method of measuring the above impact was proposed, following a comprehensive review of currently available numerical methods in Chapter 2. Commonly used first-principle methods (also referred to as Physical Models - PMs) that are rooted in physical principles provide relatively accurate and, more importantly, easy-to-interpret results, however, they are far too computationally expensive to be effective in real-time monitoring ap-

plications. On the other hand, data-driven methods (also know as Data-Driven Models - DDMs) which leverage on historic observations of a vessel's operational parameters to make estimations about its real-time/future performance are highly accurate and are able to output results much quicker, however, they lack any physical interpretability, only operating as a 'black box'. Hybrid Models (HMs) seek to combine the advantages of PMs and DDMs, while bypassing their individual setbacks. These incorporate physical knowledge into the data-driven structure in order to find the ideal middle ground between the two widely-spread families of models, and, in fact, have shown great promise in other engineering applications. As, to the best of the author's knowledge, there have been no HMs proposed to tackle the biofouling problem and, also, the fact the current industry standard method for assessing a vessel's state of biofouling (the approach set out by ISO19030) has previously received criticism, an opportune research gap was identified.

The overall aim of the project - to combine state-of-the-art approaches from the fields of Machine Learning (ML) and Marine engineering and develop hybridised decision-support tools for supplementing predictive maintenance strategies, was set out in Chapter 3. Moreover, this was broken down in ordered objectives, which then successfully guided the completion of the research work. Based on the above, a robust methodology for the project was set out in Chapter 4 and was visualised in Figure 4.1. A rich operational dataset for one of the Holland Class OPVs, collected by on-board sensors, was described in detail and used as a stepping stone for the subject data-driven and hybrid models. It was taken through a rigorous pre-processing process, cleaned of erroneous entries, outliers, and sensory noise, as well as transient periods of operation which are often characterised by high degrees of volatility. Following a detailed explanation of the ISO19030 approach, the structure of the project's own base DDMs was established. Six separate promising ML algorithms were brought forward in order to ultimately select a well-performing method.

In order to create the target Hybrid methodology, a set of first-principle enhancements were brought forward. A physical estimate of the approach's target parameter - speed through water, was deterministically calculated through the vessel's open water performance curves, along

with the ShipX software suite which was used to create a wide set of resistance curves for a large variety of operating conditions. To further supplement the sensory dataset, other physical features were also added - Calm Water Resistance & Hydrostatic Parameters, Thrust, and Added Wind Resistance. Additionally, based on knowledge of the biofouling phenomenon, a further set of features was developed to encapsulate knowledge about the time the vessel has spent operational since its last cleaning event, and the length of time it has spent stationary. These are known to be highly correlated to the extend of biofouling development on underwater surfaces.

After constructing both the DDMs and their HM adaptations, a robust & extensive model training, validation and testing procedure was conducted in Section 4.8, where the candidate methods were compared in terms of their error in predicting the vessel's speed on data representative of its 'cleanest' operational state. The proposed HMs consistently outperformed their DDM counterparts for all proposed ML algorithms, where the Random Forest algorithm with the complete suite of hybridisation achieved the best overall results with an impressively low Mean Absolute Percentage Error (MAPE) of $1.719\% \pm 0.031\%$. In fact, this could be further improved by increasing the amount of data used for its Training & Cross-Validation, as was shown in Figure 4.9.

In order to demonstrate the proposed method's performance, a case study was then conducted in Chapter 5, utilising the best performing Hybrid and Data-Driven models in order to assess the percentage speed loss the vessel has experienced over a 7 month period, representative of a fouled hull & propeller condition. This was directly compared to the results following the ISO19030 approach on the same set of data. The Hybrid Method achieved the most accurate and realistic assessment of the impact of biofouling on the vessel's performance. While the ISO19030 approach struggled to detect a definitive performance drop, the HM consistently identified losses in performance in both the short-term (per voyage) and long-term (for the entire period). Moreover, when compared to the purely data-driven approach, the HM provided substantial improvements in terms of its practical application. This is most likely due to the real-world & physical knowledge of the biofouling phenomenon that was embedded into it through the two hybridisation packages discussed in Section 4.7 These results serve to highlight the

proposed model's potential as a viable decision-support tool for maintenance planning, and its ability to provide quality insights to the vessel's owner & operator. The latter would ultimately enable a more proactive, efficient, and effective maintenance strategy.

While the developed Hybrid Methodology is unquestionably already well-capable, it can be improved, which, in the author's opinion, can be a fruitful avenue for further research. There is a large number of candidate features that can be added through hybridisation, and only a small subset of these was explored within the current work as an initial stepping stone. The methodology is, in its core, data-centric, therefore the easiest way to improve upon it, is to improve the quality & quantity of data. Most notably, it can be better validated through a more intimate knowledge of associated maintenance activities such as the cleaning schedule for the vessel's underwater surfaces. Moreover, the current work is centered around Offshore Patrol Vessels, whose operation is mission-based and, therefore, sporadic. Commercial vessel which are operated in a more continuous and constant manner would be accompanied with a 'smoother' dataset with much less downtime. Additionally, the later are profit-driven, therefore, a biofouling strategy decision-support method would be much more valuable for their owners & operators. Finally, while biofouling performance impact estimation has, hopefully, been proven to be a good candidate for hybridisation, this is not to say that there are no other niches of predictive maintenance, performance analysis, and, in more broad terms, marine engineering that can experience similar benefits.

In conclusion, within this project, a novel Hybrid Model was successfully developed and utilised to estimate the impact biofouling has on a vessel's performance, marking a noteworthy advancement in the field. The methodology used to create this output is easy to expand. In fact, in the future, more physical knowledge can be imparted into the model simply by adding further physical-based features into the sensory dataset, depending on the case-by-case availability of data. Certainly, there could be many more beneficial parameter features that have not been covered here, but would potentially provide increases in accuracy and physical robustness. Additionally, more detailed knowledge in terms of the logs of vessel cleaning events, both in dry-dock and by underwater means, could greatly increase the model's ability. All of the above

taken into account, the methodology of the current project can already successfully be used as a foundation for the development of highly performing hybrid decision-support tools to aid in the optimisation of vessel maintenance strategies.

References

[1] H. Ritchie and M. Roser, *CO2 and greenhouse gas emissions*. Our world in data, 2020.

[2] IPCC, "Global warming of 1. 5 ° C. Tech. Rep. , Intergovernmental Panel on Climate Change," 2018. [Online]. Available: https://www.ipcc.ch/sr15/

[3] K. Anderson and G. Peters, "The trouble with negative emissions," *Science*, vol. 354, no. 6309, pp. 182–183, 2016.

[4] J. Hoffmann and S. Kumar, "Globalisation-the maritime nexus," in *The handbook of maritime economics and business*, 2013.

[5] E. A. Bouman, E. Lindstad, A. I. Rialland, and A. H. Strømman, "State-of-the-art technologies, measures, and potential for reducing GHG emissions from shipping-a review," *Transportation Research Part D: Transport and Environment*, vol. 52, pp. 408–421, 2017.

[6] D. Owen, Y. Demirel, E. Oguz, T. Tezdogan, and A. Incecik, "Investigating the effect of biofouling on propeller characteristics using cfd," *Ocean Engineering*, vol. 159, pp. 505–516, 2018.

[7] K. Seo, M. Atlar, and B. Goo, "A study on the hydrodynamic effect of biofouling on marine propeller," *Journal of the Korean Society of Marine Environment & Safety*, vol. 22, no. 1, pp. 123–128, 2016.

[8] Ø. Buhaug, J. J. Corbett, O. Endresen, V. Eyring, J. Faber, S. Hanayama, D. Lee, H. Lindstad, A. Mjelde, C. Palsson *et al.*, "Second IMO greenhouse

gas study," 2009. [Online]. Available: https://www.imo.org/en/OurWork/Environment/Pages/Second-IMO-GHG-Study-2009.aspx

[9] T. Smith, J. Jalkanen, B. Anderson, J. J. Corbett, J. Faber, S. Hanayama, E. O'Keeffe, S. Parker, L. Johansson, L. Aldous, C. Raucci, M. Traut *et al.*, "Third IMO greenhouse gas study," 2014. [Online]. Available: https://www.imo.org/en/OurWork/Environment/Pages/Greenhouse-Gas-Studies-2014.aspx

[10] MEPC, "Fourth IMO greenhouse gas study," 2020. [Online]. Available: https://docs.imo.org

[11] A. Coraddu, L. Oneto, F. Baldi, and D. Anguita, "Vessels fuel consumption forecast and trim optimisation: a data analytics perspective," *Ocean Engineering*, vol. 130, pp. 351–370, 2017.

[12] I. Ho-Chun Fang, F. Cheng, A. Incecik, and P. Carnie, "Global marine trends 2030," 2013. [Online]. Available: http://www.futurenautics.com/wp-content/uploads/2013/10/GlobalMarineTrends2030Report.pdf

[13] P. Gilbert, C. Walsh, M. Traut, U. Kesieme, K. Pazouki, and A. Murphy, "Assessment of full life-cycle air emissions of alternative shipping fuels," *Journal of cleaner production*, vol. 172, pp. 855–866, 2018.

[14] P. Balcombe, J. Brierley, C. Lewis, L. Skatvedt, J. Speirs, A. Hawkes, and I. Staffell, "How to decarbonise international shipping: Options for fuels, technologies and policies," *Energy conversion and management*, vol. 182, pp. 72–88, 2019.

[15] R. Adland, P. Cariou, H. Jia, and F. Wolff, "The energy efficiency effects of periodic ship hull cleaning," *Journal of Cleaner Production*, vol. 178, pp. 1–13, 2018.

[16] J. Chen, Y. Fei, and Z. Wan, "The relationship between the development of global maritime fleets and ghg emission from shipping," *Journal of environmental management*, vol. 242, pp. 31–39, 2019.

[17] MEPC, "Resolution mepc.203(62)," 2011. [Online]. Available: https://wwwcdn.imo.org/localresources/en/KnowledgeCentre/IndexofIMOResolutions/MEPCDocuments/MEPC.203(62).pdf

[18] L. Bilgili, "Life cycle comparison of marine fuels for imo 2020 sulphur cap," *Science of The Total Environment*, vol. 774, p. 145719, 2021.

[19] IMO, "Meeting summary of the Marine Environment Protection Committee, 72nd session." 2018. [Online]. Available: https://www.imo.org/en/MediaCentre/MeetingSummaries/Pages/MEPC-72nd-session.aspx

[20] N. Rehmatulla, J. Calleya, and T. Smith, "The implementation of technical energy efficiency and CO2 emission reduction measures in shipping," *Ocean engineering*, vol. 139, pp. 184–197, 2017.

[21] M. S. Eide, T. Longva, P. Hoffmann, Ø. Endresen, and S. B. Dalsøren, "Future cost scenarios for reduction of ship CO2 emissions," *Maritime Policy & Management*, vol. 38, no. 1, pp. 11–37, 2011.

[22] H. Johnson, M. Johansson, and K. Andersson, "Barriers to improving energy efficiency in short sea shipping: an action research case study," *Journal of Cleaner Production*, vol. 66, pp. 317–327, 2014.

[23] M. Acciaro, P. Hoffmann, and M. Eide, "The energy efficiency gap in maritime transport," *Journal of Shipping and Ocean Engineering*, vol. 3, no. 1-2, p. 1, 2013.

[24] S. Moussault, J. Pruijn, E. van der Voort, and G. van IJserloo, "Modelling maintenance–cost optimised maintenance in shipping," in *Proceedings of the 12th Symposium on High-Performance Marine Vehicles, HIPER'20*. Technische Universität Hamburg-Harburg, 2020.

[25] G. Tsaganos, N. Nikitakos, D. Dalaklis, A. I. Ölcer, and D. Papachristos, "Machine learning algorithms in shipping: improving engine fault detection and diagnosis via ensemble methods," *WMU Journal of Maritime Affairs*, pp. 1–22, 2020.

[26] P. Karagiannidis and N. Themelis, "Data-driven modelling of ship propulsion and the effect of data pre-processing on the prediction of ship fuel consumption and speed loss," *Ocean Engineering*, vol. 222, p. 108616, 2021.

[27] R. Halim, L. Kirstein, O. Merk, and L. Martinez, "Decarbonization pathways for international maritime transport: A model-based policy impact assessment," *Sustainability*, vol. 10, no. 7, p. 2243, 2018.

[28] A. Farkas, N. Degiuli, and I. Martić, "Assessment of the effect of biofilm on the ship hydrodynamic performance by performance prediction method," *International Journal of Naval Architecture and Ocean Engineering*, vol. 13, pp. 102–114, 2021.

[29] M. Legg, M. K. Yücel, I. G. De Carellan, V. Kappatos, C. Selcuk, and T. H. Gan, "Acoustic methods for biofouling control: A review," *Ocean Engineering*, vol. 103, pp. 237–247, 2015.

[30] H. Flemming, P. S. Murthy, R. Venkatesan, and K. Cooksey, *Marine and industrial biofouling*. Springer, 2009.

[31] D. Oliveira and L. Granhag, "Matching forces applied in underwater hull cleaning with adhesion strength of marine organisms," *Journal of Marine Science and Engineering*, vol. 4, no. 4, p. 66, 2016.

[32] N. Rehmatulla and T. Smith, "Barriers to energy efficient and low carbon shipping," *Ocean Engineering*, vol. 110, pp. 102–112, 2015.

[33] M. P. Schultz, J. A. Bendick, E. R. Holm, and W. M. Hertel, "Economic impact of biofouling on a naval surface ship," *Biofouling*, vol. 27, no. 1, pp. 87–98, 2011.

[34] A. Farkas, N. Degiuli, and I. Martić, "The impact of biofouling on the propeller performance," *Ocean Engineering*, vol. 219, p. 108376, 2021.

[35] B. S. Institute, "Bs en 13306:2017: Maintenance. maintenance terminology," 2017.

[36] I. Lazakis, O. Turan, and S. Aksu, "Increasing ship operational reliability through the implementation of a holistic maintenance management strategy," *Ships and Offshore Structures*, vol. 5, no. 4, pp. 337–357, 2010.

[37] D. Simion, A. Purcărea, A. Cotorcea, and F. Nicolae, "Maintenance onboard ships using computer maintenance management system," *Scientific Bulletin" Mircea cel Batran" Naval Academy*, vol. 23, no. 1, pp. 134A–141, 2020.

[38] I. Zaman, K. Pazouki, R. Norman, S. Younessi, and S. Coleman, "Challenges and opportunities of big data analytics for upcoming regulations and future transformation of the shipping industry," *Procedia engineering*, vol. 194, pp. 537–544, 2017.

[39] Ø. J. Rødseth, L. P. Perera, and B. Mo, "Big data in shipping-challenges and opportunities," 2016.

[40] L. P. Perera, "Handling big data in ship performance and navigation monitoring," *Smart Ship Technology*, pp. 89–97, 2017.

[41] T. W. F. Hasselaar, "An investigation into the development of an advanced ship performance monitoring and analysis system," Ph.D. dissertation, Newcastle University, 2011.

[42] M. I. Foteinos, E. I. Tzanos, and N. P. Kyrtatos, "Ship hull fouling estimation using shipboard measurements, models for resistance components, and shaft torque calculation using engine model," *Journal of Ship Research*, vol. 61, no. 2, pp. 64–74, 2017.

[43] B. P. Pedersen and J. Larsen, "Modeling of ship propulsion performance," in *World Maritime Technology Conference WMTC2009*, 2009.

[44] E. B. Beşikçi, O. Arslan, O. Turan, and A. I. Ölçer, "An artificial neural network based decision support system for energy efficient ship operations," *Computers & Operations Research*, vol. 66, pp. 393–401, 2016.

[45] L. Aldous, T. Smith, R. Bucknall, and P. Thompson, "Uncertainty analysis in ship performance monitoring," *Ocean Engineering*, vol. 110, pp. 29–38, 2015.

[46] G. Li, H. Zhang, B. Kawan, H. Wang, O. L. Osen, and A. n. Styve, "Analysis and modeling of sensor data for ship motion prediction," in *OCEANS 2016-Shanghai*. IEEE, 2016, pp. 1–7.

[47] I. Valchev, A. Coraddu, M. Kalikatzarakis, R. Geertsma, and L. Oneto, "Numerical methods for monitoring and evaluating the biofouling state and effects on vessels' hull and propeller performance: A review," *Ocean Engineering*, vol. 251, p. 110883, 2022.

[48] R. L. Townsin, "The ship hull fouling penalty," *Biofouling*, vol. 19, no. S1, pp. 9–15, 2003.

[49] Z. Koboević, D. Bebić, and Z. Kurtela, "New approach to monitoring hull condition of ships as objective for selecting optimal docking period," *Ships and Offshore Structures*, vol. 14, no. 1, pp. 95–103, 2019.

[50] A. Farkas, S. Song, N. Degiuli, I. Martić, and Y. K. Demirel, "Impact of biofilm on the ship propulsion characteristics and the speed reduction," *Ocean Engineering*, vol. 199, p. 107033, 2020.

[51] M. Candries, M. Atlar, and C. D. Anderson, "Estimating the impact of new-generation antifoulings on ship performance: the presence of slime," *Journal of Marine Engineering & Technology*, vol. 2, no. 1, pp. 13–22, 2003.

[52] I. C. Davidson, G. Smith, G. V. Ashton, G. M. Ruiz, and C. Scianni, "An experimental test of stationary lay-up periods and simulated transit on biofouling accumulation and transfer on ships," *Biofouling*, vol. 36, no. 4, pp. 455–466, 2020.

[53] D. Uzun, Y. K. Demirel, A. Coraddu, and O. Turan, "Time-dependent biofouling growth model for predicting the effects of biofouling on ship resistance and powering," *Ocean Engineering*, vol. 191, p. 106432, 2019.

[54] C. Hewitt, S. Gollasch, and D. Minchin, "The vessel as a vector-biofouling, ballast water and sediments," in *Biological invasions in marine ecosystems*, 2009.

[55] C. Moser, T. Wier, J. Grant, M. First, M. Tamburri, G. Ruiz, A. Miller, and L. Drake, "Quantifying the total wetted surface area of the world fleet: a first step in determining the potential extent of ships' biofouling," *Biological invasions*, vol. 18, no. 1, pp. 265–277, 2016.

[56] M. Atlar, I. A. Yeginbayeva, S. Turkmen, Y. K. Demirel, A. Carchen, A. Marino, and D. Williams, "A rational approach to predicting the effect of fouling control systems on "in-service" ship performance," *GMO Journal of Ship and Marine Technology*, vol. 24, no. 213, pp. 5–36, 2018.

[57] M. P. Schultz, "Effects of coating roughness and biofouling on ship resistance and powering," *Biofouling*, vol. 23, no. 5, pp. 331–341, 2007.

[58] S. Song, Y. K. Demirel, C. D. M. Muscat-Fenech, T. Tezdogan, and M. Atlar, "Fouling effect on the resistance of different ship types," *Ocean Engineering*, vol. 216, p. 107736, 2020.

[59] E. G. Haslbeck and G. S. Bohlander, "Microbial biofilm effects on drag-lab and field," in *The National Shipbuilding Research Program, Ship Production Symposium Proceedings*, 1992.

[60] S. Watanabe, N. Nagamatsu, K. Yokoo, and Y. Kawakami, "The augmentation in frictional resistance due to slime," *Journal of the Kansai Society of Naval Architects*, vol. 131, pp. 45–51, 1969.

[61] G. Kempf, "On the effect of roughness on the resistance of ships," *Trans INA*, vol. 79, pp. 109–119, 1937.

[62] Y. K. Demirel, D. Uzun, Y. Zhang, H. C. Fang, A. H. Day, and O. Turan, "Effect of barnacle fouling on ship resistance and powering," *Biofouling*, vol. 33, no. 10, pp. 819–834, 2017.

[63] M. P. Schultz, "Frictional resistance of antifouling coating systems," *Journal of Fluids Engineering*, vol. 126, no. 6, pp. 1039–1047, 2004.

[64] A. Coraddu, L. Oneto, F. Baldi, F. Cipollini, M. Atlar, and S. Savio, "Data-driven ship digital twin for estimating the speed loss caused by the marine fouling," *Ocean Engineering*, vol. 186, p. 106063, 2019.

[65] CSC, "A transparent and reliable hull and propeller performance standard," 2011. [Online]. Available: https://bellona.no/assets/sites/3/2015/06/fil_MEPC_63-4-8_-_A_transparent_and_reliable_hull_and_propeller_performance_standard_CSC1.pdf

[66] IMO, "A transparent and reliable hull and propeller performance standard, MEPC 63-4-8." 2011. [Online]. Available: http://fs.fish.govt.nz/Page.aspx?pk=7&sc=SUR

[67] F. Sylvester, O. Kalaci, B. Leung, A. Lacoursière-Roussel, C. C. Murray, F. M. Choi, M. A. Bravo, T. W. Therriault, and H. J. MacIsaac, "Hull fouling as an invasion vector: can simple models explain a complex problem?" *Journal of Applied Ecology*, vol. 48, no. 2, pp. 415–423, 2011.

[68] F. T. Chan, H. J. MacIsaac, and S. A. Bailey, "Relative importance of vessel hull fouling and ballast water as transport vectors of nonindigenous species to the canadian arctic," *Canadian Journal of Fisheries and Aquatic Sciences*, vol. 72, no. 8, pp. 1230–1242, 2015.

[69] C. Song and W. Cui, "Review of underwater ship hull cleaning technologies," *Journal of Marine Science and Application*, pp. 1–15, 2020.

[70] D. J. Morrisey and C. Woods, *In-water cleaning technologies: Review of information*. Ministry for Primary Industries, Manatū Ahu Matua, 2015.

[71] J. Hua, Y. Chiu, and C. Tsai, "En-route operated hydroblasting system for counteracting biofouling on ship hull," *Ocean Engineering*, vol. 152, pp. 249–256, 2018.

[72] J. Bohlander and M. Zealand, *Review of options for in-water cleaning of ships*. Ministry of Agriculture and Forestry, 2009.

[73] C. Scianni and E. Georgiades, "Vessel in-water cleaning or treatment: identification of environmental risks and science needs for evidence-based decision making," *Frontiers in Marine Science*, vol. 6, p. 467, 2019.

[74] M. Tamburri, I. Davidson, M. First, C. Scianni, K. Newcomer, G. Inglis, E. Georgiades, J. Barnes, and G. Ruiz, "In-water cleaning and capture to remove ship biofouling: An initial evaluation of efficacy and environmental safety," *Frontiers in Marine Science*, 2020.

[75] M. Cheliotis, I. Lazakis, and G. Theotokatos, "Machine learning and data-driven fault detection for ship systems operations," *Ocean Engineering*, vol. 216, p. 107968, 2020.

[76] S. Lim, K. Pazouki, and A. J. Murphy, "Monitoring systems in design of ships," in *Practical Design of Ships and Other Floating Structures*, 2019.

[77] S. D. Kaminaris, E. Tripolitakis, G. S. Stavrakakis, and C. Diakaki, "An intelligent data acquisition and transmission platform for the development of voyage and maintenance plans for ships," in *International Conference on Information, Intelligence, Systems and Applications*, 2014.

[78] Ø. Ø. Dalheim and S. Steen, "Uncertainty in the real-time estimation of ship speed through water," *Ocean Engineering*, vol. 235, p. 109423, 2021.

[79] Y. Raptodimos, I. Lazakis, G. Theotokatos, T. Varelas, and L. Drikos, "Ship sensors data collection and analysis for condition monitoring of ship structures and machinery systems," in *Smart Ship Technology*, 2016.

[80] R. Costantini and S. Susstrunk, "Virtual sensor design," in *Sensors and Camera Systems for Scientific, Industrial, and Digital Photography Applications V*, 2004.

[81] A. Ikonomakis, U. D. Nielsen, K. K. Holst, J. Dietz, and R. Galeazzi, "How good is the stw sensor? an account from a larger shipping company," *Journal of Marine Science and Engineering*, vol. 9, no. 5, p. 465, 2021.

[82] A. Brandsæter and E. Vanem, "Ship speed prediction based on full scale sensor measurements of shaft thrust and environmental conditions," *Ocean Engineering*, vol. 162, pp. 316–330, 2018.

[83] A. Coraddu, S. Lim, L. Oneto, K. Pazouki, R. Norman, and A. J. Murphy, "A novelty detection approach to diagnosing hull and propeller fouling," *Ocean Engineering*, vol. 176, pp. 65–73, 2019.

[84] ISO, "ISO 19030-1, Ships and marine technology measurement of changes in hull and propeller performance - Part 1: General principles," 2016.

[85] ——, "ISO 19030-2, Ships and marine technology measurement of changes in hull and propeller performance - Part 2: Default method," 2016.

[86] ——, "ISO 19030-3, Ships and marine technology measurement of changes in hull and propeller performance - Part 3: Alternative methods," 2016.

[87] L. Liang, Y. Pang, Y. Tang, H. Zhang, H. Liu, and Y. Liu, "Combined wear of slurry erosion, cavitation erosion, and corrosion on the simulated ship surface," *Advances in mechanical engineering*, vol. 11, no. 3, 2019.

[88] A. Carchen and M. Atlar, "Four kpis for the assessment of biofouling effect on ship performance," *Ocean Engineering*, vol. 217, p. 107971, 2020.

[89] K. P. Logan, "Using a ship's propeller for hull condition monitoring," *Naval Engineers Journal*, vol. 124, no. 1, pp. 71–87, 2012.

[90] E. Erol, C. E. Cansoy, and O. Ö. Aybar, "Assessment of the impact of fouling on vessel energy efficiency by analyzing ship automation data," *Applied Ocean Research*, vol. 105, p. 102418, 2020.

[91] A. Farkas, N. Degiuli, I. Martić, and I. Ančić, "Performance prediction method for fouled surfaces," *Applied Ocean Research*, vol. 99, p. 102151, 2020.

[92] Y. K. Demirel, S. Song, O. Turan, and A. Incecik, "Practical added resistance diagrams to predict fouling impact on ship performance," *Ocean Engineering*, vol. 186, p. 106112, 2019.

[93] S. Song, Y. K. Demirel, and M. Atlar, "Penalty of hull and propeller fouling on ship self-propulsion performance," *Applied Ocean Research*, vol. 94, p. 102006, 2020.

[94] S. García, A. Trueba, D. Boullosa-Falces, H. Islam, and C. G. Soares, "Predicting ship frictional resistance due to biofouling using reynolds-averaged navier-stokes simulations," *Applied Ocean Research*, vol. 101, p. 102203, 2020.

[95] A. Senteris, A. Kanellopoulou, and G. N. Zaraphonitis, "A machine learning approach to assess vessel performance based on operational profile," *Sustainable Development and Innovations in Marine Technologies*, pp. 496–502, 2019.

[96] A. Laurie, E. Anderlini, J. Dietz, and G. Thomas, "Machine learning for shaft power prediction and analysis of fouling related performance deterioration," *Ocean Engineering*, p. 108886, 2021.

[97] S. Song, Y. K. Demirel, and M. Atlar, "Propeller performance penalty of biofouling: Computational fluid dynamics prediction," *Journal of Offshore Mechanics and Arctic Engineering*, vol. 142, no. 6, p. 061901, 2020.

[98] A. Carchen, M. Atlar, S. Turkmen, K. Pazouki, and A. J. Murphy, "Ship performance monitoring dedicated to biofouling analysis: Development on a small size research catamaran," *Applied Ocean Research*, vol. 89, pp. 224–236, 2019.

[99] A. Coraddu, L. Oneto, F. Cipollini, M. Kalikatzarakis, G. J. Meijn, and R. Geertsma, "Physical, data-driven and hybrid approaches to model engine exhaust gas temperatures in operational conditions," *Ships and Offshore Structures*, pp. 1–22, 2021.

[100] M. Haranen, P. Pakkanen, R. Kariranta, and J. Salo, "White, grey and black-box modelling in ship performance evaluation," in *Hull performence & insight conference*, 2016.

[101] A. Coraddu, L. Oneto, F. Baldi, and D. Anguita, "Ship efficiency forecast based on sensors data collection: Improving numerical models through data analytics," in *OCEANS-Genova*, 2015.

[102] A. Coraddu, L. Oneto, A. Ghio, S. Savio, D. Anguita, and M. Figari, "Machine learning approaches for improving condition-based maintenance of naval propulsion plants," *Proceedings of the Institution of Mechanical Engineers, Part M: Journal of Engineering for the Maritime Environment*, vol. 230, no. 1, pp. 136–153, 2016.

[103] L. Leifsson, H. Sævarsdóttir, S. Sigurdsson, and A. Vésteinsson, "Grey-box modeling of an ocean vessel for operational optimization," *Simulation Modelling Practice and Theory*, vol. 16, no. 8, pp. 923–932, 2008.

[104] S. Song, Y. K. Demirel, and M. Atlar, "An investigation into the effect of biofouling on the ship hydrodynamic characteristics using cfd," *Ocean Engineering*, vol. 175, pp. 122–137, 2019.

[105] O. Turan, Y. K. Demirel, S. Day, and T. Tezdogan, "Experimental determination of added hydrodynamic resistance caused by marine biofouling on ships," *Transportation Research Procedia*, vol. 14, pp. 1649–1658, 2016.

[106] P. F. Wang, S. Lieberman, and L. Ho, "Unsupervised learning neural network for classification of ship-hull fouling conditions," in *IEEE International Joint Conference on Neural Network Proceedings*, 2006.

[107] N. J. Bloomfield, S. Wei, B. A. Woodham, P. Wilkinson, and A. P. Robinson, "Automating the assessment of biofouling in images using expert agreement as a gold standard," *Scientific reports*, vol. 11, no. 1, pp. 1–10, 2021.

[108] C. S. Chin, J. T. Si, A. S. Clare, and M. Ma, "Intelligent image recognition system for marine fouling using softmax transfer learning and deep convolutional neural networks," *Complexity*, vol. 2017, 2017.

[109] P. S. Granville, "The frictional resistance and turbulent boundary layer of rough surfaces," *Journal of ship research*, vol. 2, no. 04, pp. 52–74, 1958.

[110] ——, "Three indirect methods for the drag characterization of arbitrarily rough surfaces on flat plates," *Journal of Ship Research*, vol. 31, no. 1, 1987.

[111] F. H. Todd, "Ch. VIII, "Resistance and Propulsion"," in *Principles of Naval Architecture*, 1967.

[112] J. Montewka, F. Goerlandt, M. Lensu, L. Kuuliala, and R. Guinness, "Toward a hybrid model of ship performance in ice suitable for route planning purpose," *Proceedings of the Institution of Mechanical Engineers, Part O: Journal of Risk and Reliability*, vol. 233, no. 1, pp. 18–34, 2019.

[113] M. P. Schultz, J. M. Walker, C. N. Steppe, and K. A. Flack, "Impact of diatomaceous biofilms on the frictional drag of fouling-release coatings," *Biofouling*, vol. 31, no. 9-10, pp. 759–773, 2015.

[114] A. Farkas, N. Degiuli, and I. Martić, "Towards the prediction of the effect of biofilm on the ship resistance using cfd," *Ocean Engineering*, vol. 167, pp. 169–186, 2018.

[115] V. Bertram, "Some heretic thoughts on ISO 19030," in *HullPIC Hull Performance & Insight Conference*, 2017.

[116] D. R. Oliveira, L. Granhag, and L. Larsson, "A novel indicator for ship hull and propeller performance: Examples from two shipping segments," *Ocean Engineering*, vol. 205, p. 107229, 2020.

[117] F. J. Montáns, F. Chinesta, R. Gómez-Bombarelli, and J. N. Kutz, "Data-driven modeling and learning in science and engineering," *Comptes Rendus Mécanique*, vol. 347, no. 11, pp. 845–855, 2019.

[118] B. P. Pedersen and J. Larsen, "Prediction of full-scale propulsion power using artificial neural networks," in *International conference on computer and IT applications in the maritime industries*, 2009.

[119] I. Goodfellow, Y. Bengio, and A. Courville, *Deep learning*. MIT press, 2016.

[120] A. Swider, S. Skjong, and E. Pedersen, "Complementarity of data-driven and simulation modeling based on the power plant model of the offshore vessel," in *International Conference on Offshore Mechanics and Arctic Engineering*, 2017.

[121] A. Coraddu, M. Kalikatzarakis, L. Oneto, G. J. Meijn, M. Godjevac, and R. D. Geertsmad, "Ship diesel engine performance modelling with combined physical and machine learning approach," in *International Naval Engineering Conference and Exhibition*, 2018.

[122] L. Yang, G. Chen, N. G. M. Rytter, J. Zhao, and D. Yang, "A genetic algorithm-based grey-box model for ship fuel consumption prediction towards sustainable shipping," *Annals of Operations Research*, pp. 1–27, 2019.

[123] M. Liu, Q. Zhou, X. Wang, C. Yu, and M. Kang, "Voyage performance evaluation based on a digital twin model," *IOP Conference Series: Materials Science and Engineering*, vol. 929, no. 1, p. 012027, 2020.

[124] S. Walfish, "A review of statistical outlier methods," *Pharmaceutical technology*, vol. 30, no. 11, p. 82, 2006.

[125] W. Chauvenet, *A manual of spherical and practical astronomy: embracing the general problems of spherical astronomy, the special applications to nautical astronomy, and the theory and use of fixed and portable astronomical instruments, with an appendix on the method of least squares*. JB Lippincott Company, 1871.

[126] S. Shalev-Shwartz and S. Ben-David, *Understanding machine learning: From theory to algorithms*. Cambridge university press, 2014.

[127] J. D. Hamilton, *Time series analysis*. Princeton university press, 1994.

[128] V. N. Vapnik, *Statistical Learning Theory*. Wiley-Interscience, 1998.

[129] J. Shawe-Taylor, N. Cristianini *et al.*, *Kernel methods for pattern analysis*. Cambridge university press, 2004.

[130] L. Oneto, *Model selection and error estimation in a nutshell*. Springer, 2020.

[131] R. Kohavi *et al.*, "A study of cross-validation and bootstrap for accuracy estimation and model selection," in *Ijcai*, vol. 14, no. 2. Montreal, Canada, 1995, pp. 1137–1145.

[132] B. Efron and R. J. Tibshirani, *An introduction to the bootstrap*. CRC press, 1994.

[133] N. Metropolis and S. Ulam, "The monte carlo method," *Journal of the American statistical association*, vol. 44, no. 247, pp. 335–341, 1949.

[134] L. Rosasco, E. De Vito, A. Caponnetto, M. Piana, and A. Verri, "Are loss functions all the same?" *Neural computation*, vol. 16, no. 5, pp. 1063–1076, 2004.

[135] A. N. Tikhonov and V. Y. Arsenin, *Methods of solution of ill-posed problems*. Nauka, Moscow, 1979.

[136] V. Vovk, "Kernel ridge regression," in *Empirical inference*. Springer, 2013, pp. 105–116.

[137] B. Schölkopf, R. Herbrich, and A. J. Smola, "A generalized representer theorem," in *International conference on computational learning theory*. Springer, 2001, pp. 416–426.

[138] N. Cristianini, J. Shawe-Taylor *et al.*, *An introduction to support vector machines and other kernel-based learning methods*. Cambridge university press, 2000.

[139] B. Schölkopf, "The kernel trick for distances," *Advances in neural information processing systems*, vol. 13, 2001.

[140] S. S. Keerthi and C.-J. Lin, "Asymptotic behaviors of support vector machines with gaussian kernel," *Neural computation*, vol. 15, no. 7, pp. 1667–1689, 2003.

[141] L. Oneto, A. Ghio, S. Ridella, and D. Anguita, "Support vector machines and strictly positive definite kernel: The regularization hyperparameter is more important than the kernel hyperparameters," in *2015 International Joint Conference on Neural Networks (IJCNN)*. IEEE, 2015, pp. 1–4.

[142] M. Fernández-Delgado, E. Cernadas, S. Barro, and D. Amorim, "Do we need hundreds of classifiers to solve real world classification problems?" *The journal of machine learning research*, vol. 15, no. 1, pp. 3133–3181, 2014.

[143] M. Wainberg, B. Alipanahi, and B. J. Frey, "Are random forests truly the best classifiers?" *The Journal of Machine Learning Research*, vol. 17, no. 1, pp. 3837–3841, 2016.

[144] D. M. Young, *Iterative solution of large linear systems*. Dover Publications, 2003.

[145] T. Hastie, R. Tibshirani, J. H. Friedman, and J. H. Friedman, *The elements of statistical learning: data mining, inference, and prediction*. Springer, 2009, vol. 2.

[146] C.P.Bathula, "Machine Learning concept 53: XGBoosting & ADABoosting." 2023. [Online]. Available: https://medium.com/@chandu.bathula16/machine-learning-concept-53-xgboosting-adaboosting-663cd8c920e2

[147] T. Chen and C. Guestrin, "Xgboost: A scalable tree boosting system," in *Proceedings of the 22nd acm sigkdd international conference on knowledge discovery and data mining*, 2016, pp. 785–794.

[148] L. Breiman, "Random forests," *Machine learning*, vol. 45, pp. 5–32, 2001.

[149] S. Haykin, *Neural networks: a comprehensive foundation*. Prentice Hall PTR, 1998.

[150] J. Holtrop, G. Mennen *et al.*, "An approximate power prediction method," *International shipbuilding progress*, vol. 29, no. 335, pp. 166–170, 1982.

A Data-driven model performance plots

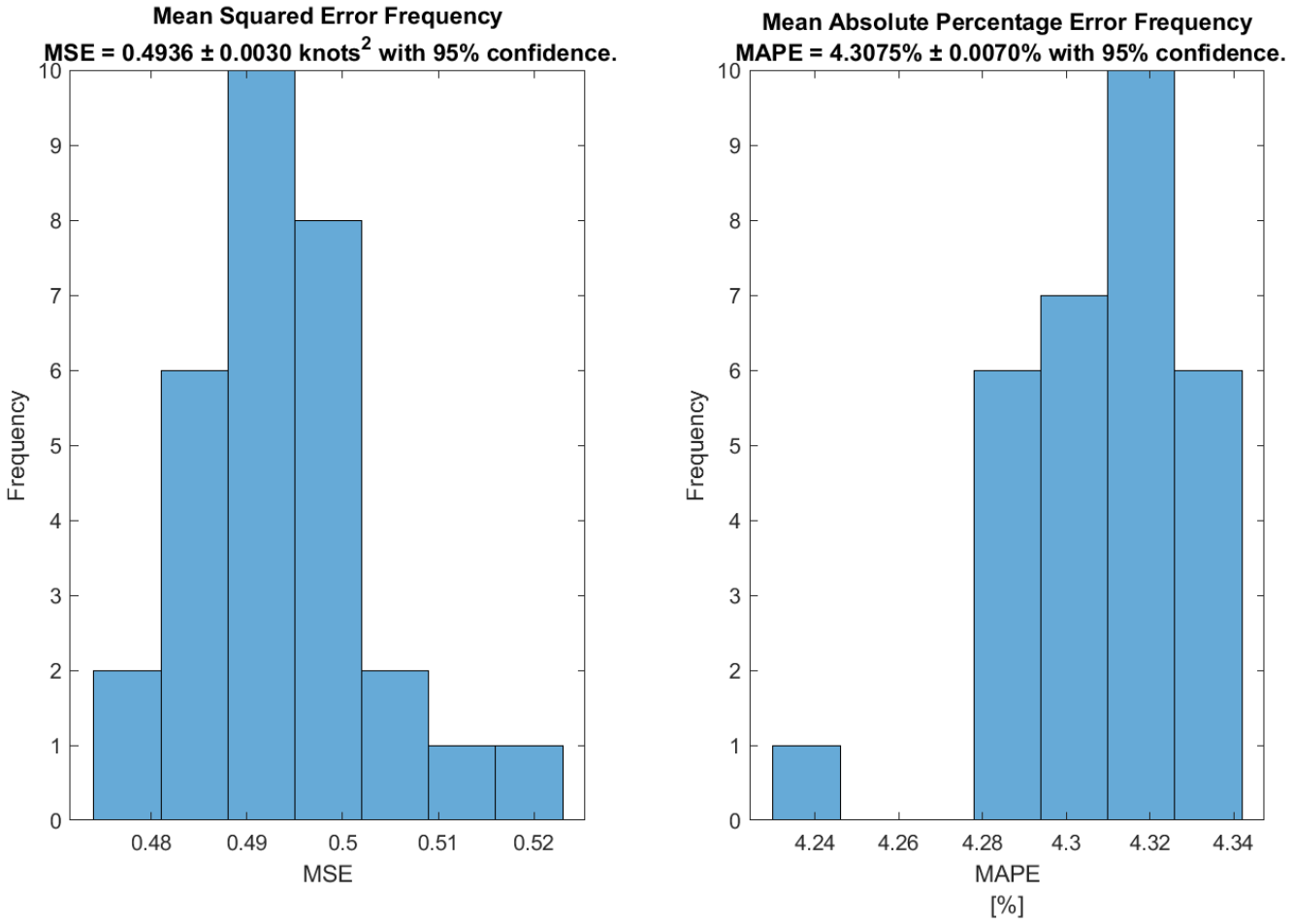

(a) RLS - DDM Training Error histograms

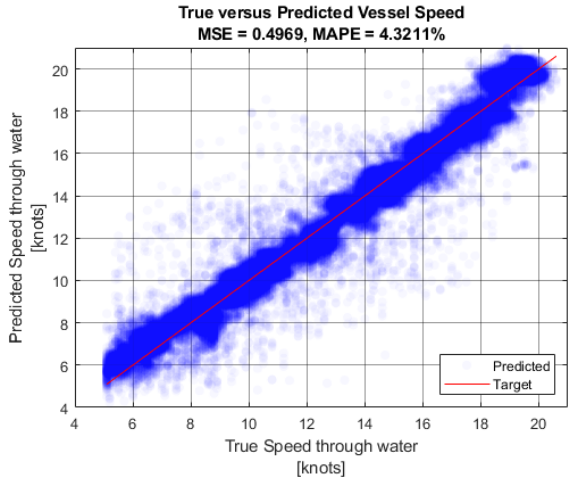

(b) RLS - DDM Test performance

Figure A.1: RLS Data-driven Model performance

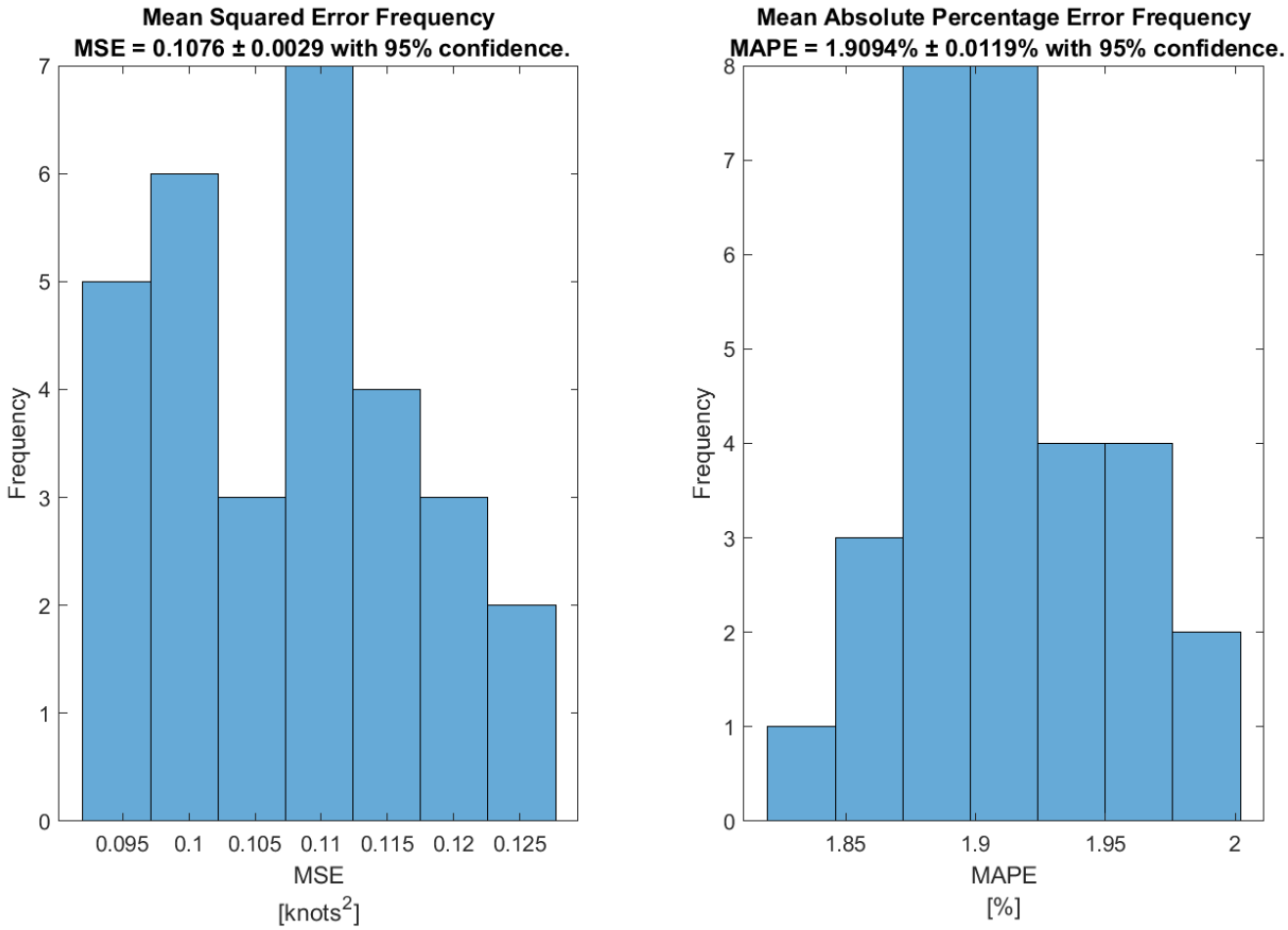

(a) KRLS - DDM Training Error histograms

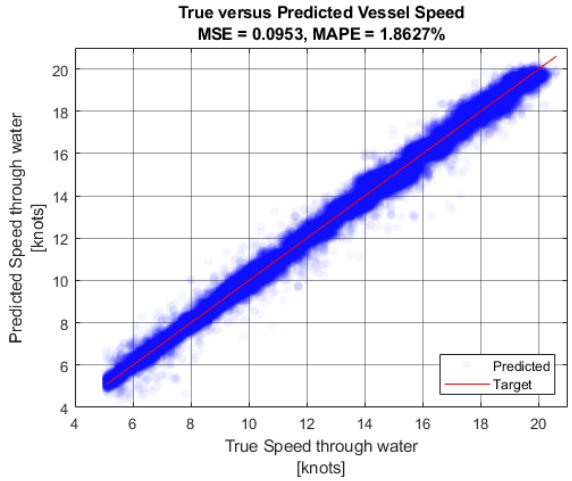

(b) KRLS - DDM Test performance

Figure A.2: KRLS Data-driven Model performance

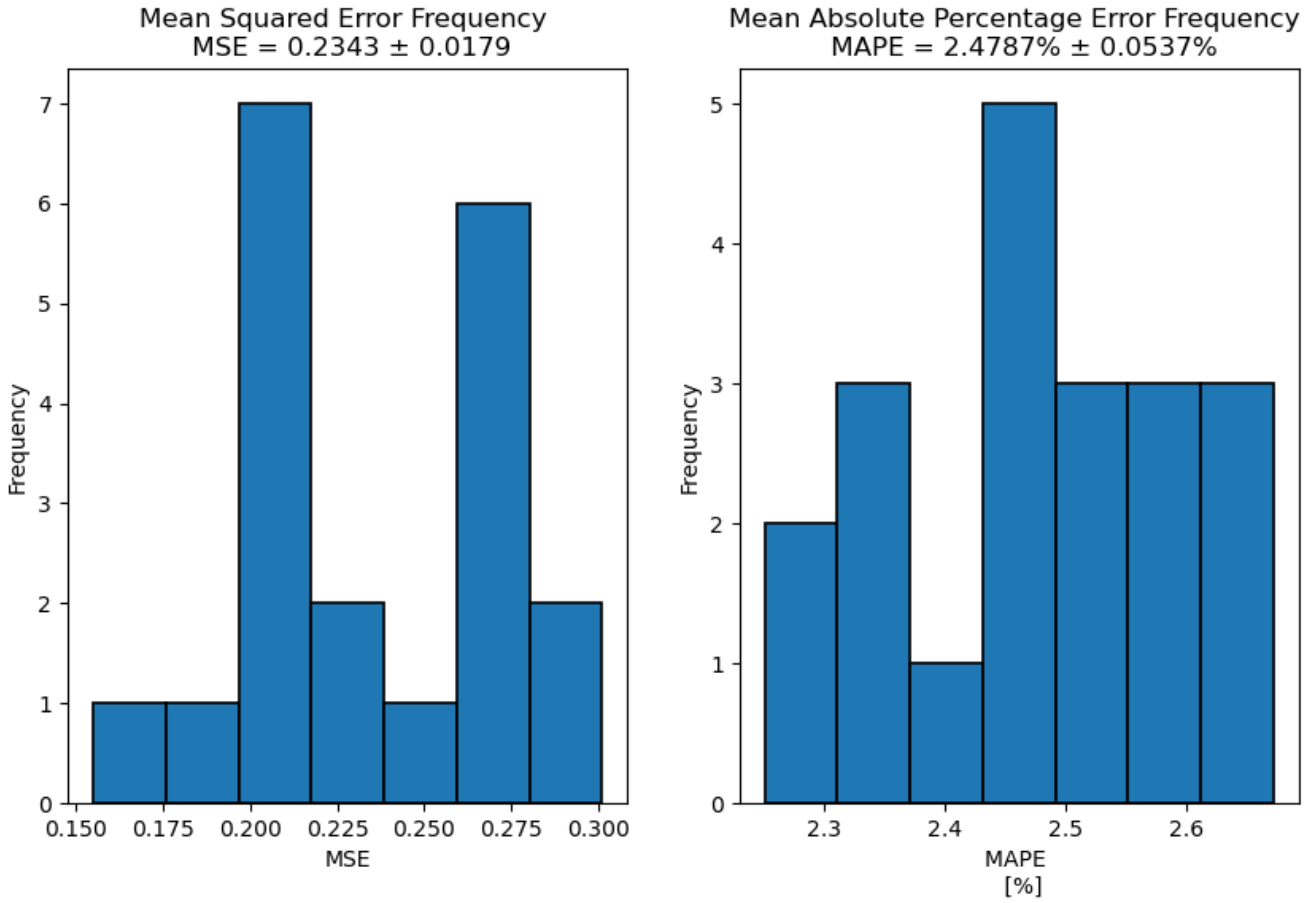

(a) Decision Tree - DDM Training Error histograms

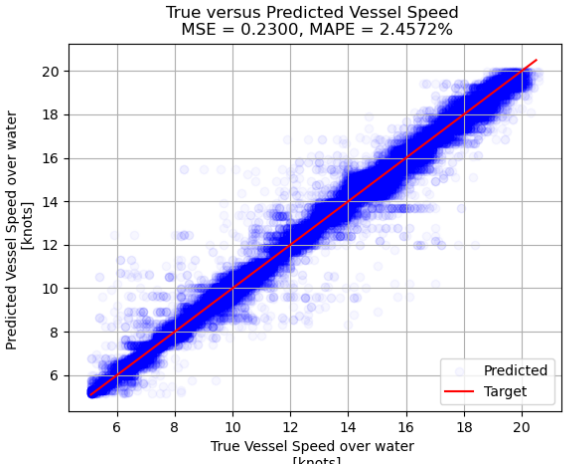

(b) Decision Tree - DDM Test performance

Figure A.3: Decision Tree Data-driven Model performance

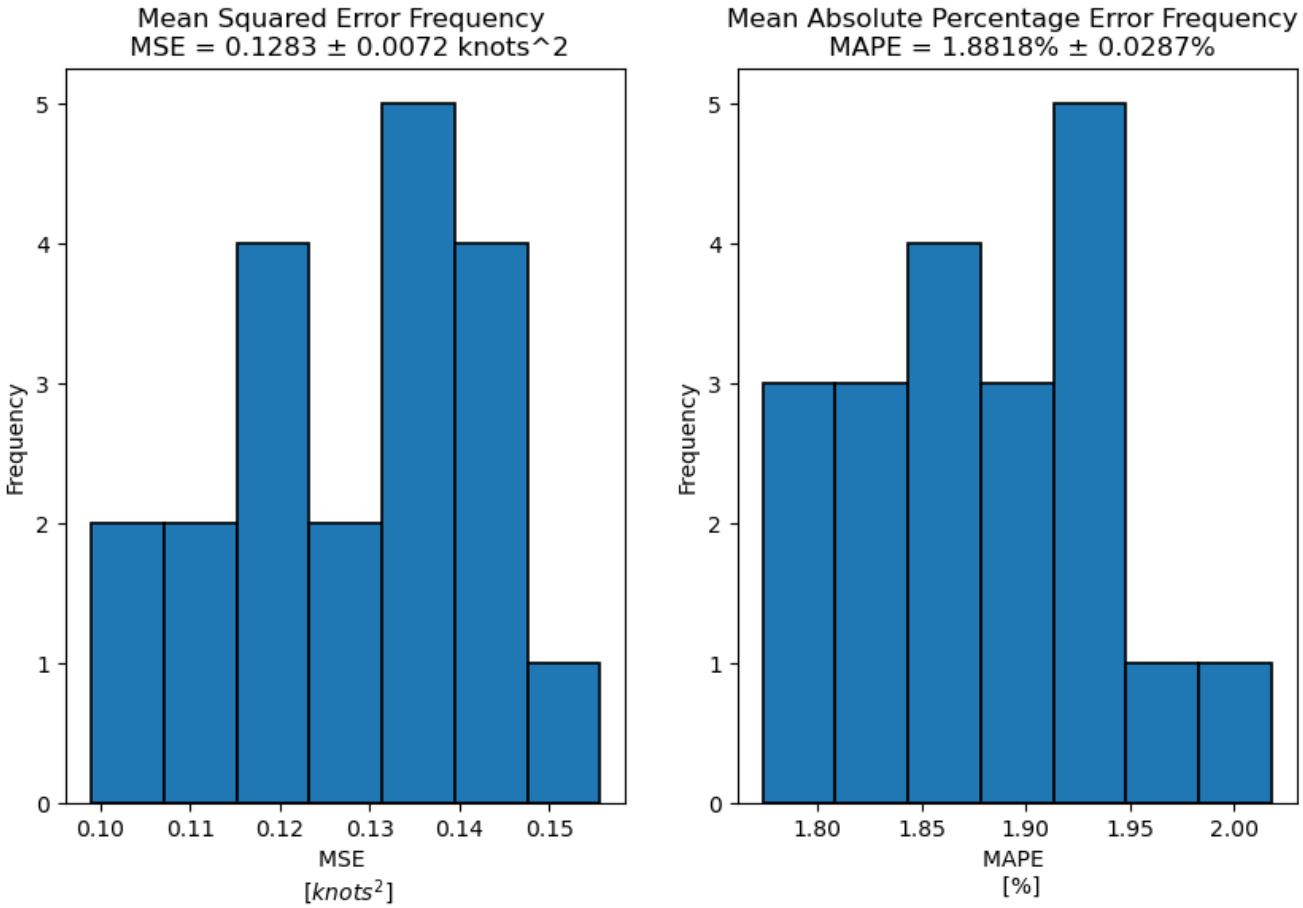

(a) Random Forest - DDM Training Error histograms

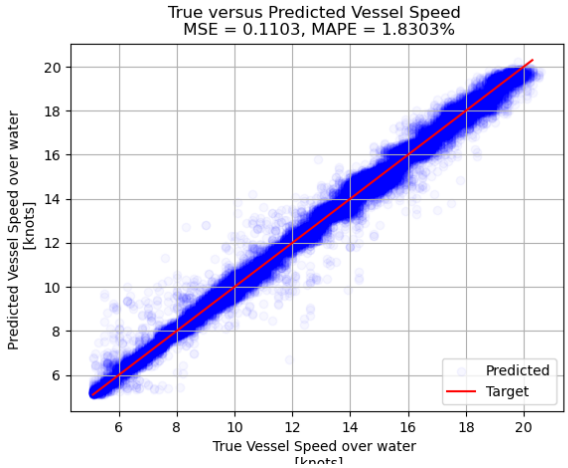

(b) Random Forest - DDM Test performance

Figure A.4: Random Forest Data-driven Model performance

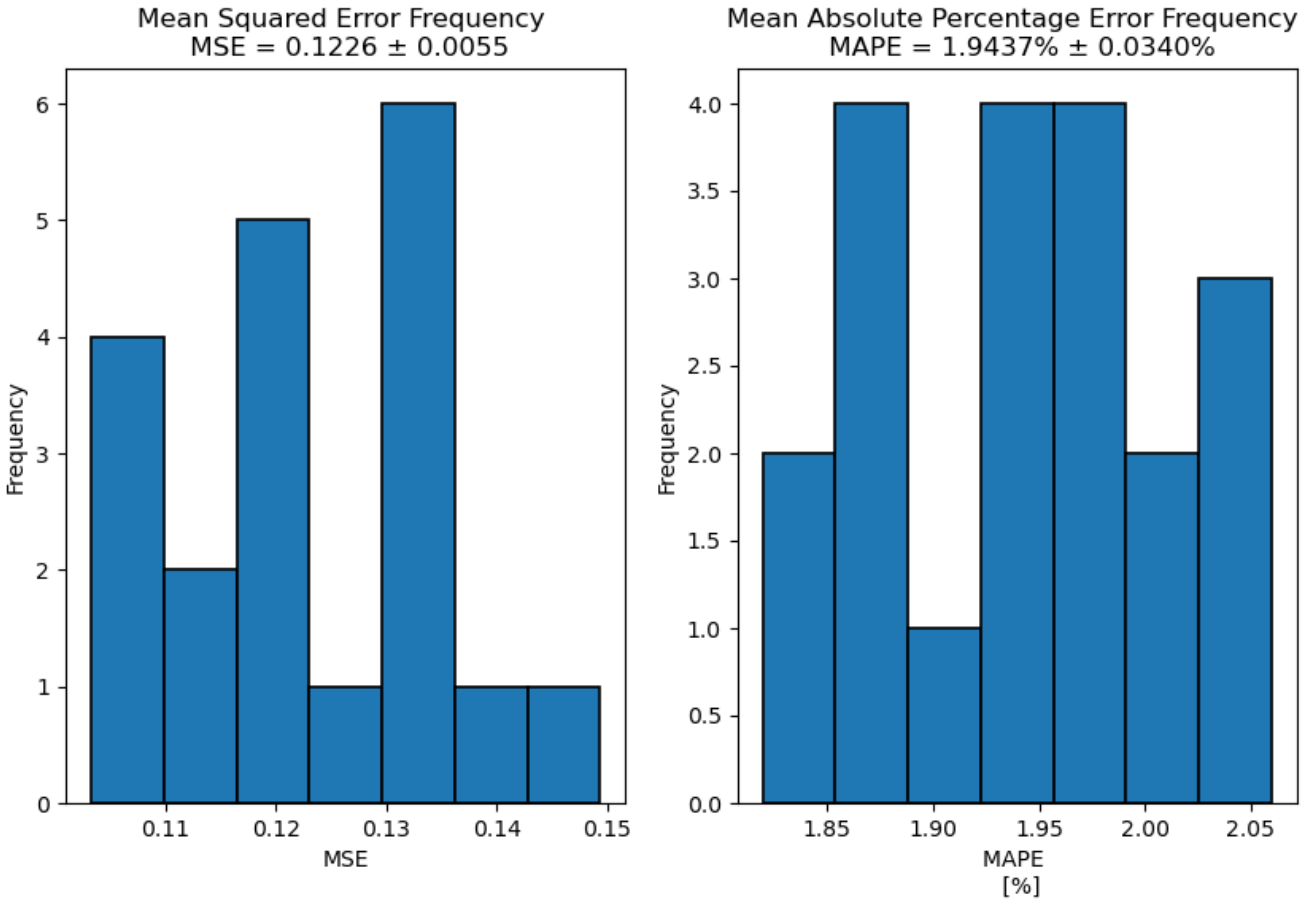

(a) XG Boost - DDM Training Error histograms

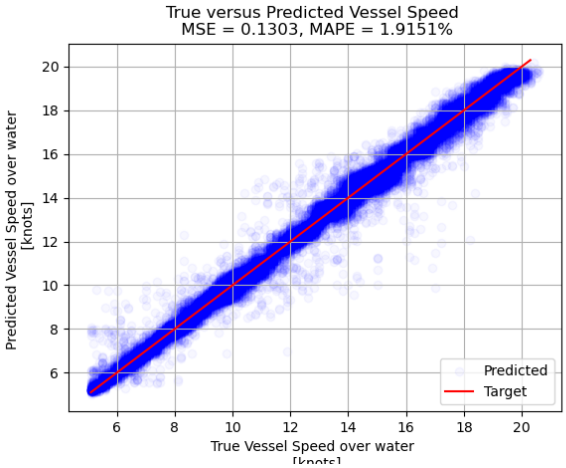

(b) XG Boost - DDM Test performance

Figure A.5: XG Boost Data-driven Model performance

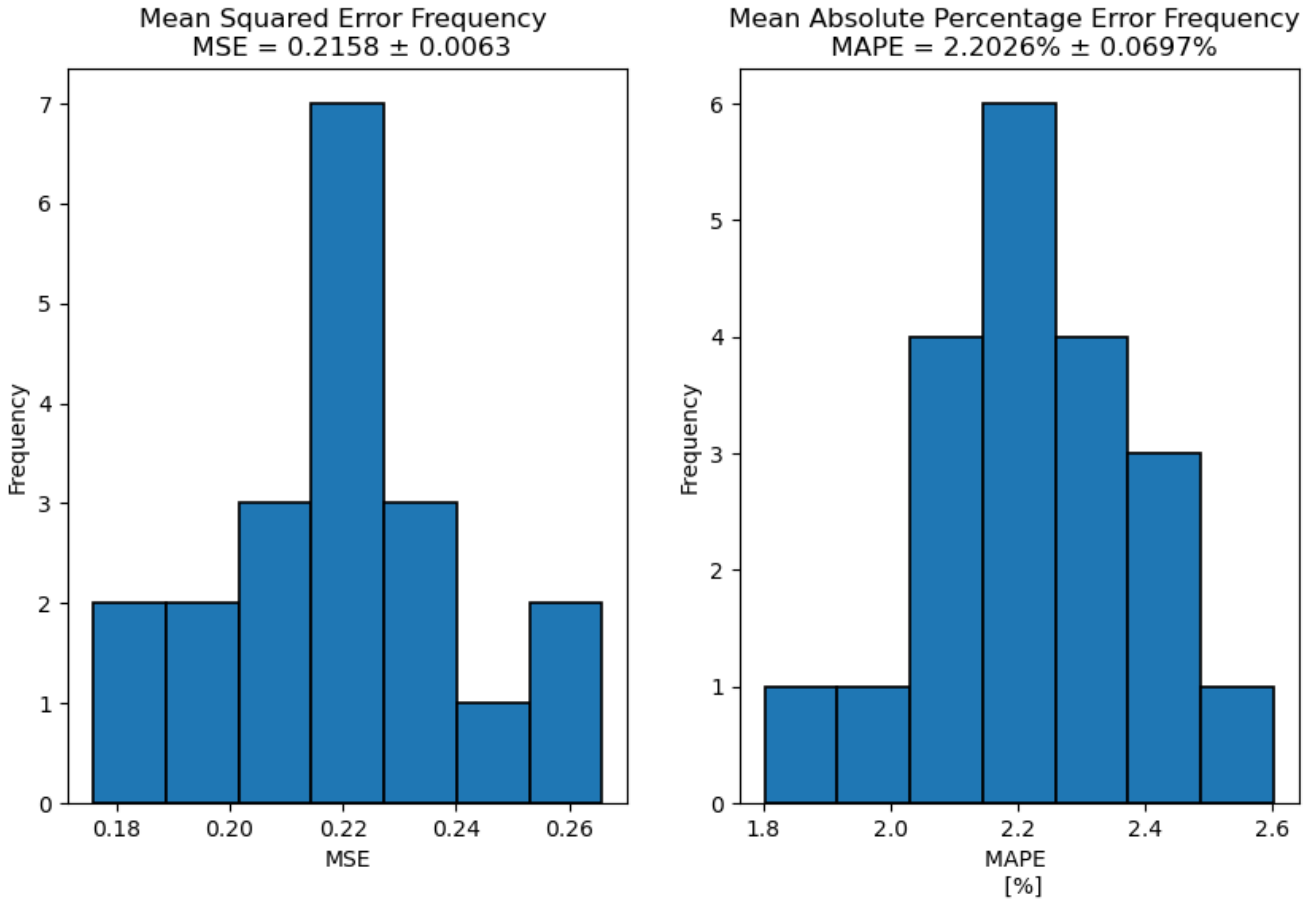

(a) Neural Network - DDM Training Error histograms

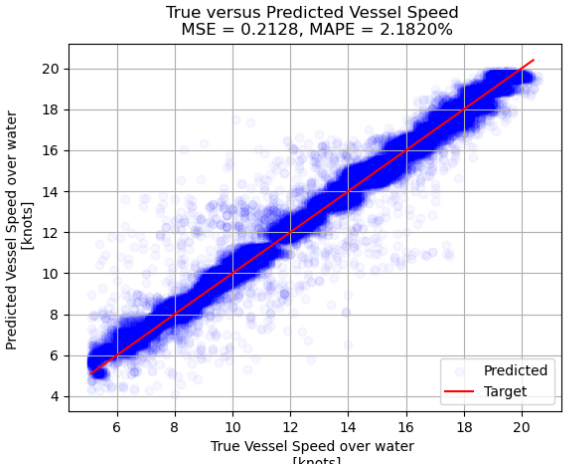

(b) Neural Network - DDM Test performance

Figure A.6: Neural Network Data-driven Model performance

B Hybrid model performance plots

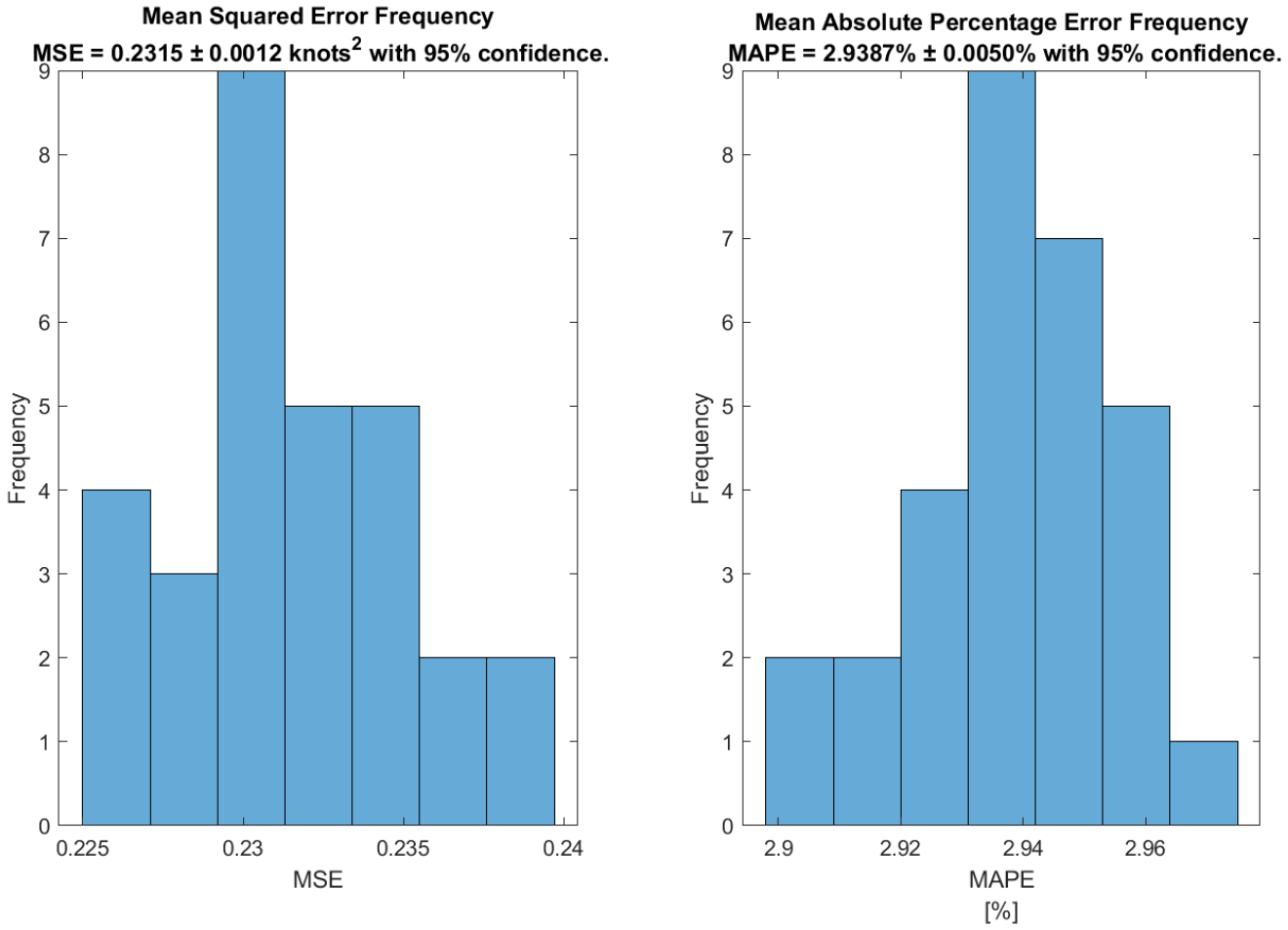

(a) RLS - HM Training Error histograms

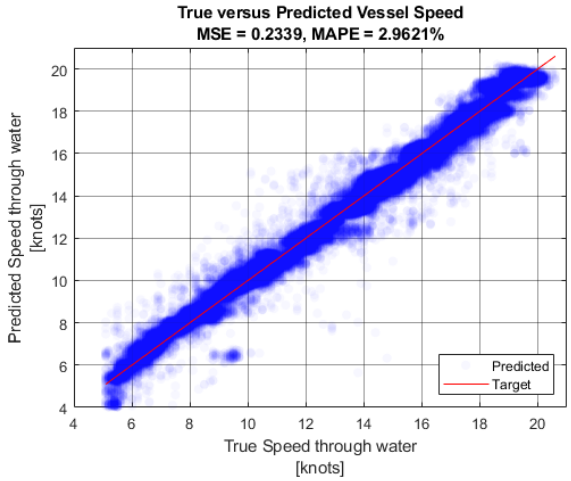

(b) RLS - HM Test performance

Figure B.1: RLS Hybrid model performance

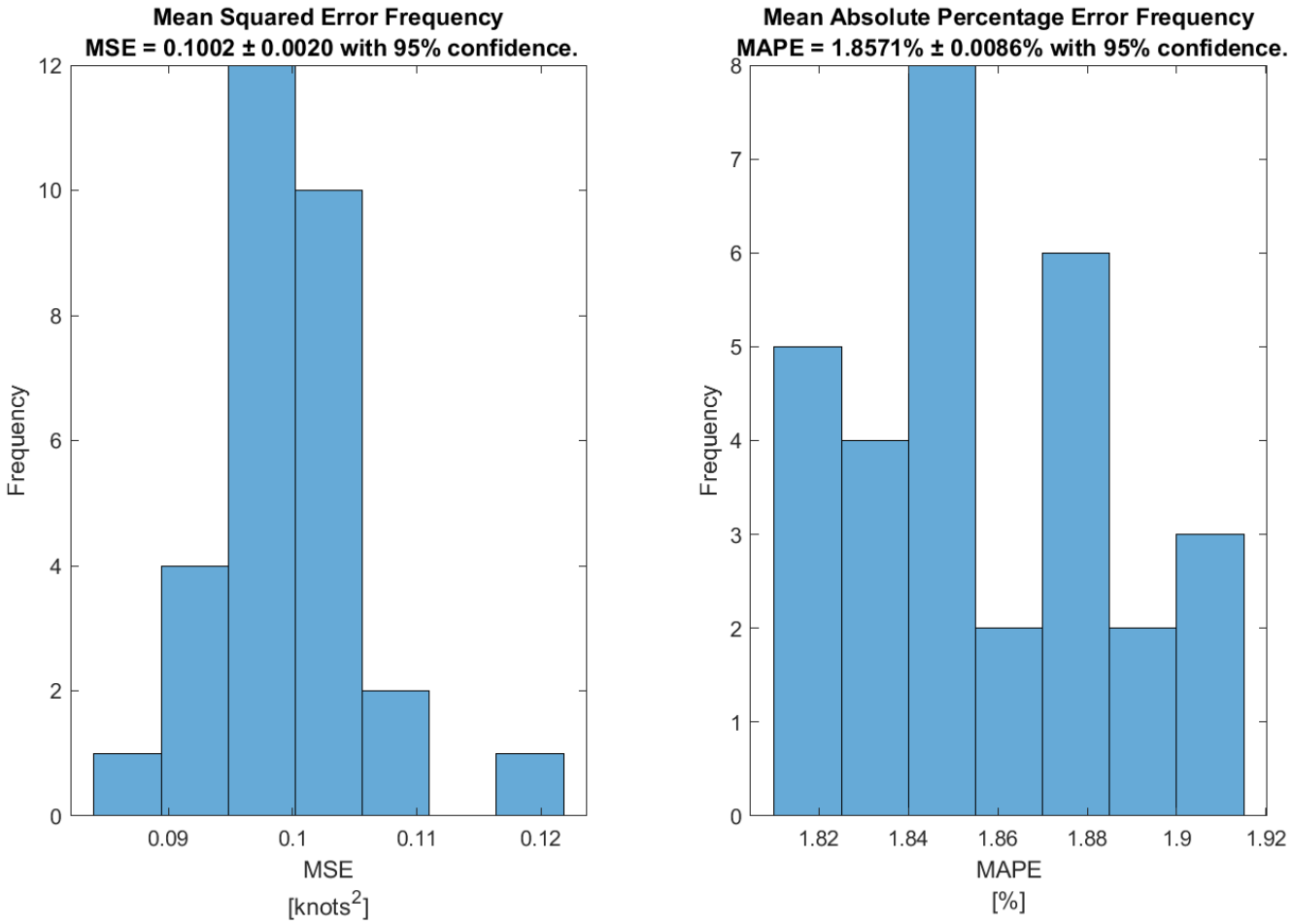

(a) KRLS - HM Training Error histograms

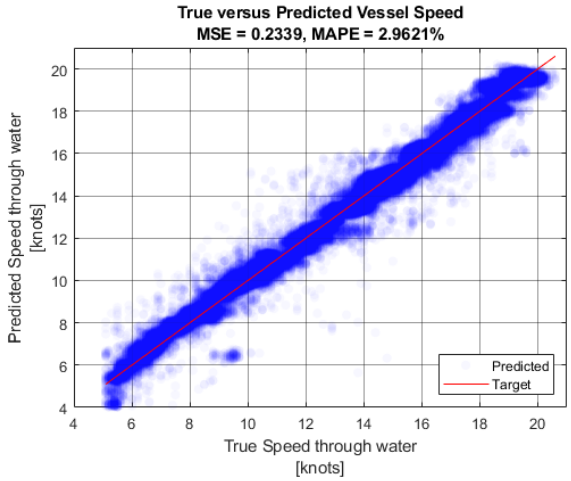

(b) KRLS - HM Test performance

Figure B.2: KRLS Hybrid model performance

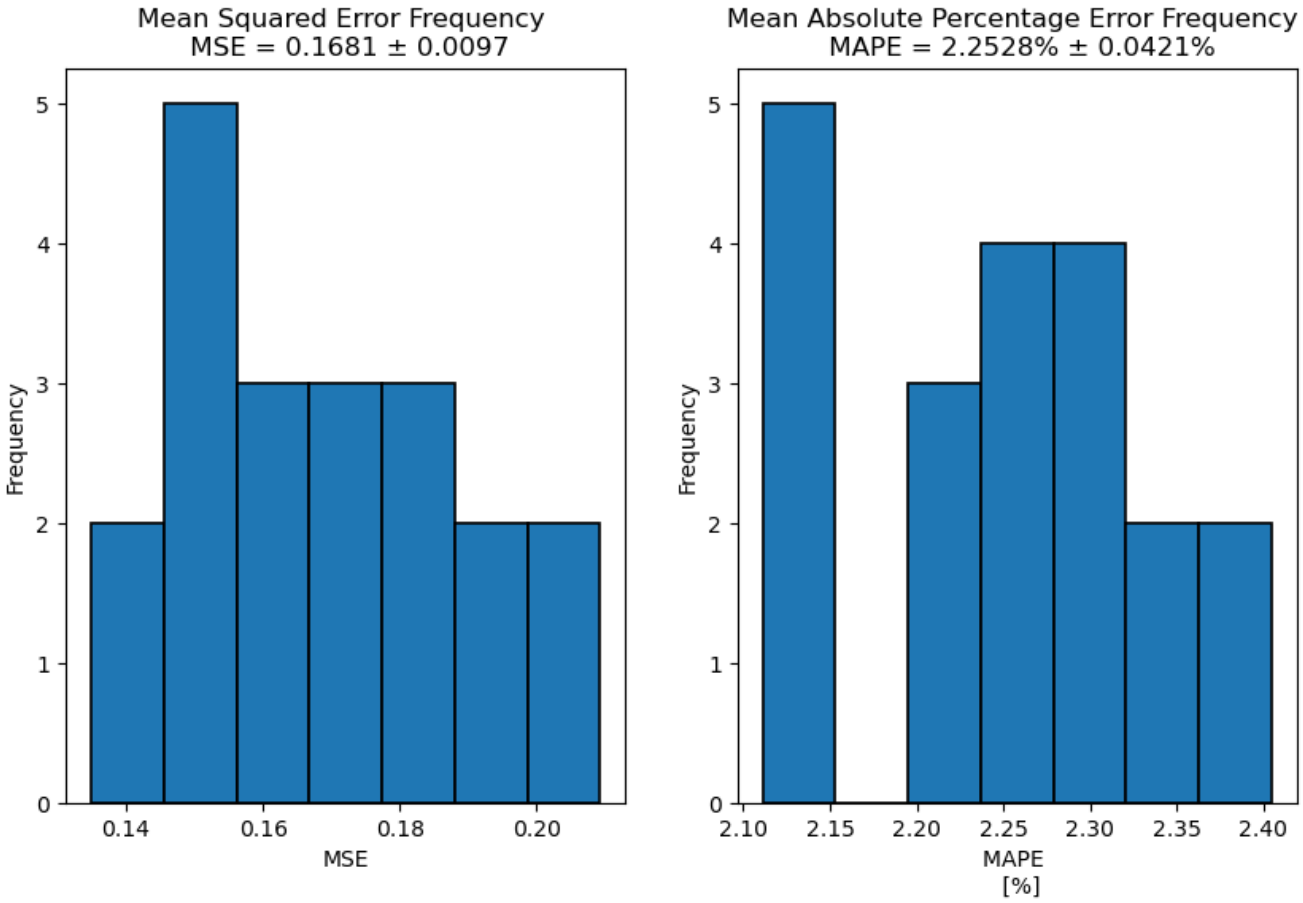

(a) Decision Tree - HM Training Error histograms

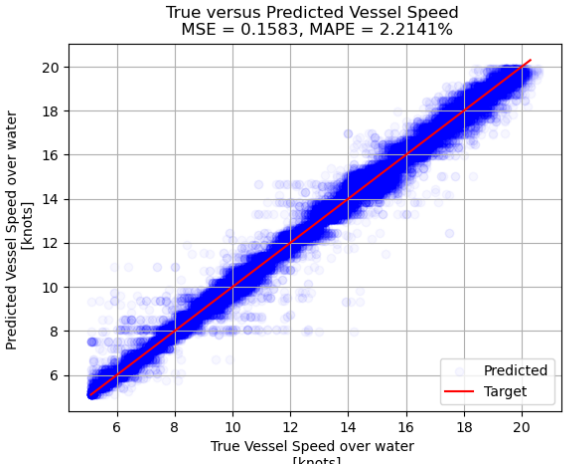

(b) Decision Tree - HM Test performance

Figure B.3: Decision Tree Hybrid model performance

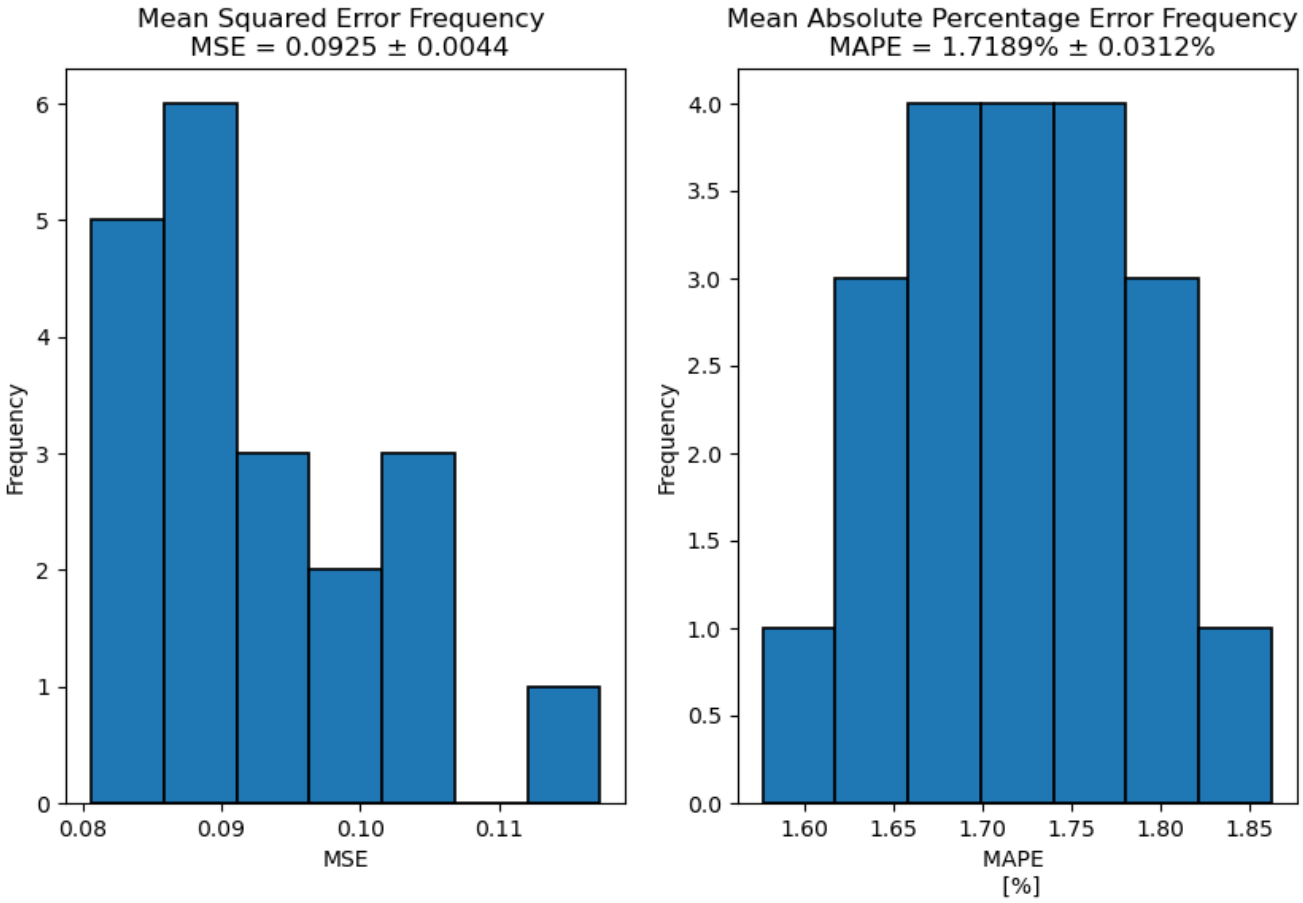

(a) Random Forest - HM Training Error histograms

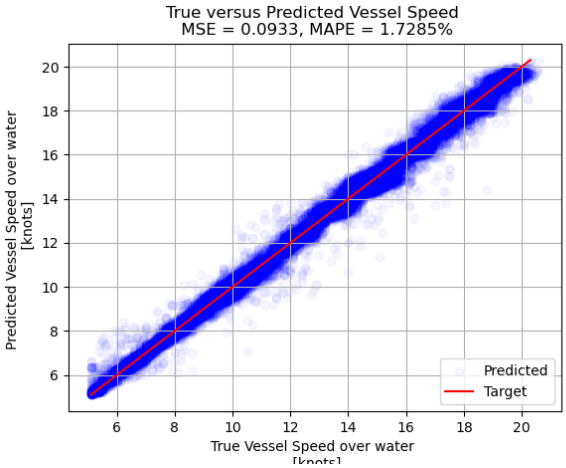

(b) Random Forest - HM Test performance

Figure B.4: Random Forest Hybrid Model performance

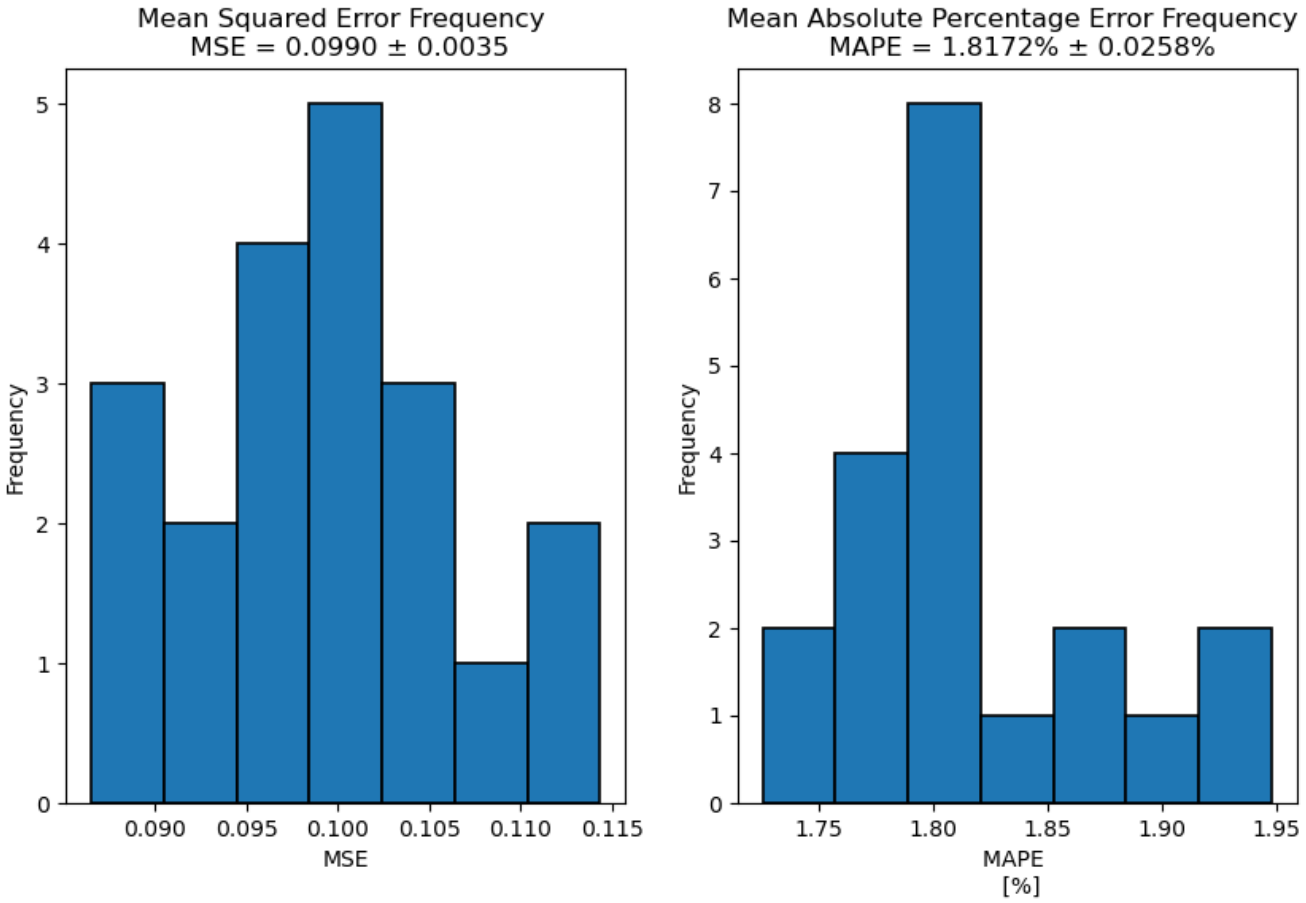

(a) XG Boost - HM Training Error histograms

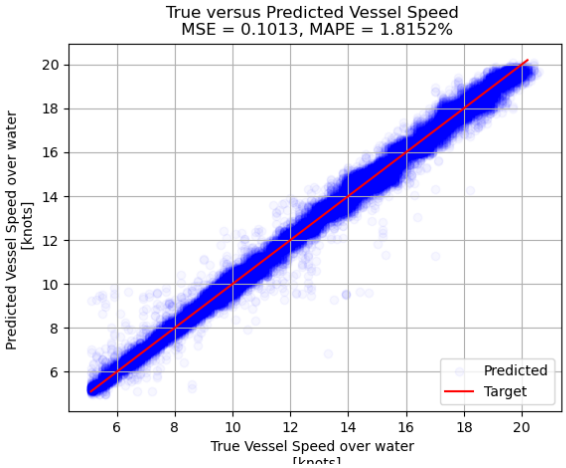

(b) XG Boost - HM Test performance

Figure B.5: XG Boost Hybrid Model performance

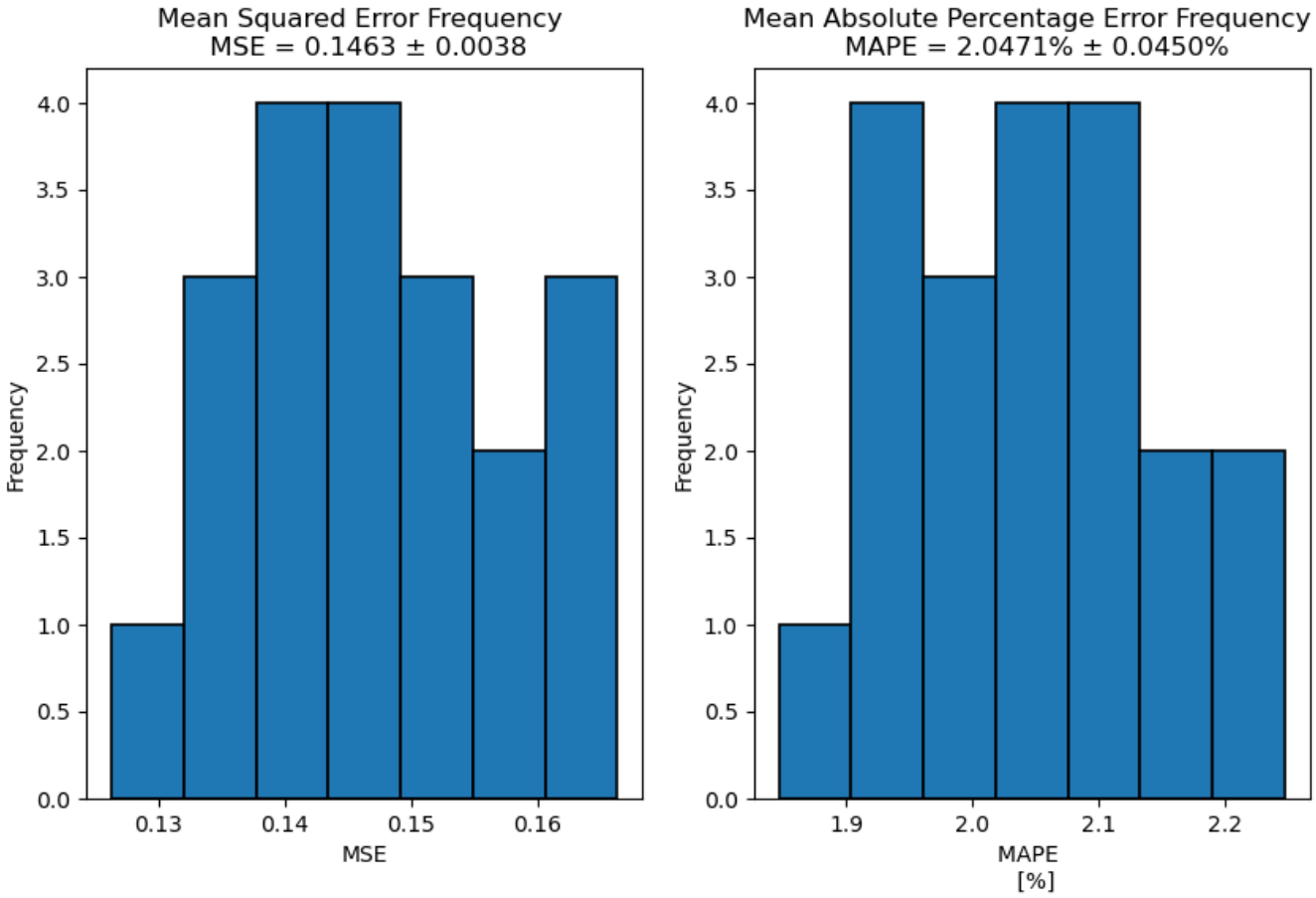

(a) Neural Network - HM Training Error histograms

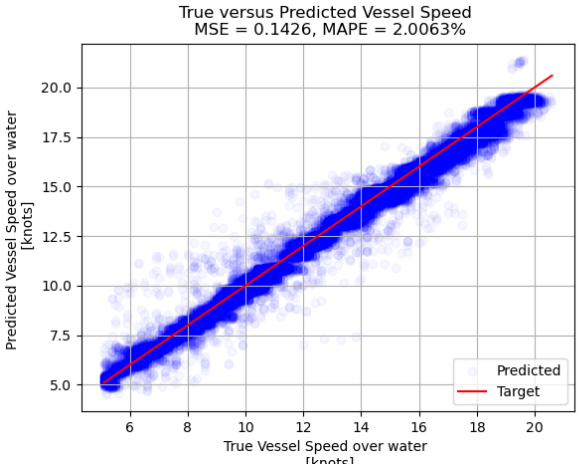

(b) Neural Network - HM Test performance

Figure B.6: Neural Network Hybrid Model performance